Copyright Warning & Restrictions

The copyright law of the United States (Title 17, United States Code) governs the making of photocopies or other reproductions of copyrighted material.

Under certain conditions specified in the law, libraries and archives are authorized to furnish a photocopy or other reproduction. One of these specified conditions is that the photocopy or reproduction is not to be "used for any purpose other than private study, scholarship, or research." If a, user makes a request for, or later uses, a photocopy or reproduction for purposes in excess of "fair use" that user may be liable for copyright infringement,

This institution reserves the right to refuse to accept a copying order if, in its judgment, fulfillment of the order would involve violation of copyright law.

Please Note: The author retains the copyright while the New Jersey Institute of Technology reserves the right to distribute this thesis or dissertation

Printing note: If you do not wish to print this page, then select "Pages from: first page # to: last page #" on the print dialog screen

ABSTRACT

Thermal Oxidative Decomposition of Chlorobenzenein a Tubular Flow Reactor

by

Jian Liu

The thermal reaction experiments of chlorobenzene decomposition were carried out in a tubular flow reactor in hydrogen and oxygen mixtures ranged from 1% to 5% at one atmosphere total pressure. Experiment temperatures were varied over a range of 590--640^{o}C. Residence times ranged from 0.3 to 2.0 seconds.

It was found that the decomposition of chlorobenzene increased with both temperature and residence time. The oxidation of chlorobenzene occurred more rapidly when oxygen concentration was increased. 95% decomposition of chlorobenzene occurred at 620^{o}C, O_2/H_2 = 5%, and two seconds residence time.

The major products were benzene and HCl, and the minor products were CH_4, C_2H_4, C_2H_6, CO, and CO_2. Toluene and C_2H_2 were observed in several experimental conditions.

A kinetic reaction mechanism which included 220 elementary reactions was developed and modified by adding mechanism important to benzene oxidation reactions. In the 600^{o}C to 630^{o}C temperature range, the model predictions of chlorobenzene decomposition and benzene formation at one second residence time and 1% to 5% oxygen and hydrogen ratio showed significant agreement with experiment data.

THERMAL OXIDATIVE DECOMPOSITION OF CHLOROBENZENE IN A TUBULAR FLOW REACTOR

by
Jian Liu

A Thesis
Submitted to the Faculty of the
New Jersey Institute of Technology
in Partial Fulfillment of the Requirements for the Degree
of Master of Science
Department of Chemical Engineering, Chemistry,
and Environmental Science
May 1992

APPROVAL PAGE

Thermal Oxidative Decomposition of

Chlorobenzene in a Tubular Flow Reactor

by

Dr. Joseph W. Bozzelli, Thesis Adviser
Distinguished Professor of
Chemical Engineering, Chemistry,
and Environmental Science, NJIT

Dr. Barbara B. Kebbekus, Committee Member
Associate Chairperson and Professor of
Chemical Engineering, Chemistry,
and Environmental Science, NJIT

Dr. Somenath Mitra, Committee Member
Assistant Professor of Chemical Engineering,
Chemistry, and Environmental Science, NJIT

BIOGRAPHICAL SKETCH

Author: Jian Liu

Degree: Master of Science in Environmental Science

Date: May, 1992

Undergraduate and Graduate Education:

- Master of Science in Environmental Science,
  New Jersey Institute of Technology, Newark, NJ, 1992
- Bachelor of Science in Environmental Science,
  Beijing Normal University, Beijing, PR China, 1984

Major: Environmental Science

Publication:

Liu, Jian. "Transport and Accumulation of the Heavy Metals in Soil-Plant System and the Relation Between Heavy Metals and the Condition of Soil Environment", ACTA ECOLOGICA SINICA, Vol. 5, 1985.

ACKNOWLEDGEMENT

I wish to express appreciation to Professor Joseph W. Bozzelli for his advice and encouragement. I am deeply indebted to him for the opportunities which he made available to me.

Specical thanks to Dr. Barbara B. Kebbekus and Dr. Somenath Mitra for the helpful corrections.

I also wish to express appreciation to my colleagues, Yo-Ping Wu and Wen-Pin Ho, at Kinetics Research Laboratory at the New Jersey Institute of Technology for the assistance their gave to me.

For love and inspiration I shall be eternally grateful to my wife, Li Li , and my parents.

TABLE OF CONTENTS

LIST OF TABLES

LIST OF FIGURES

CHAPTER 1
INTRODUCTION

Incineration of chlorocarbons in refuse recovery and in hazardous waste incinerators are of considerable concern to federal, state, and local environmental regulatory and community groups because of the possibility of hazardous emissions from these incinerators. High temperature oxygen-rich incineration often seems to produce trace amounts of undesirable and thermally stable combustion products. Shaub and Tsang[1] and Harris, et al[2] have cited species such as polychlorobiphenyls (PCBs) and polychlorinated dibenzodioxins(PCDDs) as effluent. These chlorinated compounds are thought to be highly toxic, and as a consequence they are highly undesirable products of incomplete combustion. It would be valuable to understand the fundamental reaction mechanisms by which these species are produced during incineration or oxidation processes. Graham, Hall, and Dellinger[3] have investigated the oxidation of a mixture of five organic hazardous compounds in a thermal reactor at temperature 300°C - 1000°C. This toxic compound mixture was composed of 2.5% carbon tetrachloride, 2.5% trichloro-etylene, 2.5% monochlorobenzene, 2.5% 1,1,2-trichloro-1,2,2-trifluoroethane, and 90% toluene by weight for a total distribution of 84.6% C, 8.0% H, 6.6% Cl, and 0.8% F. Results from their studies under pyrolytic conditions showed that more than 50 stable

products were observed over a temperature range of 300-1000°C with a mean residence time at 2 seconds. Out of these products, more than 27 were halogenated compounds such as chlorinated furans, phenols, and polycyclic aromatic hydrocarbons (PCAHs). All of these are believed to be significantly more toxic than the starting materials.[4]

Rubey, et. al.[5], have studied the oxidation of a mixture of PCBs over temperature ranges of 500°C - 1000°C using a 1 mm ID flow reactor with 2 second residence times. They found that polychlorinated dibenzofuran (PCDBF) and polychlorinated polyaromatic hydrocarbons (PCPAHs) were produced as a result of the PCB oxidation. Moreover, they found that at any given temperature in the range that was studied, an increase in the oxygen available for oxidation resulted in an increase in the amount of PCDBF produced. Gochfeld, et. al.[6], have reported that dioxin exposure to humans is a serious health problem. Public attention has recently focused on both municipal and hazardous waste incineratosr as sources of dioxin fallout .

Pyrolysis studies of chlorobenzene (Hydrodechlorination) have been performed by R. Louw, H. Dijks, and P. Mulder[7] and by E. Ritter[8] in hydrogen atmospheres with reaction temperatures 800 - 1010°C. Ritter found significant quantities of soot formation and incomplete mass balance for Cl (as HCl). However, the addition of

small amount of oxygen to the excess H_2 in reactions with chlorobenzene may lower the pyrolysis temperature and possibly reduce high molecular weight compounds and improve Cl conversion to HCl.

This work is the continuation of the study of our group on thermal reactions of chlorobenzene in hydrogen and oxygen mixtures. Ritter and Bozzelli[9] reported some chlorobenzene oxidation results in their study Yang, Chunchen[10] studied thermal decomposition of chlorobenzene in tubular flow reactor in 1989. Some of experimental results have to be reexamined, and we try to modify the kinetic reaction mechanism by adding to the benzene oxidation mechanism.

CHAPTER 2
PREVIOUS STUDIES

The thermal decomposition of chlorobenzene was earlier studied by Cullis and Priday[11] in 1954. This study was limited to a static (batch) reactor. Cullis and Manton[12], in 1958, extended this work to a flow system which was operated at a low pressure in a flow tank reactor at the temperature range 770 ^{o}C to 890 ^{o}C. They found that addition of hydrogen gas to the system accelerated the decomposition of chlorobenzene.

In 1973, Louw, Rothuizen and Wegman[13] published a study on the reaction of chlorobenzene with chlorine and hydrogen atoms at 500^{o}C in a low pressure reactor. The residence time within their reactor system averaged two minutes. Reactant and product information is available and a part of a mechanistic model was proposed. In 1983, Louw, Dijks, and Mulder[7] published a second study on the decomposition of chlorobenzene by using a tank flow reactor in hydrogen bath gas at 1 atm pressure. The residence time ranged from 5 - 10 seconds and the temperatures were 500^{o}C - 1000^{o}C. A reaction mechanistic scheme for the formation of methane through a methyl - cyclopentadiene intermediate was proposed. In the study, they also observed C_2 hydrocarbons such as C_2H_2, C_2H_4 and C_2H_6. CH_4 is about 0.5 percent of initial reagent at 750^{o}C. C_2H_4 and C_2H_6 rise to much smaller amounts. C_2H_2 is produced in

trace amounts only. Biaryls were found in 1-2 mole percent proportions to the HCl level together with trace amounts of naphthalene and biphenylene. They also indicated that pyrolysis in excess H_2 would be a promising method for dechlorination of organic chlorine compounds.

In 1985, Manion, Mulder, and Louw[14] examined the hydrodechlorination of a mixture of polychlorobiphenyls (PCB's) using a spiralized quartz reactor, which was 3.5 meters long and of 4 mm ID. The temperature ranged from 700°C to 925°C with residence time ranging from 5 to 15 seconds. Their results showed that the hydrodechlorination of PCB yields polychlorinated benzenes such as: chlorobenzene, di-chlorobenzene, and tri-chlorobenzene, and non-chlorinated organic products, mainly benzene. They pointed out that the dechlorination of aliphatic and olefinic chlorides reacted much faster than chlorobenzenes in an excess of H_2.

In 1986, Yang, Y. D.[15] studied the hydrodechlorination of chlorobenzene over a palladium catalyst at atmosphere pressure in the temperature range from 35°C to 85 °C. The conversions of 45 - 60 % were reported, but deactivation of the catalyst was considered to be a problem. The major products of this reaction were benzene and carbon.

Ritter, E. R.[8] studied the thermal decomposition of chlorobenzene in a tubular flow reactor system at one atmosphere pressure and average residence times of 0.02 to 2.5 seconds. Experiments carried out in 3 different diameter quartz reactor tubes, to examine the wall reactions in these reactors by the application of pseudo first order reaction kinetics and assumption of plug flow reactor. The major products he reported were benzene, HCl, and a small amount of polycyclic aromatic hydrocarbons (PAHs). His study also found minor products such as cyclopentadiene, toluene, biphenyl, chlorobiphenyl, terphenyl, triphenylene, and naphthalene. He also studied the pyrolysis of chlorobenzene in a helium atmosphere.

Mingta Hung[16] studied the high temperature pyrolysis of dichlorobenzene in a plug flow reactor, where reaction temperature ranged from 800^{o}C to 1000^{o}C at one atmosphere pressure of hydrogen bath gas. This study found the major products: chlorobenzene, benzene, HCl and C(s). The carbon formation was significant and sometimes amounting to 50% of the reacted dichlorobenzene. However, he also did not report any data about light hydrocarbons analysis.

In 1988, Zhu, L. J.[17] further studied the kinetic of thermal decomposition of chlorobenzene and dichlorobenzene in a hydrogen and helium atmospheres. He examined formation of light hydrocarbons and soot. The experiments were performed at atmosphere pressure with residence times

ranging from 0.2 to 1.2 seconds, and temperature ranged from 850°C to 925°C. Light hydrocarbon products were identified as CH_4, C_2H_2, C_2H_4, and C_2H_6. Under a hydrogen atmosphere, C_2H_4 was formed but no C_2H_2, where in a helium atmosphere C_2H_2 was produced as a higher concentration end product. All light hydrocarbons from the pyrolysis of chlorobenzene in this study of Zhu were less than 5% of the initial reactant chlorobenzene or dichlorobenzene concentration.

In 1989, Yang, C. C.[10] studied the thermal reaction of chlorobenzene on addition of small percentages of oxygen (1% - 5%) in the pyrolysis of dilute chlorobenzene in H_2. By addition of oxygen, the reaction temperatures of chlorobenzene were significantly reduced and ranged only from 560°C to 660°C, much lower than the 900°C required for the non-oxygen atmospheres of Ritter and Hung. In addition, Yang investigated reaction products to initiate development of a mechanistic model.

We note that we need to pay more attention to benzene reaction because it is the major product on chlorobenzene decomposition. There are many studies on benzene oxidation in the literature such as those of Tsang[18], Felder[19] et al, Brezinsky[20] et al, and Bozzelli[21]. Brezinsky[22] and Venkat et. al.[20] have published general reaction schemes with no rate constants or thermodynamic properties. Bittker[23] published a mecha-

nism which is based upon previously published reaction paths and presents rate constants which fit experimental data for ignition delay times and toluene loss profiles.

Bozzelli[21]'s study focused on thermodynamic and kinetic analysis for reaction of cyclopentadiene and cyclopentadienyl radical with O_2, O, H, OH, and HO_2 using bimolecular QRRK theory and prediction from mechanism with reaction data.

CHAPTER 3
RESEARCH BACKGROUND

3.1 Destruction Mechanism of Chlorinated Hydrocarbons in Combustion Process

Organic molecules can be decomposed into thermodynamicly more stable products, fragments and atoms at sufficiently high temperature. In the presence of oxygen, this process is expedited by the great thermodynamic stability of the products, H_2O and CO_2. The most specific and accurate way to describe such process is in terms of single step elementary reactions. It is important to distinguish this approach from the more general or global approach of simply describing the system in terms of the directly observed input and output species. For the optimization of a reactor this may, in some cases, be the most cost efficient method.[24]

There are two primary types of reactions which will lead to destruction of organic compounds in the gas phase, unimolecular and bimolecular processes. The unimolecular reaction can be considered to depend on temperature. The physical situation is that of a molecule receiving energy from the heat bath until some reaction threshold is surpassed and decomposition occurs. Bimolecular destruction mechanism usually involves a radical attacking the molecule. This can lead to the direct abstraction of an atom or addition to a site of unsaturation. In both cases the consequences are the formation of a secondary radical

which may rapidly decompose in the incineration thermal environment. Although a large number of radicals are formed during the degradation of organic compounds, it is known that a few radicals, principally OH, O, H, and Cl make the major contributions to the destruction mechanism.

Incineration involving chlorine compounds merit special attention. Chlorine atom is extremely reactive. It rapidly abstracts hydrogen and adds to unsaturated sites. Therefore, the presence of large quantities of chlorinated compound opens up additional decomposition pathways--forming HCl. This process ties up a significant amount of hydrogen and limits H_2O formation in addition to limiting other reactions.

Organic molecules under incineration conditions will decompose via a combination of pyrolytic and oxidative mechanisms. Free radicals are important intermediates. For pyrolysis, the process involves degradation to smaller and more unsaturated species. Under oxidation, the breakdown process is enhanced, carbon atoms are bonded to oxygen and many of the unsaturated structures which are precursors to soot have little or no chance to be formed.[25] The oxidation process is highly exothermic and, therefore, along with the chain induced decomposition there are sharp increases in temperatures. More radicals are created and the reaction is driven to completion. If during any stage of these processes the reaction is stopped, through quenching at the cold walls or mixing with cold gases or

if the temperature of a given plug of gas is not hot enough to drive the reaction to completion, then the remaining organic compounds persist as the products of incomplete combustion.

3.2 Estimation of Thermochemical Data

Thermochemical data are required to determine energy balance in chemical reactions and the Gibbs Free Energy of a reaction as function of temperature. It also provides a convenient way to determine reverse reaction rate constants from the calculated equilibrium constant of the reaction and the known forward rate constants. Thermodynamics also plays a very important role in determination of rate constants and there is need for continued experimental research to develop and evaluate the thermodynamic parameters. This will, consequently, improve the accuracy of rate constants determined through models such Transition State Theory(TST).

Our thermochemical data base which includes H_f, S, and C_p is based upon the best currently available data. Appendix A lists our detailed thermo database and references to each specie. When experimentally based thermochemical data are not available, the values will be estimated using the THERM computer code,[26] which is based on the group additivity techniques,[27] by Bozzelli and Ritter.

3.3 Estimation of Quantitative Kinetic Data

For unimolecular decomposition of molecules and radicals, there is a large amount of existing data as well as broad theoretical understanding. In the absence of direct experimental results, satisfactory predictions can often be made.[24] Through detailed balance the rate expressions for the reverse radical combination and radical addition reactions to unsaturates can be directly calculated.

The NIST chemical kinetics database[28] provides the chemical kinetics community with a tool for rapidly examining the literature. The program gives data on particular reaction, all of the reactions of a species, or subsets of all of the reaction.

In addition, Quantum Rice Ramsperger Kassel(QRRK) calculations provide a means of extending results over wide pressure and temperature ranges. For radical and atom attack on molecules, the reactions of radical and atoms are of great important in low as well as high temperature reaction process.

3.4 Transition State Theory

For many kinds of reactions, especially for elementary reactions, their rate constants may be expressed as a product of a temperature dependent term and a composition term.

A more detailed explanation of how the reactants transform into products is given by the Transition-State

Theory. The reactants combine to form unstable intermediates called Transition State complexes (sometimes these complexes are also termed activated complexes) which then decompose spontaneously into products. Transition-State Theory assumes that an equilibrium exists between the concentration of reactants and this activated complex at all times and that the rate of decomposition of the complex is the same for all reactions which is given by **k**T/**h**, where **k** is the Boltzmann constant and **h** is the Planck's constant. Thus for the forward elementary reaction of a reversible reaction,

$$A + B \underset{k_r}{\overset{k_f}{<========>}} AB \qquad (1)$$

we have the following conceptual elementary scheme:

$$A + B \underset{k_{-1}}{\overset{k_1}{<========>}} AB^* \xrightarrow{k_2} AB \qquad (2)$$

$$K^* = \frac{k_1}{k_{-1}} = \frac{[AB^*]}{[A][B]}$$

$$k_2 = \frac{\mathbf{k}T}{\mathbf{h}}$$

The observed rate of the forward reaction is then

$$r_{AB,\text{forward}} = (\text{concentration of activated complex}) \times (\text{rate of decomposition of activated complex})$$

$$= \frac{\mathbf{k}T}{\mathbf{h}} [AB^*]$$

$$= \frac{kT}{h} K^* C_A C_B \qquad (3)$$

By expressing the equilibrium constant of activated complex in terms of the standard free energy,

$$\triangle G^* = \triangle H^* - T\triangle S^* = -RT \ln K^* \qquad (4)$$

$$K^* = EXP(-\triangle G^*/RT) = EXP(-\triangle H^*/RT + \triangle S^*/R)$$

the rate becomes

$$r_{AB,foward} = \frac{kT}{h} EXP(\triangle S^*/R)\ EXP(-\triangle H^*/RT)\ C_A\ C_B \qquad (5)$$

Theoretically both $\triangle S^*$ and $\triangle H^*$ vary very slowly with temperature. Hence, of the three terms that make up the rate constant in Eq. 5, the middle one, $EXP(\triangle S^*/R)$, is so much less temperature-sensitive than the other two terms that we may take it to be constant. So for the forward reaction, and similarly for the reverse reaction of Eq. 1, we have approximately

$$k_f = T\ EXP(-\triangle H_f^*/RT) \qquad (6)$$

$$k_r = T\ EXP(-\triangle H_r^*/RT)$$

where $\triangle H_f^* - \triangle H_r^* = \triangle H_{RXN}$

Transition-state theory views the reaction rate to be governed by the rate of decomposition of intermediate. The rate of formation of intermediate is assumed to be governed by collisions plus thermodynamics and it is present on equilibrium concentrations at all times. That is, Transition-state theory considers the second step

combined with the complex concentration to be the rate controlling factors.

3.5 Collision Theory

The collision rate of molecules in a gas can be found from the kinetic theory of gases. For the bimolecular collisions of like molecules A we have

$$Z_{AA} = d_A^2 \, n_A^2 \left| \frac{4\,\mathbf{k}T}{M_A} \right|^{1/2} = d_A^2 \, \frac{N^2}{10^6} \left| \frac{4\,\mathbf{k}T}{M_A} \right|^{1/2} C_A^2$$

where d = diameter of molecule, cm

M = mass of molecule, gm

N = Avogadro's number

C_A = concentration of A, mol/liter

n_A = number of molecules of A/cm^3

k = Boltzmann constant

For bimolecular collisions of unlike molecules in a mixture of A and B, the kinetic theory gives

$$Z_{AB} = \left(\frac{d_A + d_B}{2}\right)^2 \frac{N^2}{10^6} \left| 8\,\mathbf{k}T \left(\frac{1}{M_A} + \frac{1}{M_B}\right) \right|^{1/2} C_A \, C_B$$

If every collision between reactant molecules results in the conversion of reactants into product, these expressions give the rate of bimolecular reaction. The actual rate is usually much lower than that predicted, and this indicates that only a small fraction of all collisions result in reaction. This suggests that only the more energetic and violent collisions, those involving

energies in excess of a given minimum energy E, lead to a reaction. From the Maxwell Boltzman distribution law of molecular energies the fraction of all bimolecular collisions that involve energies in excess of this minimum energy is given approximately by exp(-E/RT), where E is usually much greater than RT. Since we are only considering energetic collisions, this assumption is reasonable. Thus the rate of reaction is given by

$$-r_A = k\, C_A\, C_B = \left|\begin{matrix}\text{collision}\\ \text{rate}\end{matrix}\right| \left|\begin{matrix}\text{fraction of collisions}\\ \text{involving energies in}\\ \text{excess of E}\end{matrix}\right|$$

$$= Z_{AB}\frac{10^3}{N} e^{(-E/RT)}$$

$$= \left(\frac{d_A + d_B}{2}\right)^2 \frac{N}{10^3} \left| 8kT\left(\frac{1}{M_A} + \frac{1}{M_B}\right)\right|^{1/2} e^{(-E/RT)}\, C_A\, C_B$$

A similar expression can be found for the bimolecular collisions between like molecules. For both, in fact for all bimolecular reactions, the above equation shows that the temperature dependency of the rate constant is given:

$$k = T^{1/2}\, e^{(-E/RT)}$$

3.6 Comparison of Two Theories

It is interesting to note the difference in approach between the transition-state and collision theories. Consider A and B colliding and forming an unstable in-

termediate which then decomposes into product, or

$$A + B \text{ -------> } AB^{*} \text{ -------> } AB$$

collision theory views the rate to be governed by the number of energetic collisions between reactants. What happens to the unstable intermediate is of no concern. The theory assumes that this intermediate breaks down rapidly enough into products so as not to influence the rate of the overall process. Transition-state theory, on the other hand, views the reaction rate to be governed by the rate of decomposition of intermediate. The rate of formation of intermediate is assumed to be governed by collisions plus thermodynamics. It is dependent on equilibrium concentrations at all times. Thus collision theory views the first step to be slow and rate-controlling, whereas transition-state theory views the second step combined with the determination of complex concentration to be the rate controlling factors.

3.7 Prediction of Rate Constants for Radical Addition and Recombination Reactions by Bimolecular QRRK Theory

The decomposition of a radical or molecule has a unimolecular, pressure-independent rate constant in the limit of high pressure, but as pressure is reduced the rate constant eventually falls off or decreases with pressure. In the low-pressure limit, it becomes directly proportional to the pressure. Rationalizing and qualifying these effects was first accomplished in the late 1920's[29]. This

has again become an active area in kinetics research.

Radical combination or radical-molecule addition to an unsaturated molecule would seem to be simply the reverse of decomposition, having the same decay behavior by microscopic reversibility. This is true for the specific reaction channel that leads to formation of the collisionally stabilized adduct. The reason is that the adduct species has an energy distribution which is in thermal equilibrium with surrounding gas molecules, just as for a species that is thermally decomposing.

It is very important to note but not well recognized that additional products can be formed from combination and addition reactions directly through the chemical activated adduct. The initially formed adduct has a chemical energy distribution, different from a thermal energy distribution because the thermal energies of the reactants are augmented by the chemical energy released via formation of the new bond. This additional chemical energy is initially the same as the energy barrier for dissociation of the collisionally stabilized adduct to the original adducts. If the energy in the chemical activation energy distribution extends above the barrier for another dissociation (or isomerization) reaction pathway of the adduct, then that lower energy reaction pathway can also occur. Distribution of products (new channels versus dissociation back to reactants or stabilization) is often

controlled by entropic effects (relative A factors) to the different channels in addition to pressure.

Calculation of the bimolecular rate constant involves the concept that the fate of the chemically activated adduct is determined by competition among the possible pathways; stabilization by collision, redissociation to reactants, or formation of new products by dissociation or isomerization.[30]

3.7.1 Unimolecular QRRK Equation

Dean (1985)[30] has presented a formalism for calculating apparent bimolecular rate constants based on the Quantum-RRK or QRRK unimolecular reaction theory of Kassel (1928)[29], which treats the storage of excess energy (relative to the ground state) as quantized vibrational energy. He also assumes steady state condition for the complex.

In the simplest form of the theory, the assumption is made that the vibrations of the decomposing molecule can be represented by a single frequency <v>, usually a geometric mean <v> of the molecule's frequencies. Next, energy E of the initially activated complex and each barrier to reaction path relative to the ground state of the stabilized molecule is divided into E/h<v> vibrational quanta. For the total energy variable E, the symbol n is used; and for number of quanta to the energy barrier to

reaction Eo, the quantized energy is m quanta. A very general scheme for unimolecular reaction is as follows:

$$A + M \underset{k_{dex}}{\overset{k_{ex}}{<==========>}} A^* + M$$

$$A^* \xrightarrow{k_{rxn}(E)} \text{Products}$$

Here M stands for the third body and only serves to raise the reacting molecule to its energized state A^* by collisional activation.

The apparent k_{uni}:

$$k_{uni} = \frac{1}{[A]} \times \frac{d[\text{Products}]}{dt} \qquad (1)$$

is then evaluated by a sum over all energies, assuming pseudo-steady state for each energy level of A* and collisional excitation, deexcitation or stabilization with rate constants k_{ex}, k_{dex} and k_{stab}:

$$k_{uni} = \frac{1}{[A]} \; k_{rxn}(E) \; [A^*(E)]$$

$$= k_{rxn}(E) \; \frac{k_{deexc}[M] \quad K(E,T)}{k_{deexc}[M] + k_{rxn}(E)} \qquad (2)$$

where K(E,T) is the thermal-energy distribution function (k_{ex}/k_{dex}). Kassel assumed that if a molecule were excited to an energy E, then $k_{rxn}(E)$ would be proportional to the probability that one of the s oscillators could have

energy Eo or greater (sufficient energy to cause reaction). This is equivalent to saying it has, m or more of the n total quanta. The proportionality constant was shown to be A, the Arrhenius preexponential factor for dissociation of A in the high pressure limit, so the energy-dependent rate constant is:

$$k_{rxn}(E) = A \frac{n!\ (n-m+s-1)!}{(n-m)!\ (n+s-1)!} \qquad (3)$$

Likewise, he derived the quantized thermal energy distribution K(E,T) to be:

$$K(E,T) = a^n\ (1-a)^s \frac{(n+s-1)!}{n!\ (s-1)!} \qquad (4)$$

where $a = e^{(-h<v>/kT)}$.

In the present development, a collisional efficiency β has been applied to modify the traditional but incorrect strong-collision assumption that $k_{deexc} = Z\ [M]$, where Z is the hard sphere collision frequency rate constant. The strong-collision assumption implies that any collision between A^* and M would have to remove all the excess energy from A^*. Note that any species included as M would have to accommodate this energy content, regardless of its capacity for accepting the energy. Analyzing collisional energy transfer for master-equation methods, Troe (1977)[31] fit most of the temperature dependence of β with the equation:

$$\frac{\beta}{1-(\beta)^{1/2}} = \frac{-\langle \Delta E_{coll} \rangle}{F(E)\ k\ T} \qquad (5)$$

where $< E_{coll}>$ is the average amount of energy transferred per collision and F(E) is a factor, weakly dependent on energy, that is related to the number of excited states. Considering the temperature range of 300-2500 ^{o}K for a series of reactions; F(E) = 1.15 was observed as a median value. The value of β depends on the specific third-body molecule M through the value of $\langle \Delta E_{coll} \rangle$.

3.7.2 Bimolecular QRRK Equations

The bimolecular QRRK equations follow (Dean, 1985)[30] from unimolecular QRRK and the definition of the chemical activation distribution function. Consider recombination or addition to occur via the sequence:

$$R + R' \underset{k_{-1}(E)}{\overset{k_1\ f(E,T)}{\rightleftharpoons}} [RR']^* \xrightarrow{k_2(E)} P + P'$$

$$[RR']^* \xrightarrow{\beta k_s[M]} A$$

Here R is a radical, R' is a radical (recombination) or unsaturated molecule (addition), $[RR']^*$ is the energized complex which can either dissociate or be collisionally stabilized, β is the collisional deactivation efficiency,

and ks is the collisional rate constant for stabilization. k_1 is the high-pressure-limit rate constant for forming adduct and f(E,T) is the energy distribution for chemical activation:

$$f(E,T) = \frac{k_1(E)\ K(E,T)}{k_{-1}(E)\ K(E,T)} \qquad (6)$$

where K(E,T) is the QRRK thermal distribution from Eq. 4. Rate constants $k_{-1}(E)$ and $k_2(E)$ are calculated from the QRRK equation for $k_{rxn}(E)$ (Eq.3) using $m_{-1}(E_{-1}/h\langle v\rangle)$ and $m_2(E_2/h\langle v\rangle)$, respectively.

To obtain the bimolecular rate constant for a particular product channel, a pseudosteady-state analysis is made on the chemically activated adduct as before. The rate constant for forming the stabilized addition product [RR'] from R + R' is:

$$k_{stab} = \frac{d[RR']/dt}{[R][R']} = \beta\ k_s[M]\ \frac{k_1\ f(E,T)}{\beta\ k_s[M] + k_{-1}(E) + k_2(E)} \qquad (7)$$

and, for forming the addition/decomposition product (displacement reaction) P + P':

$$k_{dec} = \frac{d[Prod]/dt}{[R][R']} = k_2(E)\ \frac{k_1\ f(E,T)}{\beta\ k_s[M] + k_{-1}(E) + k_2(E)} \qquad (8)$$

If more decomposition channels are available, the $k_{rxn}(E)$ for each channel is added in the denominator of Eqs.7 and 8, and an equation in the form of Eq.8 is written for each additional channel, substituting the respective $k_{rxn}(E)$ for $k_2(E)$ as the multiplier term.

3.7.3 Low- and High-Pressure Limits

The low-pressure and high-pressure limits for these channels may be derived from Eqs. 7 and 8. As pressure changes, the rate constants change because of the relative magnitudes of terms in the denominator, $\beta k_s[M]$ vs. $k_{-1}(E)$ and $k_2(E)$.

The low-pressure limit for addition/stabilization (or recombination) is derived from Eq.7 to be

$$\lim_{M \to 0} k_{stab} = [M]\ \beta\ k_s \frac{k_1\ f(E,T)}{k_{-1}(E) + k_2(E)} \qquad (9)$$

sometimes written as [M]*ko (as a termolecular reaction), and the high-pressure limit reduces properly to k_1. At a given temperature, the fall-off curve for stabilization can be plotted as log(kstab) vs. log(P) or log(M).

Note the presence of $k_2(E)$ in Eq.9. If chemically activated conversion of $[RR']^*$ is more rapid than decomposition to reactants [$k_2(E) >> k_{-1}(E)$], then Eq.9 shows that ko_{stab} will be divided by $k_2(E)$ rather than by $k_{-1}(E)$. Thus, ignoring the chemically activated pathway could give incorrect rate constants for "simple" addition.

Similar analysis of Eq.8 implies that chemically activated decomposition has a fall-off curve that is the opposite of addition/stabilization, with a rate constant that is pressure-independent at low pressure and inversely proportional to pressure at high pressure. From Eq.8, the low-pressure limit for the chemically activated pathway to P and P' will be

$$\lim_{M \to 0} k_{dec} = k_1 \frac{k_2(E)\ f(E,T)}{k_{-1}(E) + k_2(E)} \qquad (10)$$

and the high-pressure limit will be

$$\lim_{M \to 0} k_{dec} = \frac{1}{[M]} \frac{k_1}{\beta\ k_s}\ k_2(E)\ f(E,T) \qquad (11)$$

with an inverse pressure dependence. While this result goes against past intuition about low- and high- pressure limits, it is a natural consequence of physics when chemically activated reaction are recognized as possibilities. One consequence is that a reaction of the form A + B ---> C + D with a rate constant measured to be pressure-independent may be proceeding via the described addition/elimination pathway, and show a pressure dependency at some point.

3.8 Computer Codes Used to Develop the Model

3.8.1 CHEMACT[32]

CHEMACT is a computer code that used the QRRK treatment of chemical activation reactions to estimate apparent bimolecular rate constants for various channels that can results in addition, recombination, and insertion reactions. Since these rate constants depend on both pressure and temperature, it is important that user includes the appropriate expression for specific pressure of interest in the modeling calculation.

General sources of input data for CHEMACT:

1. thermodynamic parameters: enthalpy (H_f), entropy (S), and heat capacities (C_p) as a function of temperature for reactants, adducts and products are important for accurate results.

2. molecular parameters describing the size, collisional energy transfer and energy levels of the adduct formed by the initial reaction are also needed. These in clude the mass, number of vibrational modes of the adduct, Lennard-Jones parameters and geometric mean frequency.

3. The bath gas molecule collision diameter, well depth and average energy transferred are needed.

4. High pressure limit rate constants for adduct formation and various isomerization and dissociation product channels of the adduct are also needed.

3.8.2 DISSOC

Fall-off corrections for regular unimolecular decomposition reactions were made by the unimolecular Quantum RRK method.[33] DISSOC computer code analyzed unimolecular reaction with QRRK analysis for proper treatment of fall-off dependency and estimate apparent unimolecular dissociation rate constants for various unimolecular dissociation channels. Same input data with CHEMACT computer code is required to run DISSOC program.

3.8.3 THERM[34]

THERM is a computer code which can be used to estimate, edit, or enter thermodynamic property data for gas phase radicals and molecules using Benson's group additivity method.[27] All group contributions considered for a species was recorded and thermodynamic properties are generated in NASA polynomial format in addition to listing more convenient for thermodynamic, kinetic, and equilibrium calculation.

3.8.4 CPFIT[32]

CPFIT is a computer code that determine geometric mean frequency. It accepts input in the form of heat capacities versus temperature to 1000 ^{o}K in addition to the number of vibrational modes and the number of internal rotors in the molecule.

CHAPTER 4
EXPERIMENTAL METHOD

The thermal reaction of chlorobenzene in hydrogen and oxygen mixtures has been studied in 10.5 mm i.d. tubular flow quartz reactor at one atmosphere pressure. A diagram of the experimental system is shown in Figure 4. The experimental conditions of the pyrolysis and oxidation of chlorobenzene are listed below:

1. Reactor Diameter: 10.5 mm
2. Effective Reactor Length: 39 cm
3. Reactor Temperature (^{o}C):

   590, 600, 610, 620, 630, 640
4. Reactant Ratio:

   CLBZ : O_2 : H_2 = 0.37 : 98.64 : 0.99

   CLBZ : O_2 : H_2 = 0.37 : 97.68 : 1.95

   CLBZ : O_2 : H_2 = 0.37 : 96.73 : 2.90

   CLBZ : O_2 : H_2 = 0.37 : 95.80 : 3.83

   CLBZ : O_2 : H_2 = 0.37 : 94.89 : 4.74
5. Residence Time (sec): 0.3--2.0
6. Operating Pressure: 1 atm

As carrier gas, hydrogen was passed through three saturators, two of which contained chlorobenzene. The third one, with no chlorobenzene in it, was used only for condensation. The saturators are held at $0^{o}C$ to insure complete saturation and keep constant initial mole fraction for all experimental conditions.

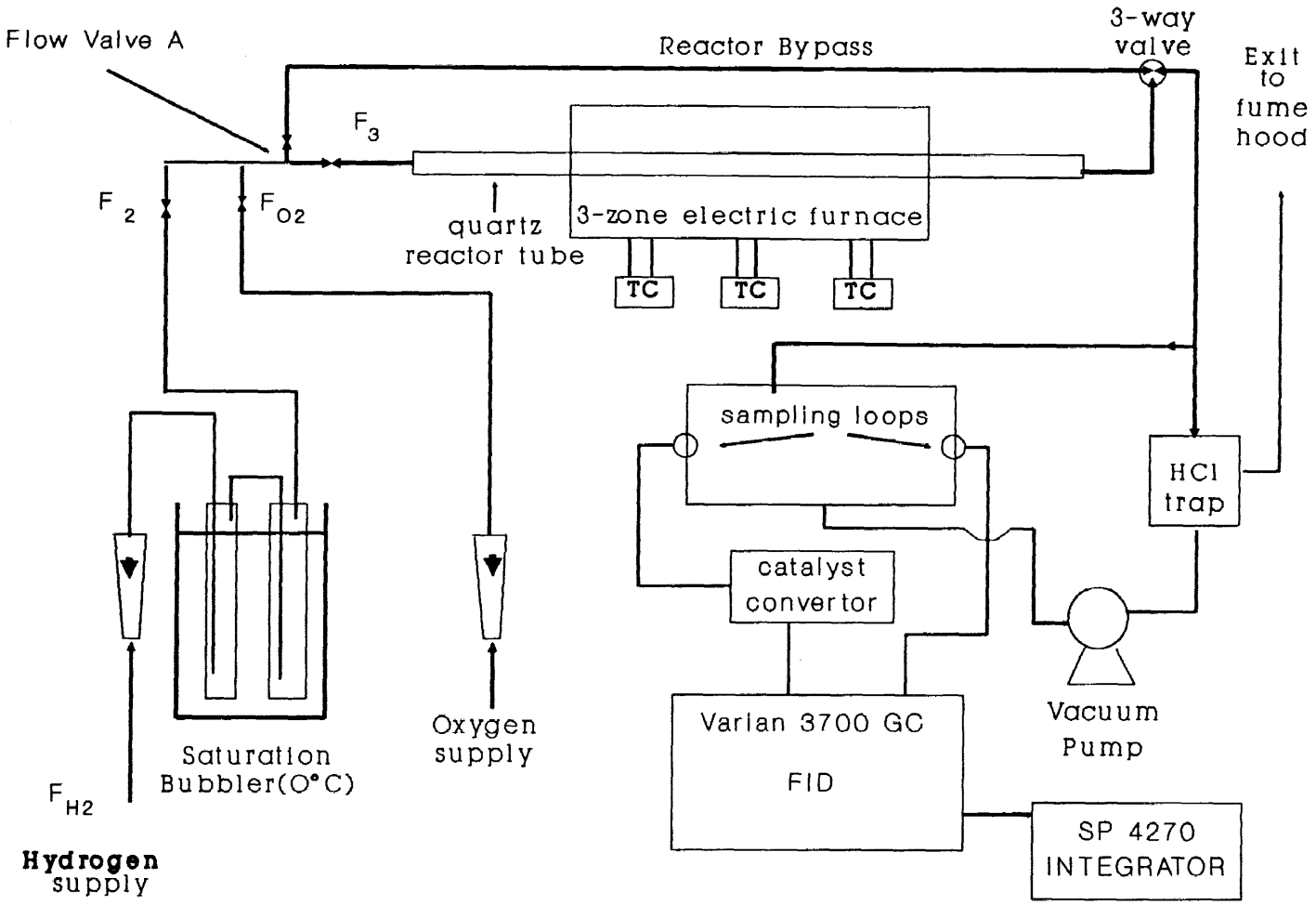

Figure 4. Experimental system

The thermal decomposition products of chlorobenzene were analyzed systematically by varying the temperature, oxygen and hydrogen ratio, and residence time. The temperature ranged from 590 to 660°C. The O_2/H_2 ranged from one percent to five percent. The residence time ranged from 0.3 to 2.0 seconds.

During the experiment, the mixture of chlorobenzene, oxygen, and hydrogen was passed through either to the bypass line or the reactor by changing the flow valve A (Figure 4). It was necessary to monitor the variance of input concentration of the mixture. The mixture was preheated to above 200°C before entering the reaction zone of the reactor to improve isothermal temperature control. All transfer lines to GC and HCl trap was heated about 90°C to limit condensation. The reactor effluent gas passed through heated transfer lines to the GC analyzers. The bulk of the effluent was passed through a sodium-bicarbonate flask before being released into a fume hood.

4.1 Temperature Control and Measurement

Tight temperature control for the flow reactor was required to obtain isothermal reaction condition. The 10.5 mm i.d. quartz reactor was housed within a three-zone furnace (46 cm length) which was controlled independently by three temperature controllers (Omega Engineering, Inc., Stamford, CT).

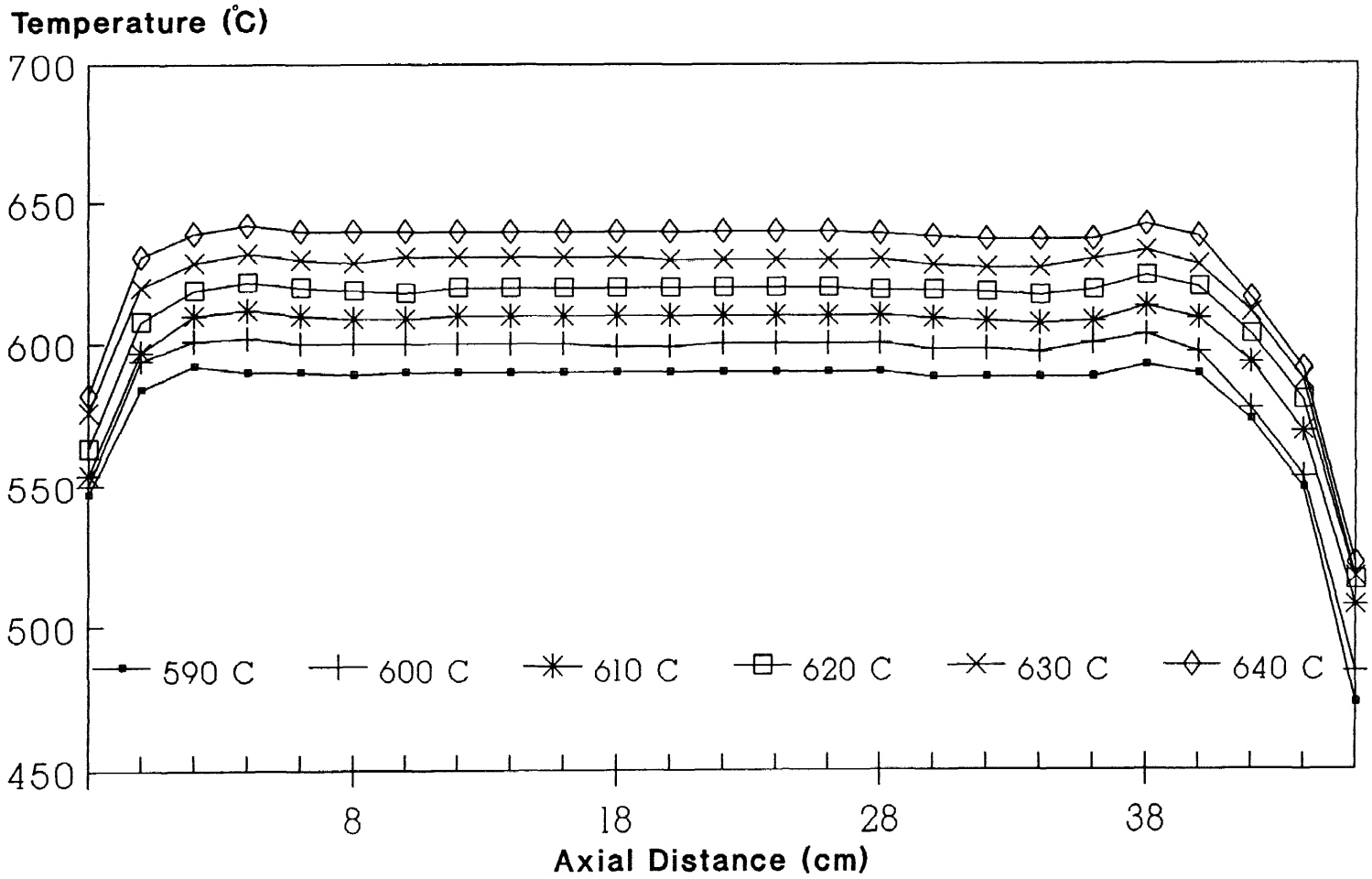

Figure 4.1.1 Temperature Profiles

Residence Time = 1.0 sec

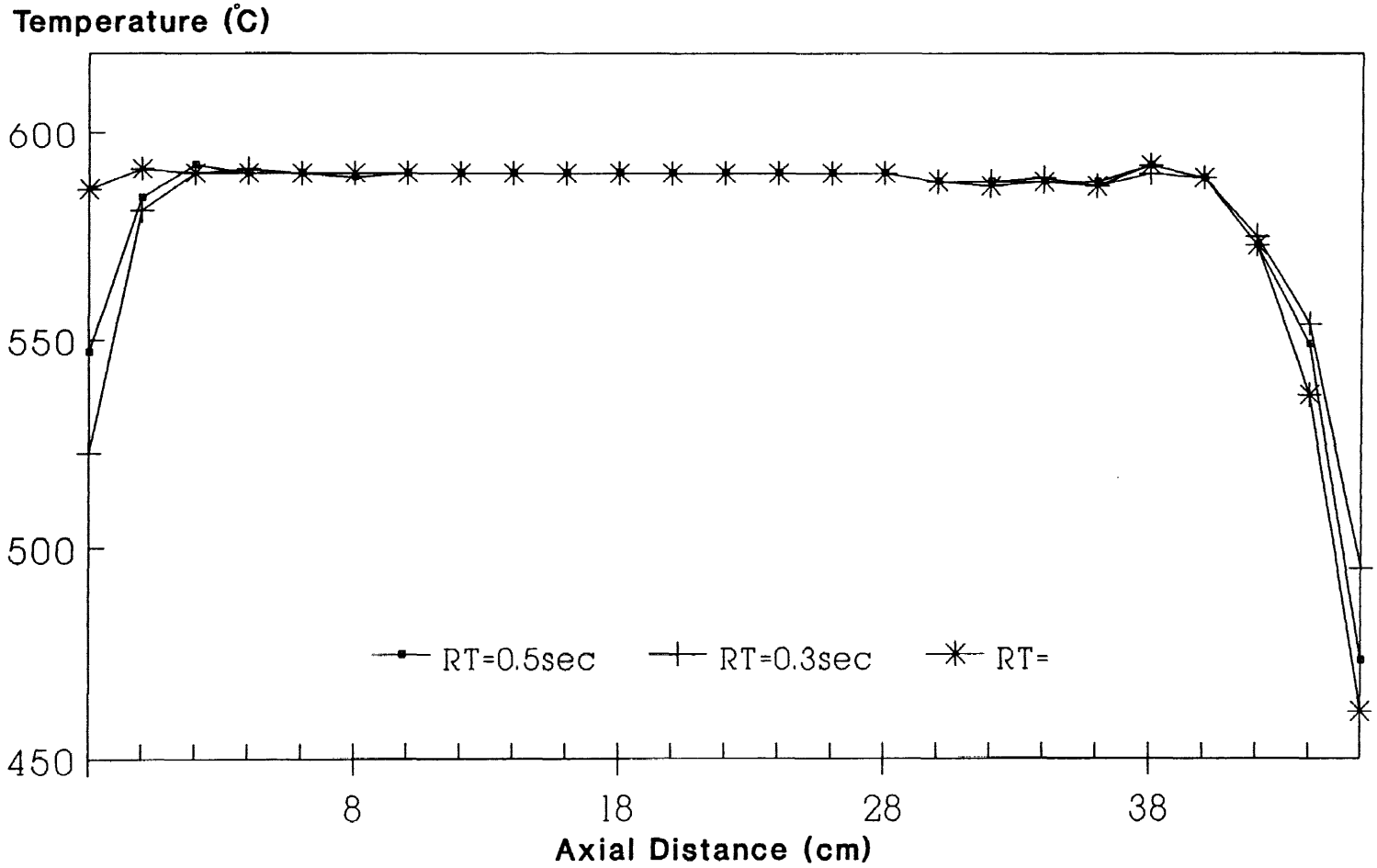

Figure 4.1.2 Temperature Profiles
590 °C with Different Residence Times

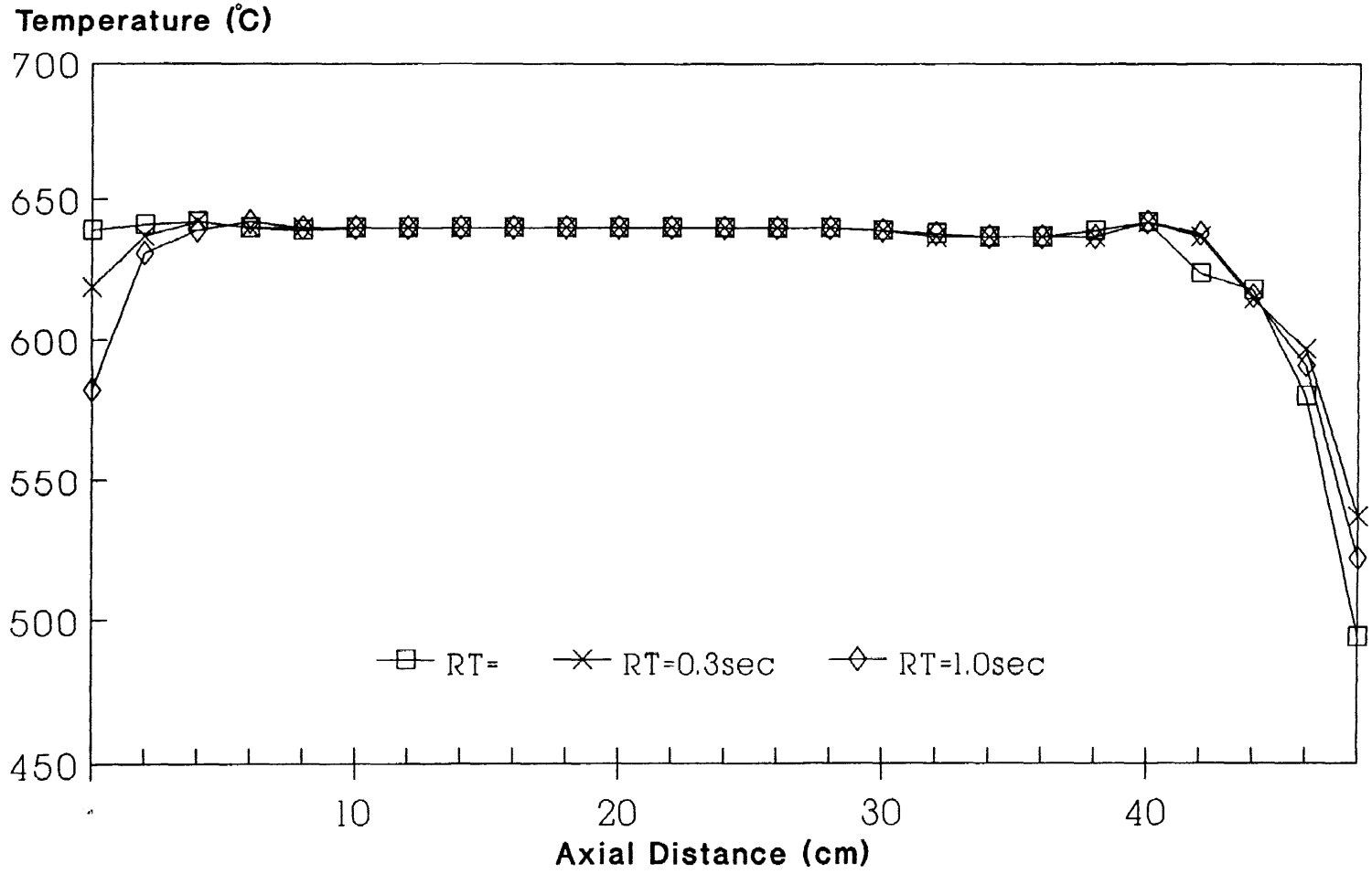

Figure 4.1.3 Temperature Profiles
640 °C with Different Residence Times

The temperature measurements were performed with varied flow rates of hydrogen. The actual temperature profile of the reactor was obtained using type K thermocouple probe moved coaxially within the reactor. The temperature profiles are shown in Figure 4.1.1 to Figure 4.1.3. They show that the temperature variation was less than 0.6% over the central zone of the reactor. The temperature profiles also shown that the length of isothermal range of the reactor is 36.75cm.

4.2A Determination of Residence Time

Different residence times can be achieved by changing flow rate through the reactor. Because the amount of chlorobenzene in F_2 (Figure 4) can be maintained in same mole fraction (0.37%), the total flow rate F_3 can be described as:

$F_3 = F_{O2} + F_2$

where F_{O2} is oxygen flow rate

$F_2 = F_{H2} + F_{CLBZ} = F_{H2} + F_2 * 0.0037$

then $F_2 = F_{H2}/(1-0.0037)$

so, $F_3 = F_{O2} + F_{H2}/(1-0.0037)$

here F_3 is the flow rate in room temperature, and it should be converted to the temperature of the reactor F_3': $F_3'/F_3 = T_{reactor}/298$

because we know the isothermal volumn (V) of the reactor, residence time can be determined by:

Residence Time = V/F_3'

4.2B Kinetic Analysis

A comparison of the kinetic values found by plug flow analysis with values obtained by applying both the numerical and analytical solution of the continuity equation for first order kinetics with laminar flow was presented by Chang and Bozzelli[35]. the study showed that the plug flow assumption for our experimental system is accurate within 5% to 7% for all temperature range (590 - 640^{o}C) and residence time ranged from 0.3 second to 2.0 seconds.

4.3 Quantitative Analysis of Reaction Products

Quantitative analysis of reaction products was performed using a on-line Varian 3700 gas chromatography (GC) equipped with two flame ionization detectors (FID). Channel A was used to analyze heavy (C_6 - C_7) hydrocarbon while channel B analyzed light (C_1 - C_2) hydrocarbons.

Two GC columns, both 1.2 m in length by 0.32 cm o.d., were used to separate reaction products. Column A packed with 1% Alltech AT-1000 to separate heavy compounds, and column B packed with Carbosphere to separate light hydrocarbon.

Two six-port gas sample valves (Valco Instrument Co.) were used to inlet a fraction of reactor effluent into the GC. Both of them were maintained at 170^{o}C. Channel A used a 1.0 ml sampling loop, and channel B used a 0.5 ml loop.

A catalytic convertor which contained 5% Ruthenium on Alumina and was heated to 300^{o}C with a constant hydrogen

flow (15.5 ml/min) was placed between column B effluent and FID B. CO and CO_2 separated by column B was then reacted with H_2 in the convertor to form CH_4 which is readily detectable by the FID B.

Calibration of the flame ionization detectors was done by injection of known concentrations of compounds to obtain appropriate molar response factors. For column A, known concentrations of Benzene and Toluene were obtained using a saturation bubbler. For column B, gas standards (Scott Specialty Gases, Plumsteadville, PA), which contained CO, CO_2, CH_4, C_2H_2, C_2H_4, and C_2H_6, were analyzed. The relative response factor was determined for each compound as shown in Table 4.3.1 and Table 4.3.2. Based on these response factors, the specific compound peak area from sample analysis was converted to the equivalent number of moles of each compound. Total error for the experimental system including variation in flow rates, temperature, and GC sampling was estimated around 15%. Typical integrator printout is shown in Figures 4.3.1 and 4.3.2.

4.4 Hydrochloric Acid Analysis

Quantitative analysis of HCl product was performed at all experimental conditions. The samples for HCl analysis were collected independently from GC sampling as shown on Figure 4. The effluent was bubbled through a two-stage bubbler. Each stage contained 10 ml of standardized

0.0083M NaOH. The gas passed through the two-stage bubbler until the first stage solution reached its phenolphthalein end point. The time required for this to occur was recorded. At this point, the bubbling was stopped, the aliquots were combined and titrated against standardized 0.0090M HCl until the end point was reached. HCl produced by reaction was then calculated since the concentration and flow rate was known.

Table 4.3.1 Relative Response Factor for channel A

Compound	Relative Response Factor
C_6H_5Cl	1.00
C_6H_6	1.22
$C_6H_5CH_3$	1.43

Table 4.3.2 Relative Response Factor for channel B

Compound	Relative Response Factor
CH_4	1.00
CO	0.92
CO_2	0.22
C_2H_2	1.33
$C2H_4$	1.70
C_2H_6	1.73

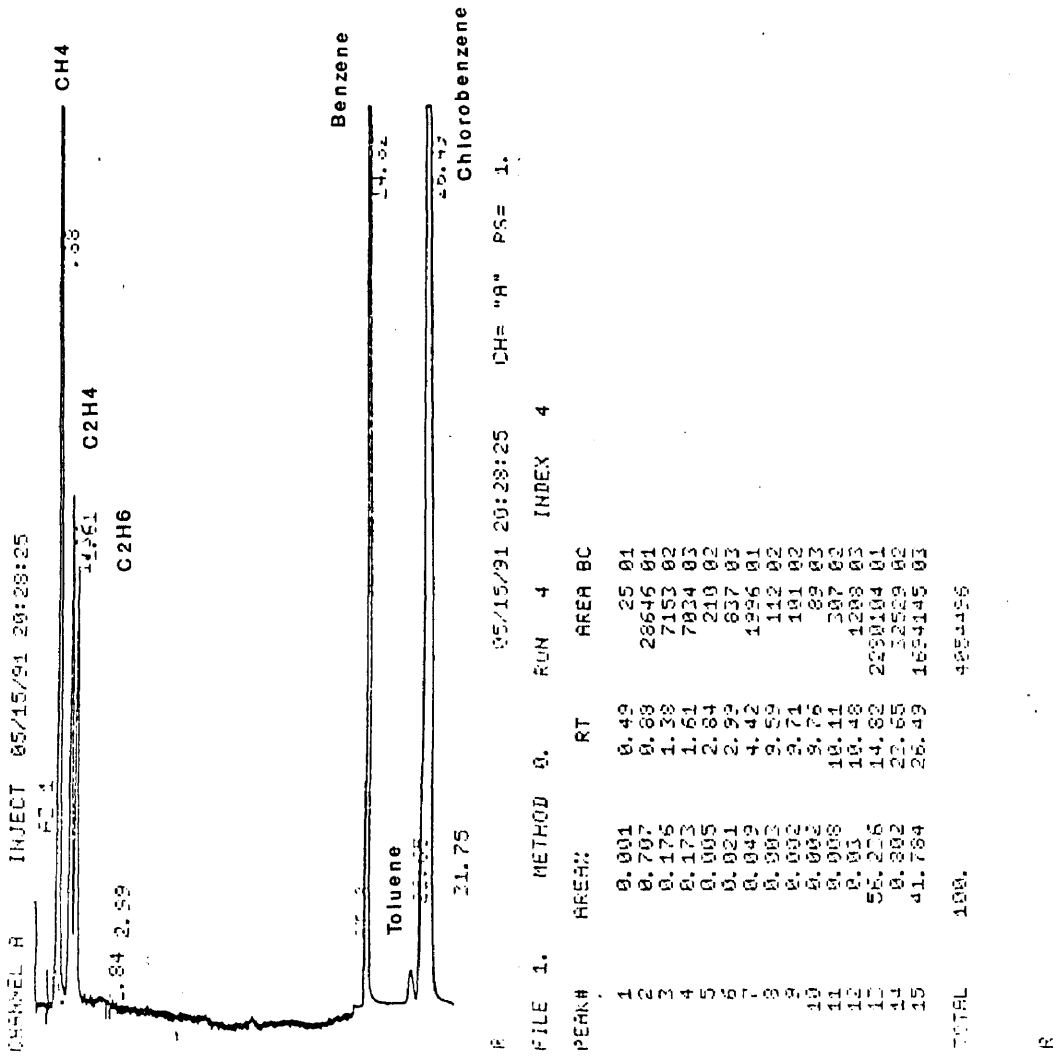

Figure 4.3.1 Column A Printout

Column A Condition:

Carrier Gas(He) Flow Rate:	14.0 ml/min
H_2 Flow Rate:	29.6 ml/min
Air Flow Rate:	335 ml/min
Injection Port Temp.:	170 ^{o}C
Detector Temp.:	220 ^{o}C
Sensitivity:	10^{-11} AMPS/MV
Attenuation:	1
Temp. Programming:	
initial temp.:	35 ^{o}C
hold:	3 min
program rate:	16 ^{o}C/min
final temp:	200 ^{o}C
hold:	19 min
Integrator Attenuation:	1
	8 after 12.5 min
Chart Speed:	0.5 cm
	0.1 cm after 12.5 min

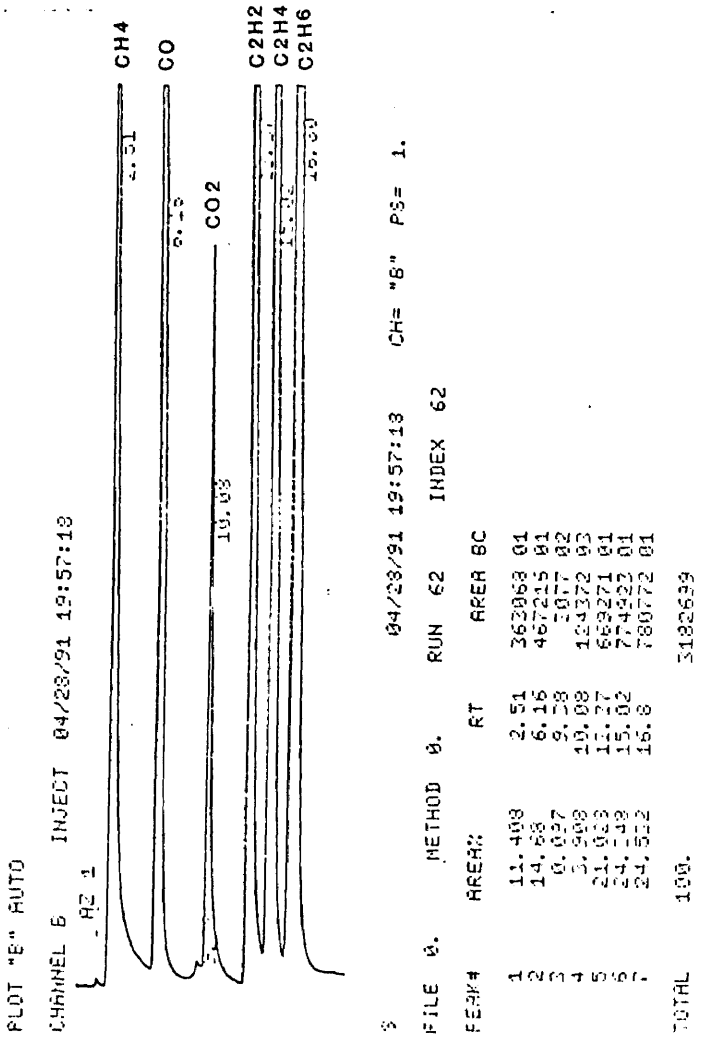

Figure 4.3.2 Column B Printout

Column B Condition:

Carrier Gas(He) Flow Rate: 32.6 ml/min
H_2 Flow Rate: 29.9 ml/min(convertor + makeup)
Air Flow Rate: 275 ml/min
Injection Port Temp.: 170 ^{o}C
Detector Temp.: 220 ^{o}C
Sensitivity: 10^{-11} AMPS/MV
Attenuation: 1
Temp. Programming:
initial temp.: 35 ^{o}C
hold: 2 min
program rate: 16 ^{o}C/min
final temp: 200 ^{o}C
hold: 19 min
Integrator Attenuation: 1

4.5 Qualitative Analysis of Reaction Products by Mass Spectrometry

The analysis of the reaction outlet gases was performed on a Finnigan 400 series GC/MS. Evacuated stainless steel sample cylinders were used for collection of gas samples at reactor exit. The sample was cryogenically focused using liquid nitrogen before injection.

CHAPTER 5
RESULTS AND DISCUSSION

5.1 Reaction of Chlorobenzene in Hydrogen and Oxygen Mixture

Experimental results on decomposition of chlorobenzene are shown in Figure 5.1.1 to Figure 5.1.11.

Figure 5.1.1 through Figure 5.1.6 show that the concentration of chlorobenzene consistently decreased with increasing residence time at a given temperature and that oxygen has a significant effect acceleration on the decomposition of chlorobenzene. Higher concentration of oxygen results in faster decay of C_6H_5Cl. Figure 5.1.7 to Figure 5.1.11 compare chlorobenzene decay as a function of temperature at different residence times. At constant residence time, increases in temperature consistently result in lower reactant concentrations, for the concentration of chlorobenzene.

95% decomposition of chlorobenzene first occurred at 620^{o}C, O_2/H_2 = 5%, and residence time = 2.0 sec (Fig.5.1.4). As the temperature rose, 95% decomposition occurred at shorter residence time (Fig. 5.1.5).

5.2 Products Distribution and Material Balance

Figure 5.2.1 through Figure 5.2.15 show the product distribution in three sets of data. At 0.5 sec residence time (Fig. 5.2.1 to Fig. 5.2.5), the complementary

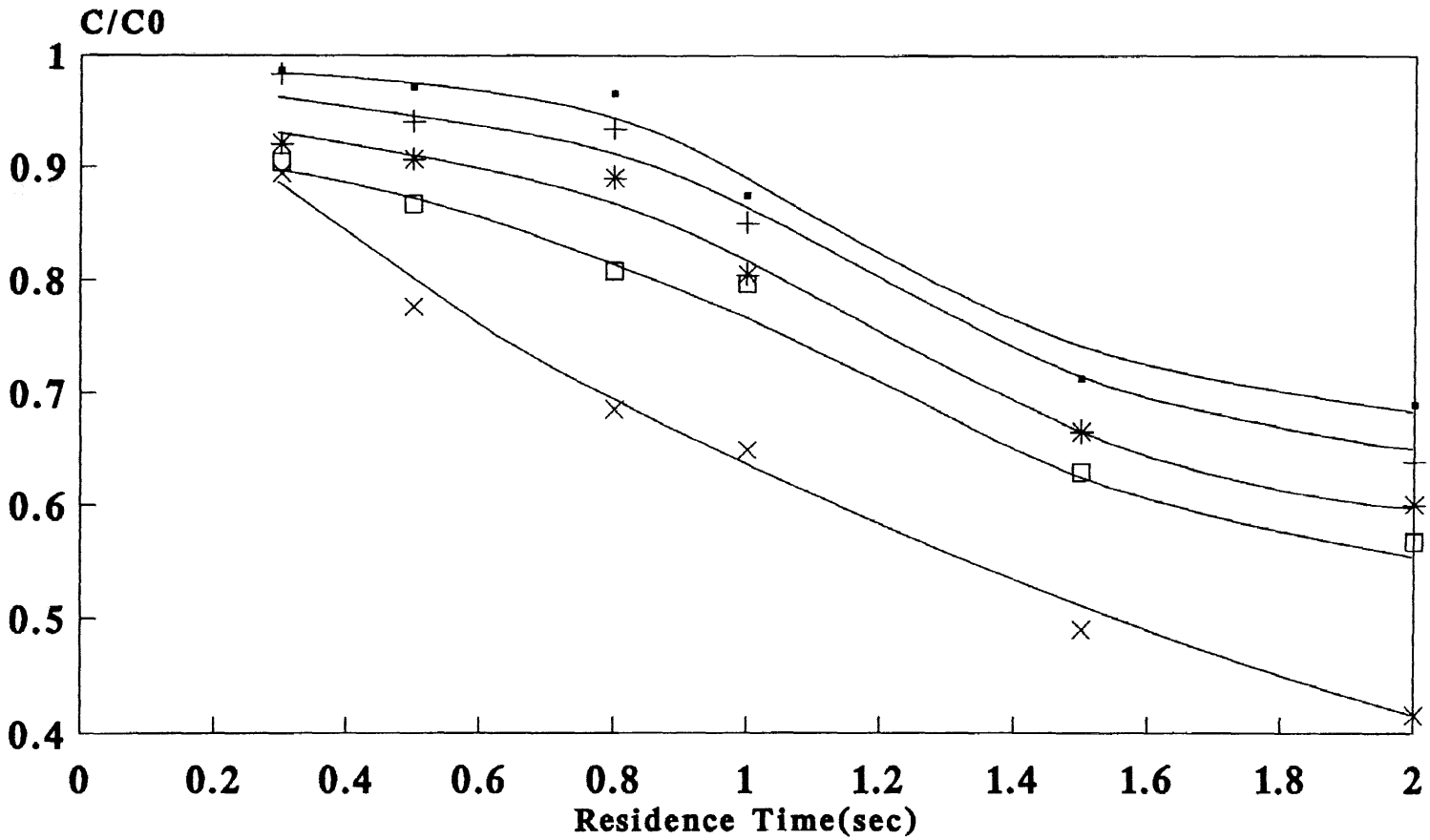

Figure 5.1.1 Decay of CLBZ in Different O2/H2 (590°C)

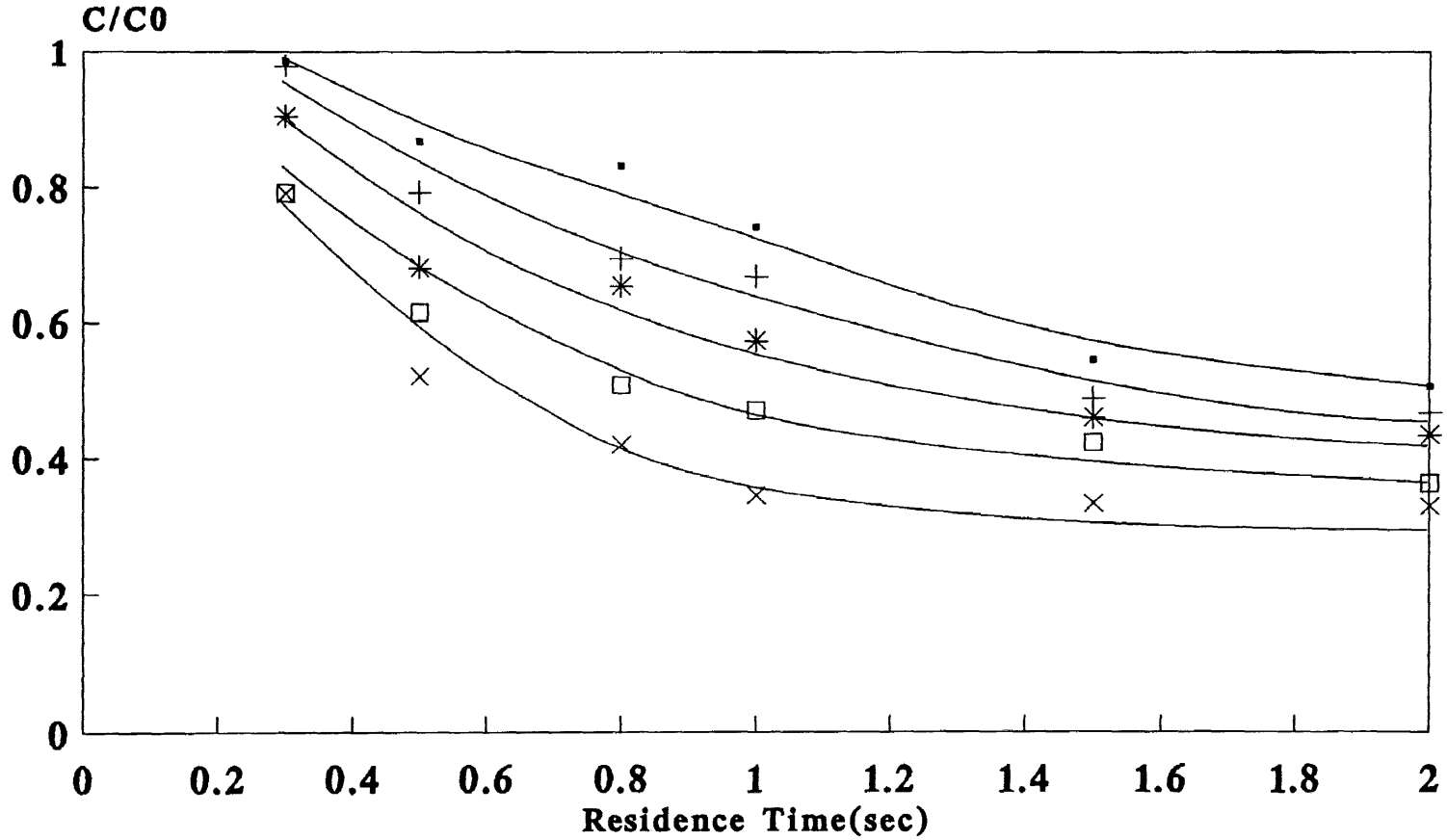

Figure 5.1.2 Decay of CLBZ in Different O2/H2 (600°C)

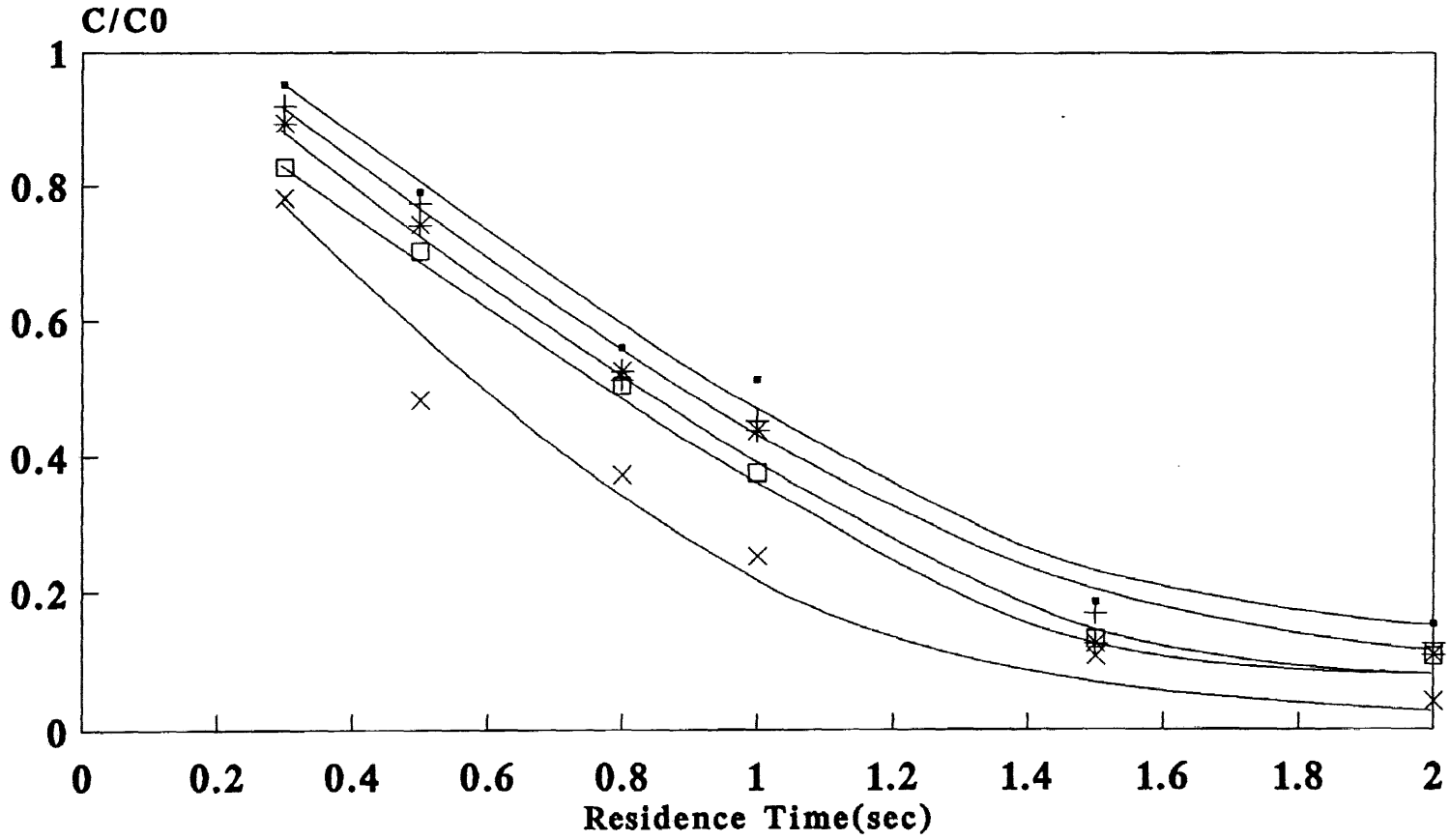

Figure 5.1.3 Decay of CLBZ in Different O2/H2 (610°C)

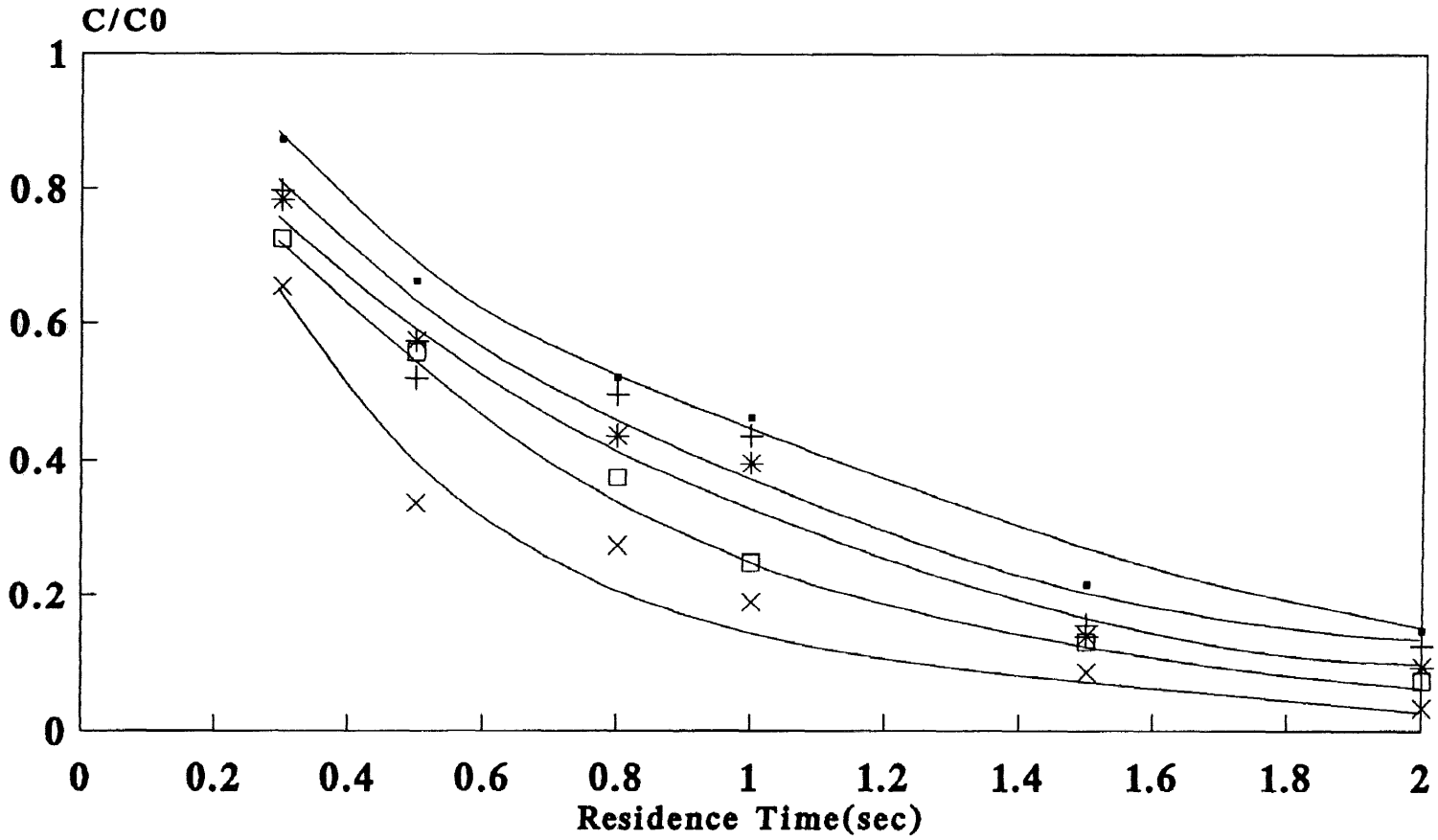

Figure 5.1.4 Decay of CLBZ in Different O2/H2 (620°C)

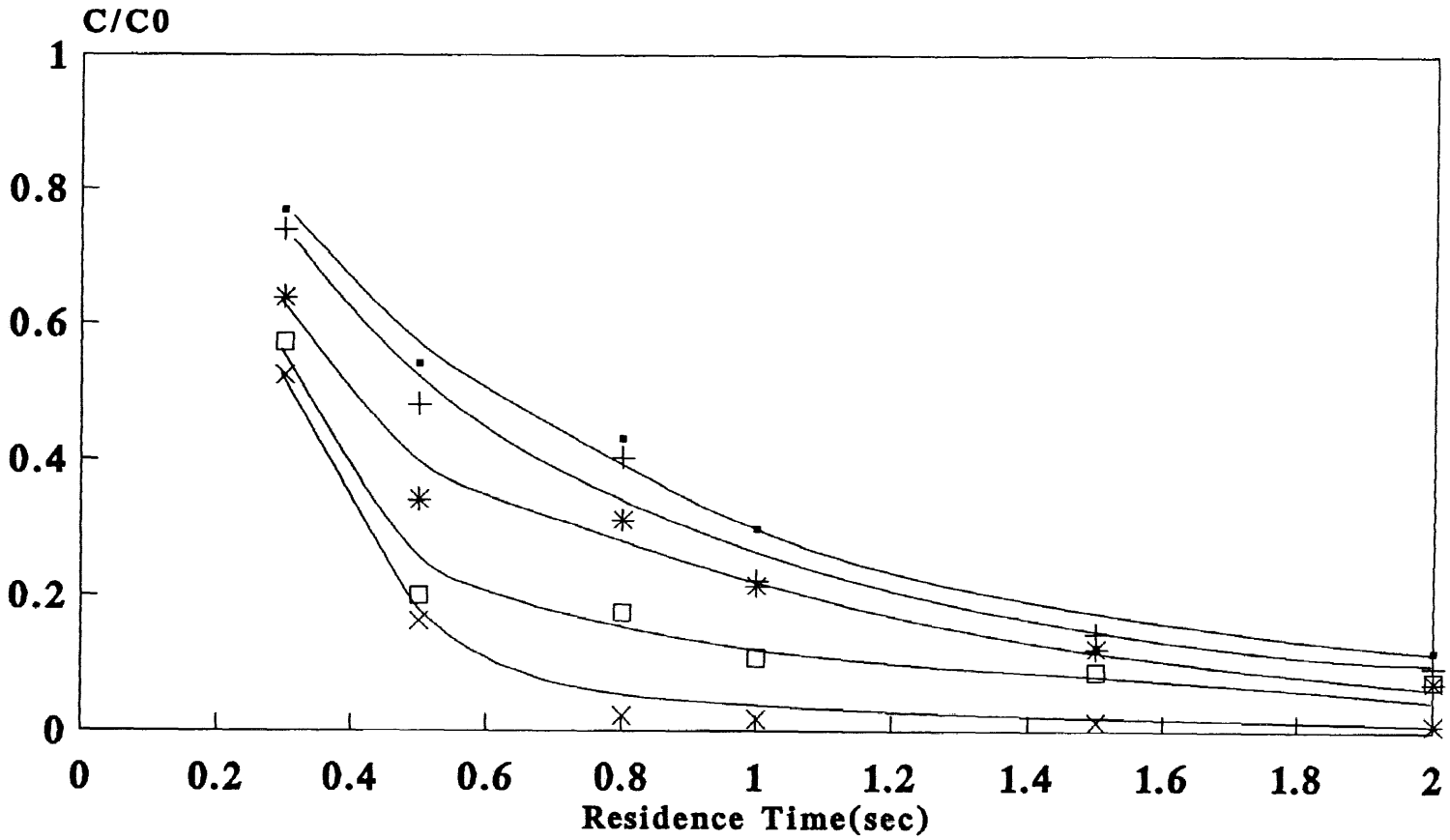

Figure 5.1.5 Decay of CLBZ in Different O2/H2 (630°C)

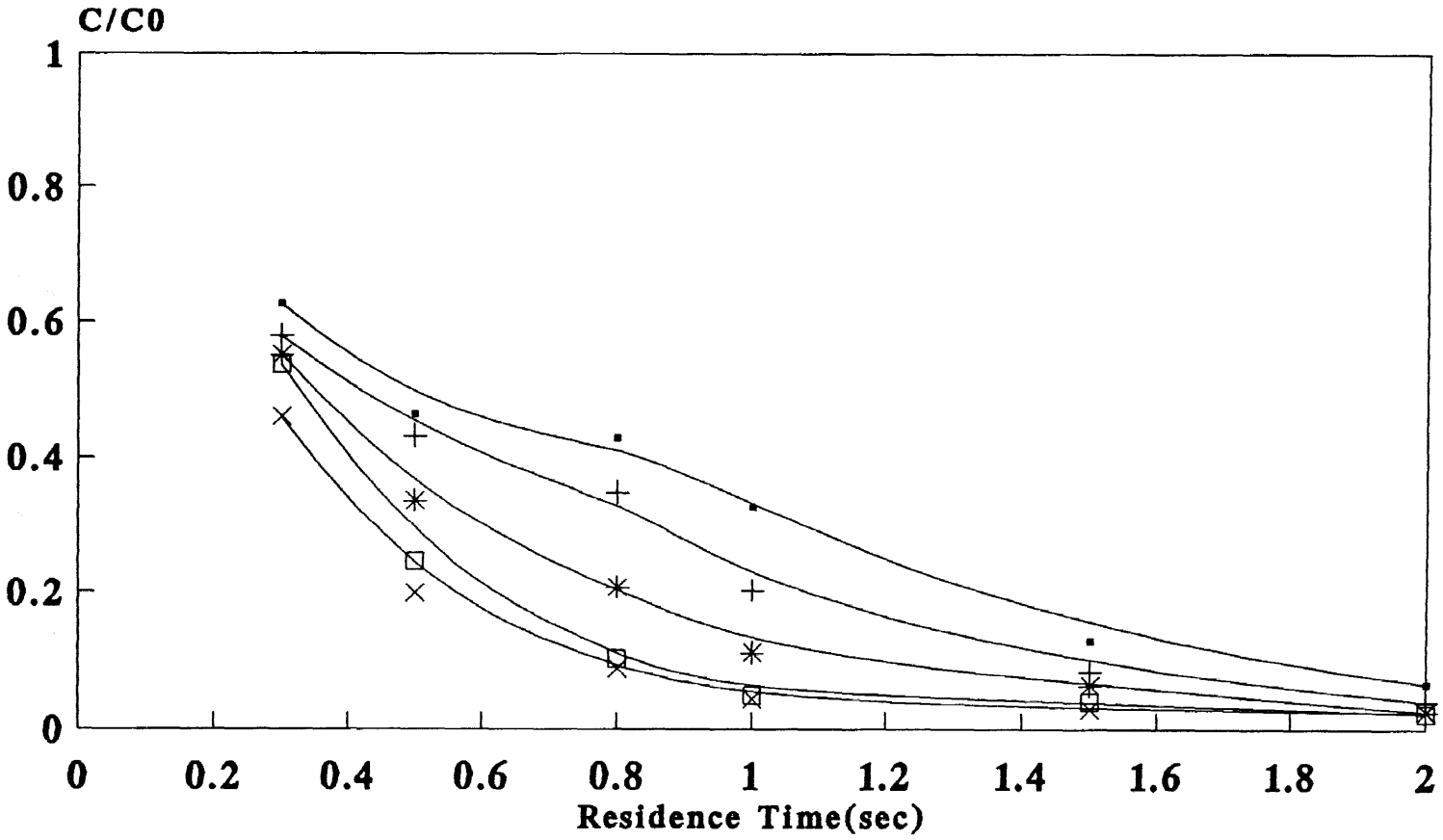

Figure 5.1.6 Decay of CLBZ in Different O2/H2 (640°C)

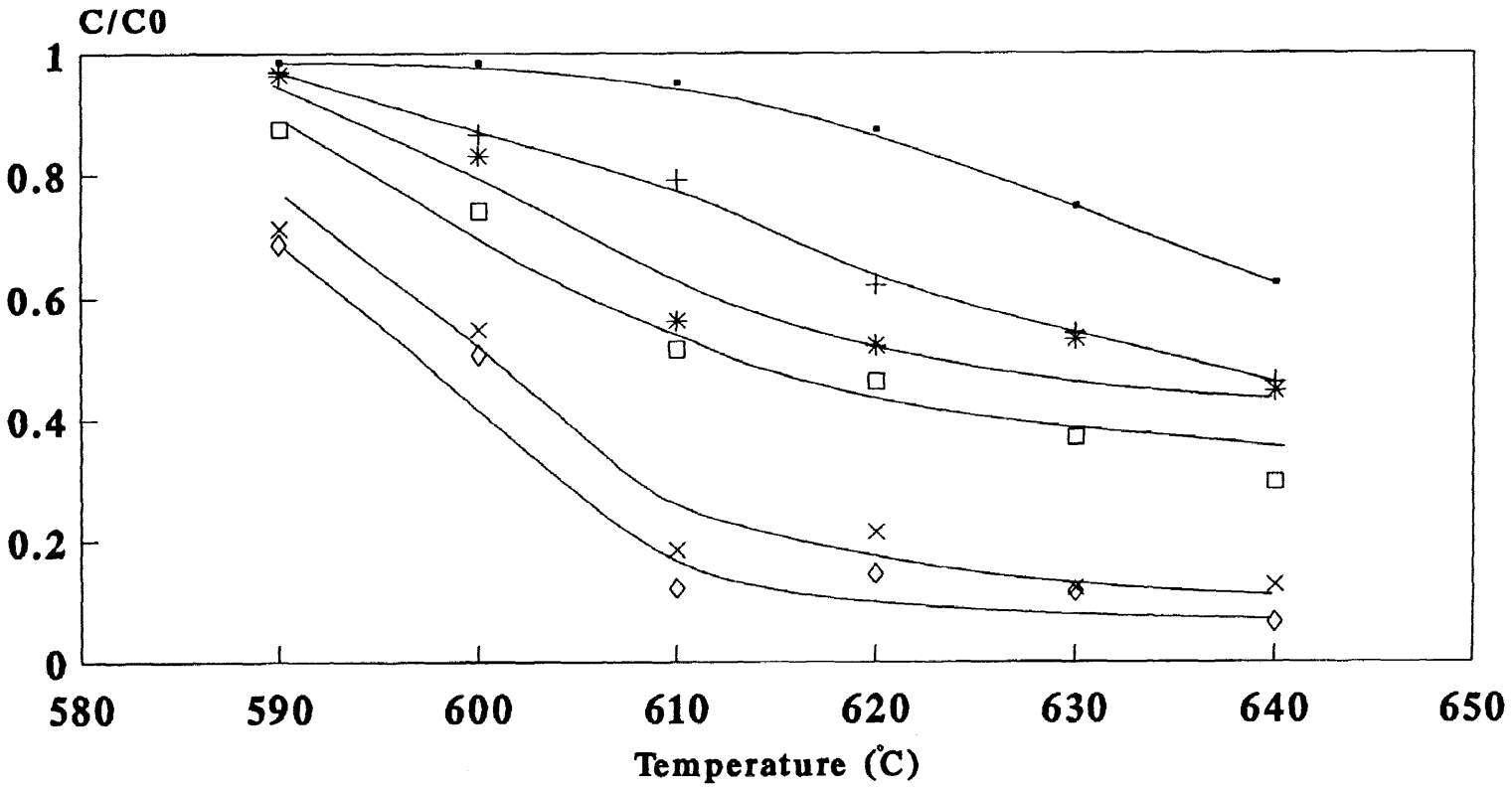

Figure 5.1.7 Decay of CLBZ vs Temperature, O2/H2=1%

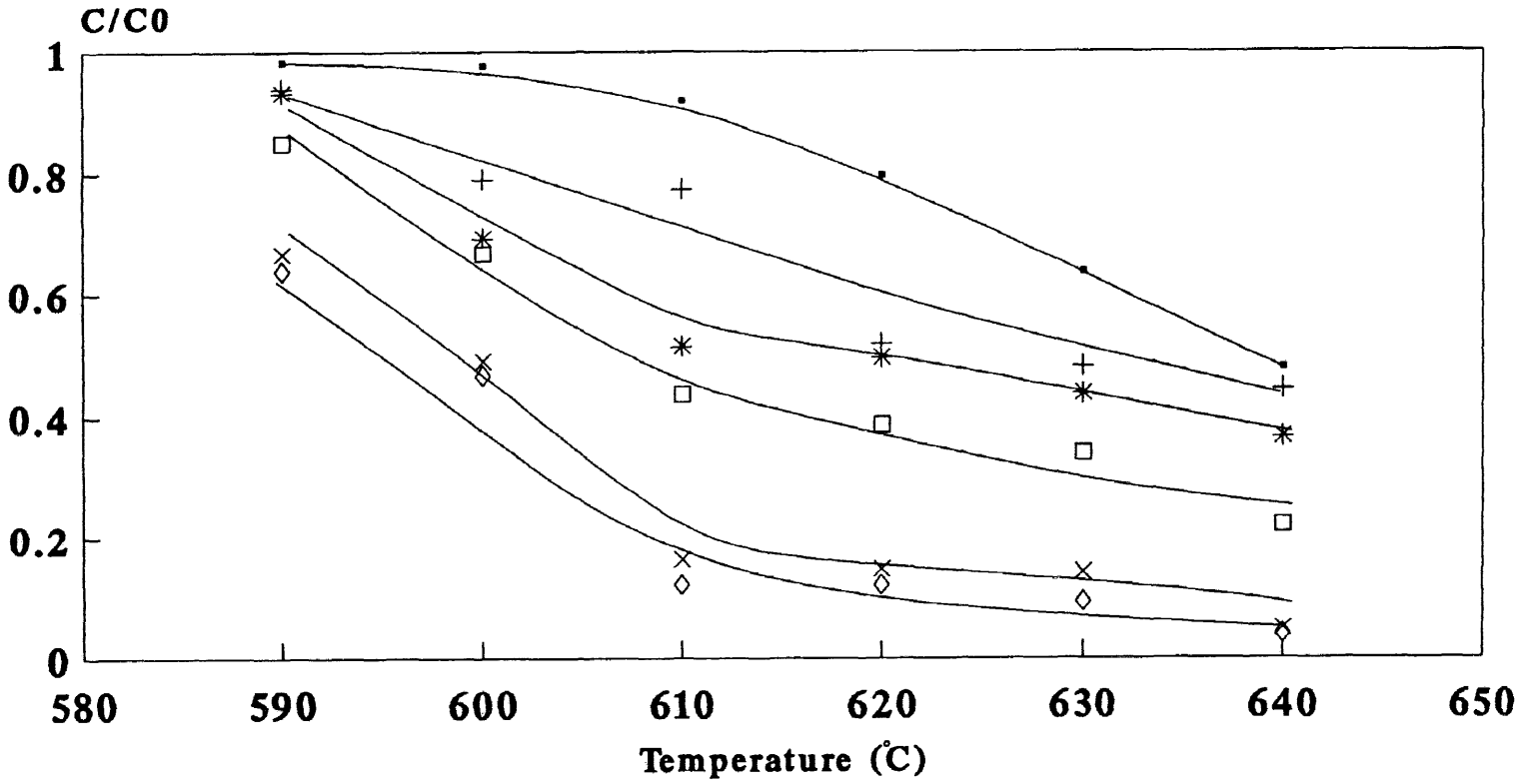

Figure 5.1.8 Decay of CLBZ vs Temperature, O2/H2=2%

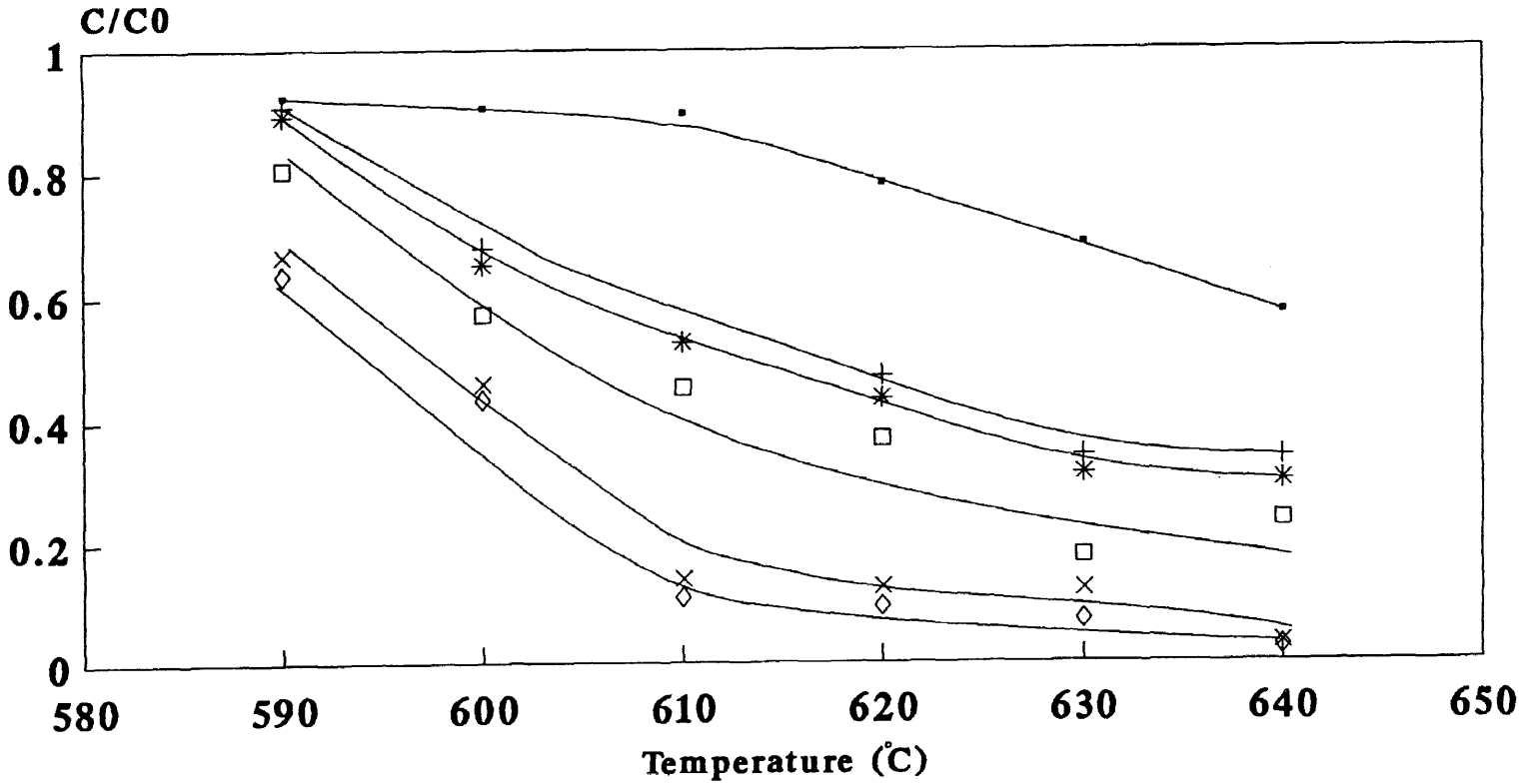

Figure 5.1.9 Decay of CLBZ vs Temperature, O2/H2=3%

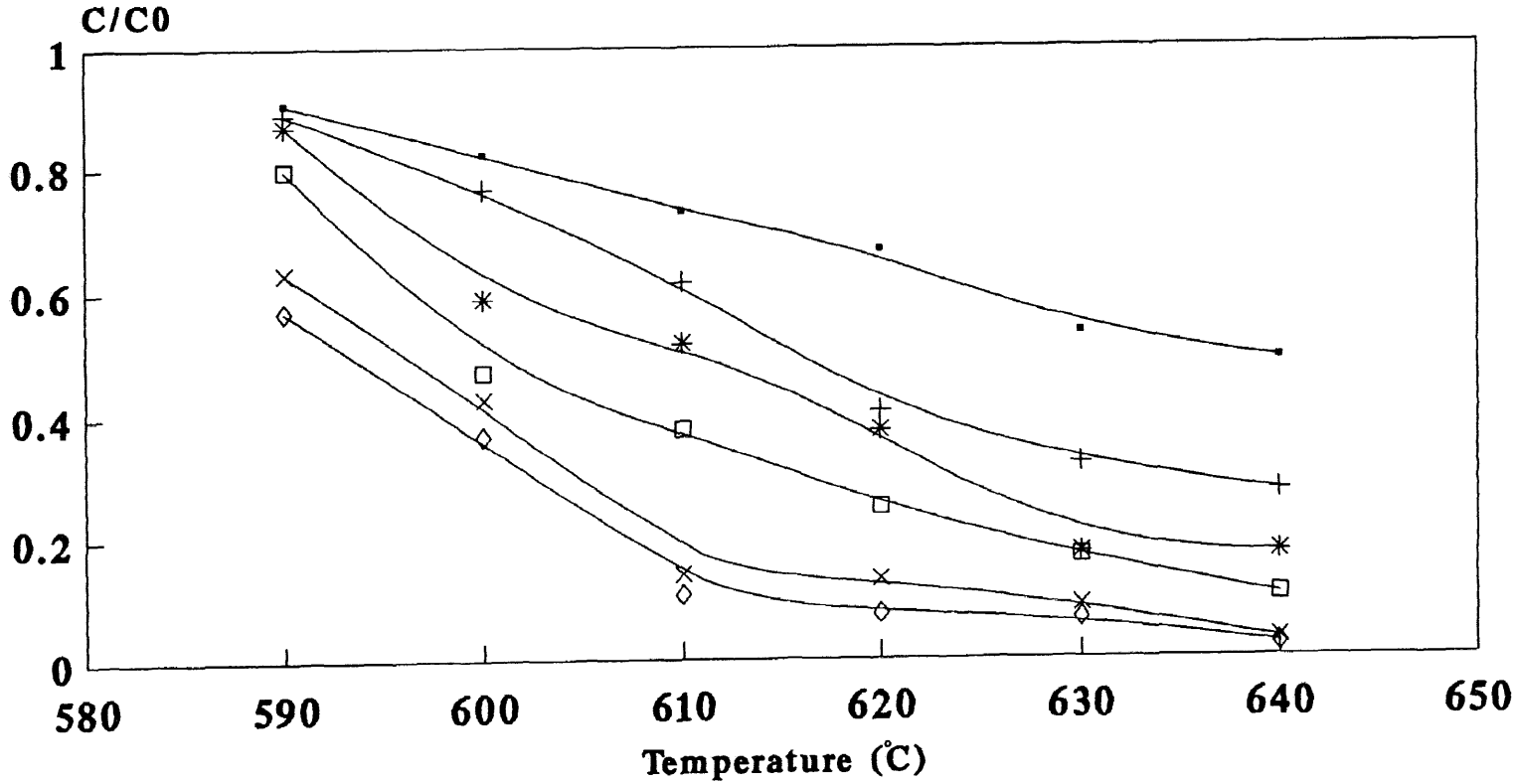

Figure 5.1.10 Decay of CLBZ vs Temperature, O2/H2=4%

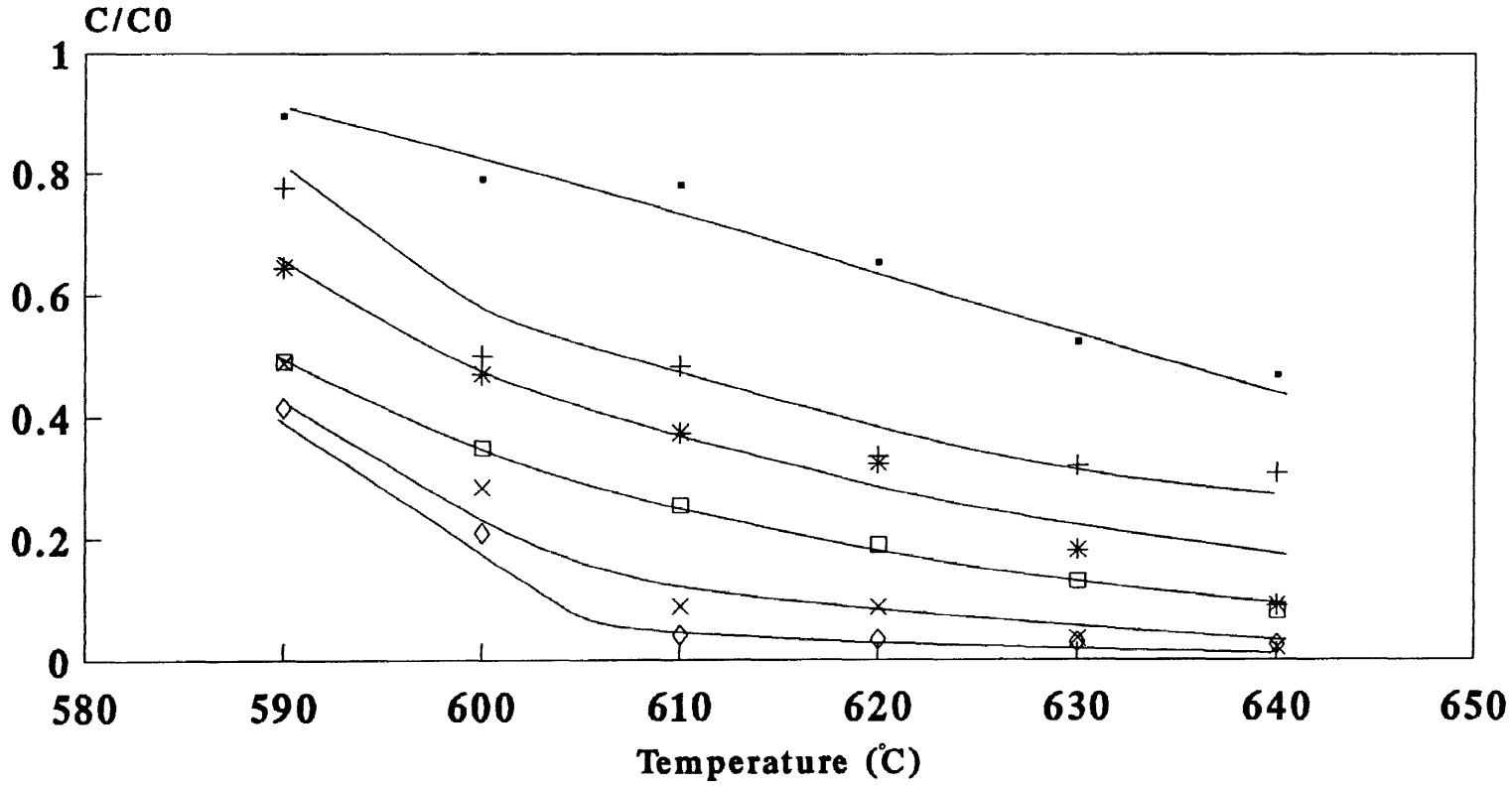

Figure 5.1.11 Decay of CLBZ vs Temperature, O2/H2=5%

relationship between chlorobenzene decomposition and benzene formation was very clear over this entire temperature range and for all oxygen to hydrogen ratios. At 1.0 sec residence time (Fig.5.2.6 to Fig. 5.2.10), the rate of benzene formation is shown to be slowed when the temperature is above 610^{o}C. Benzene decay now occurs above 640^{o}C, for the 5% O_2/H_2 condition. Benzene decomposition was observed clearly at 2.0 sec residence time (Fig. 5.2.11 to Fig. 5.2.15). Only 50% of the chlorobenzene was observed as benzene when 98% of chlorobenzene decomposed.

The normalized concentrations for carbon material balance at all temperature and oxygen to hydrogen ratios at 1.0 sec residence time, is listed in Table 5.2.1 to Table 5.2.5. Poor material balance is observed at higher oxygen to hydrogen ratio (5%) condition.

Minor products observed were CH_4, C_2H_2, C_2H_4 C_2H_6, toluene, CO and CO_2. All of the minor products increased in concentration consistently. As temperature and O_2 concentration increase, the concentration of CO and CO_2 also increase. The CO_2 concentration is always below CO concentration in all experimental conditions. Maximum CO concentration was observed under the experimental conditions of 640^{o}C, 5% oxygen to hydrogen ratio, and 2.0 sec residence time.

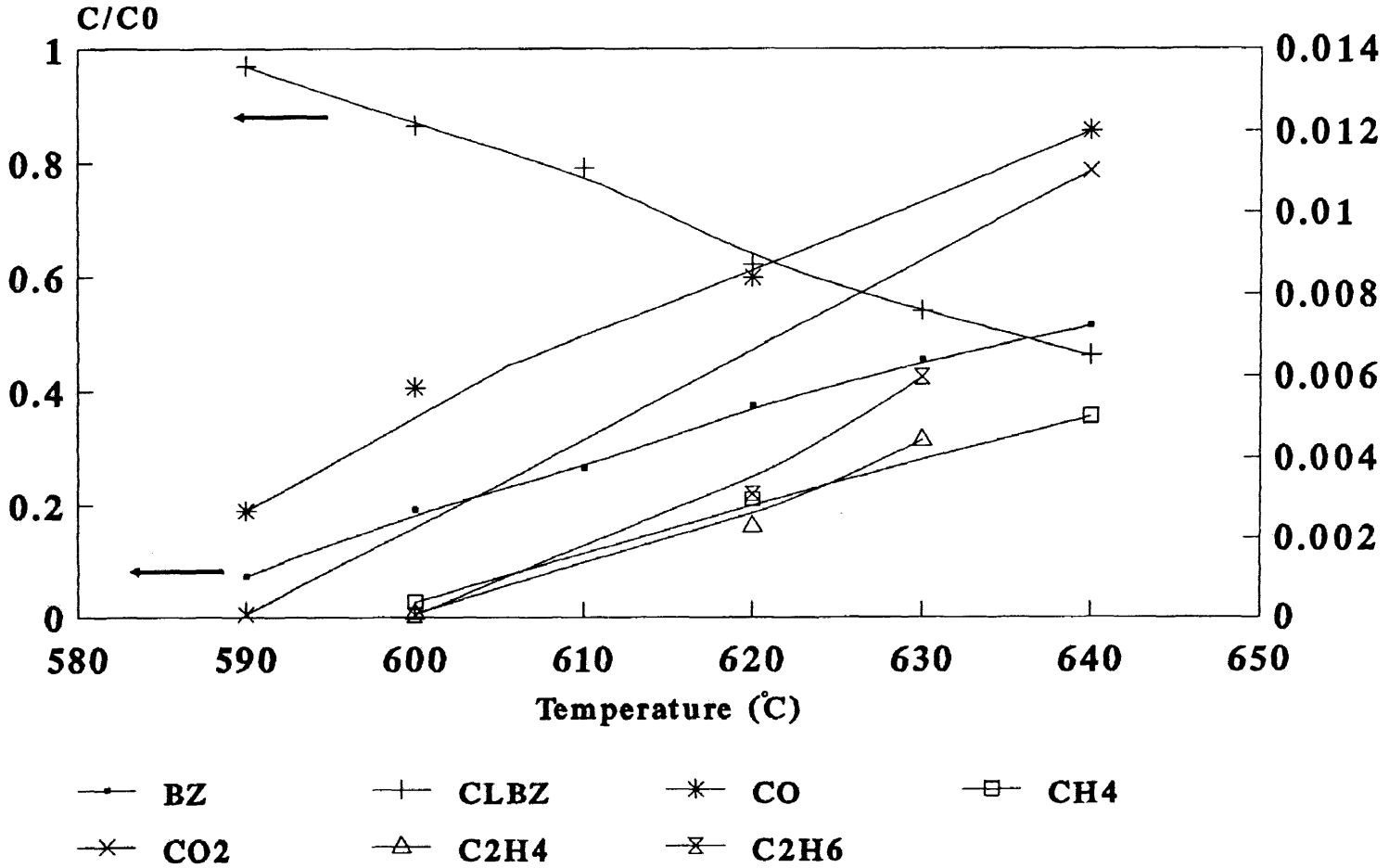

Figure 5.2.1 Product Distribution, O2/H2 = 1%, RT = 0.5sec

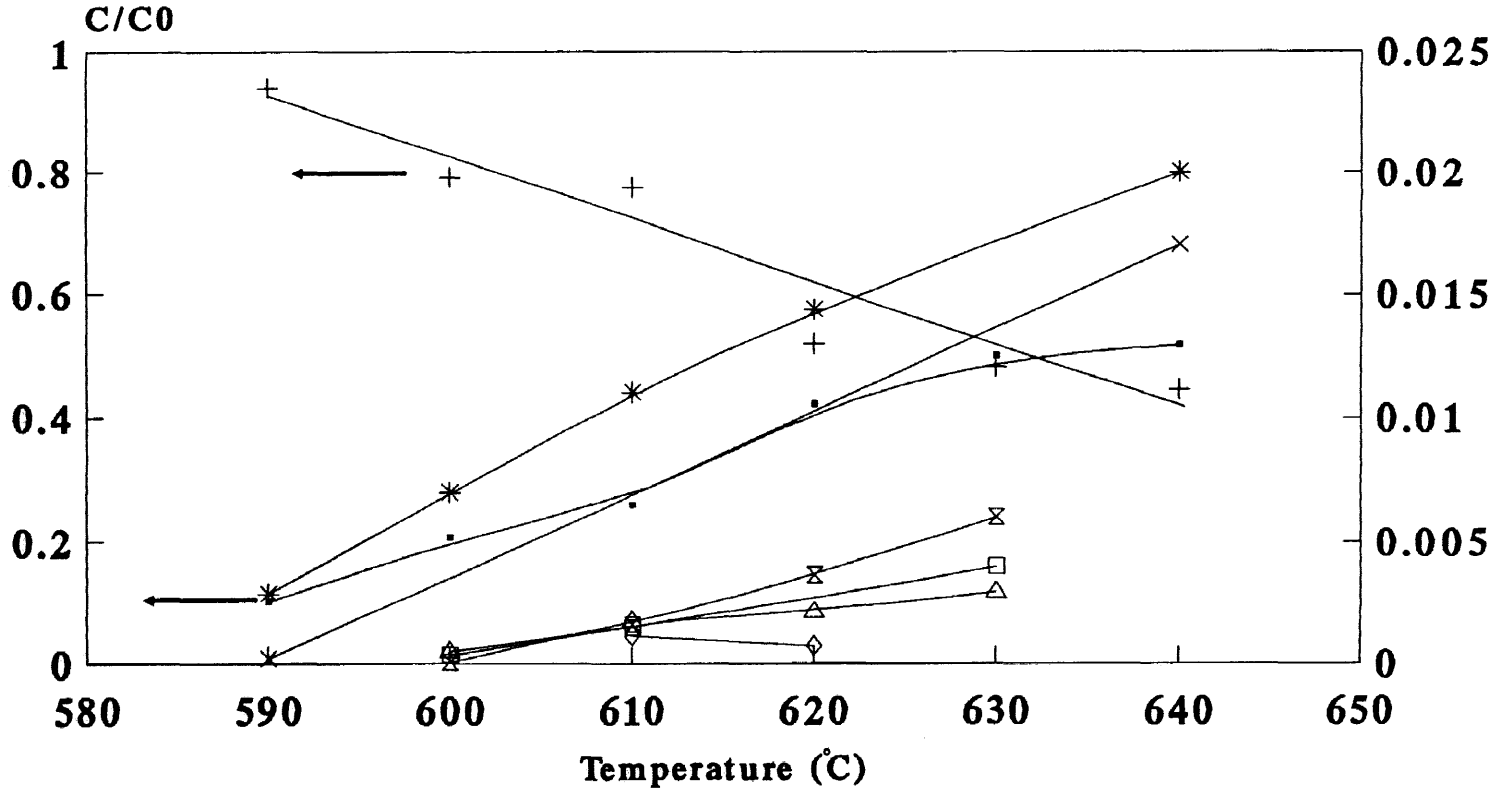

Figure 5.2.2 Product Distribution, O2/H2 = 2%, RT = 0.5sec

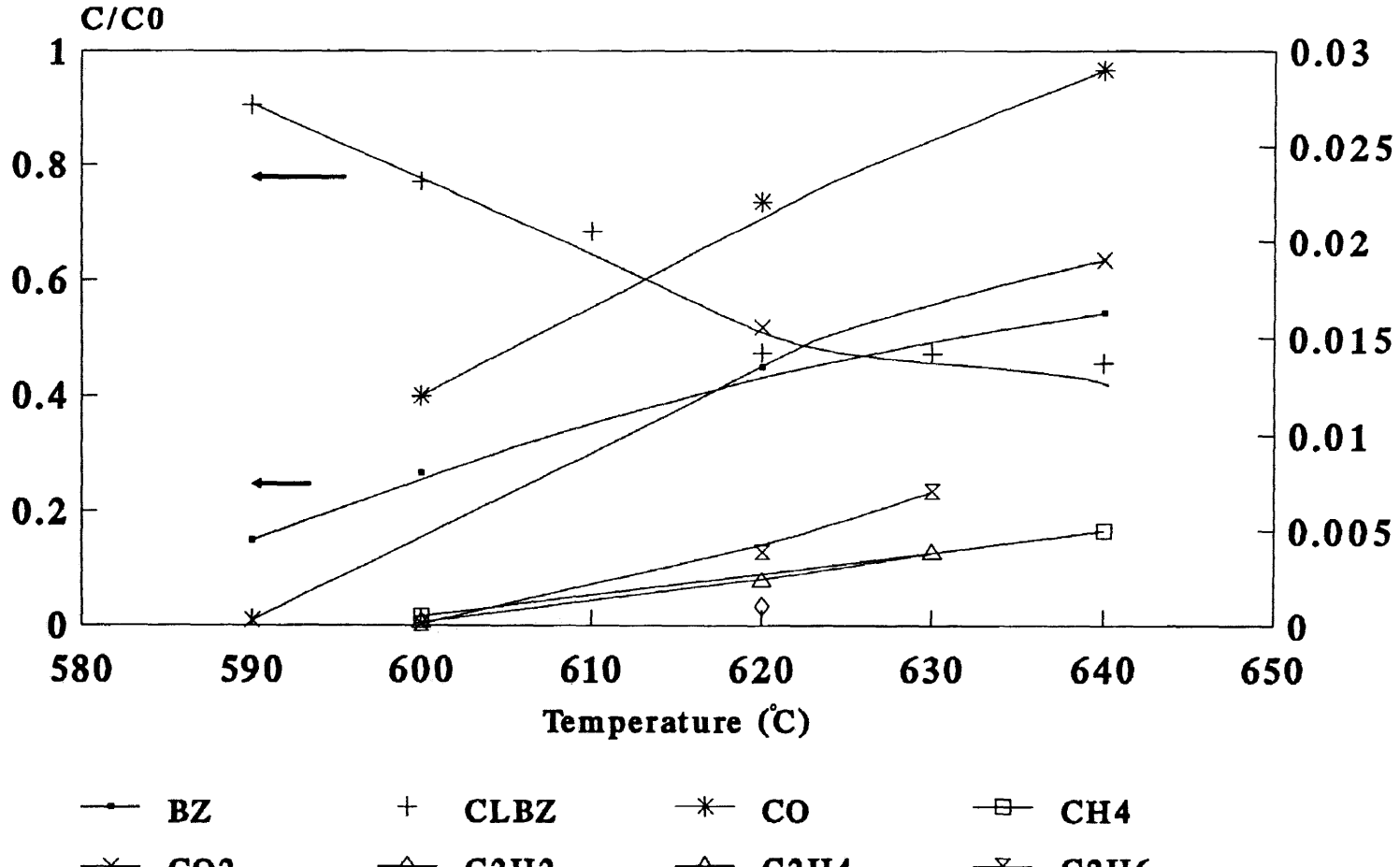

Figure 5.2.3 Product Distribution, O2/H2 = 3%, RT = 0.5sec

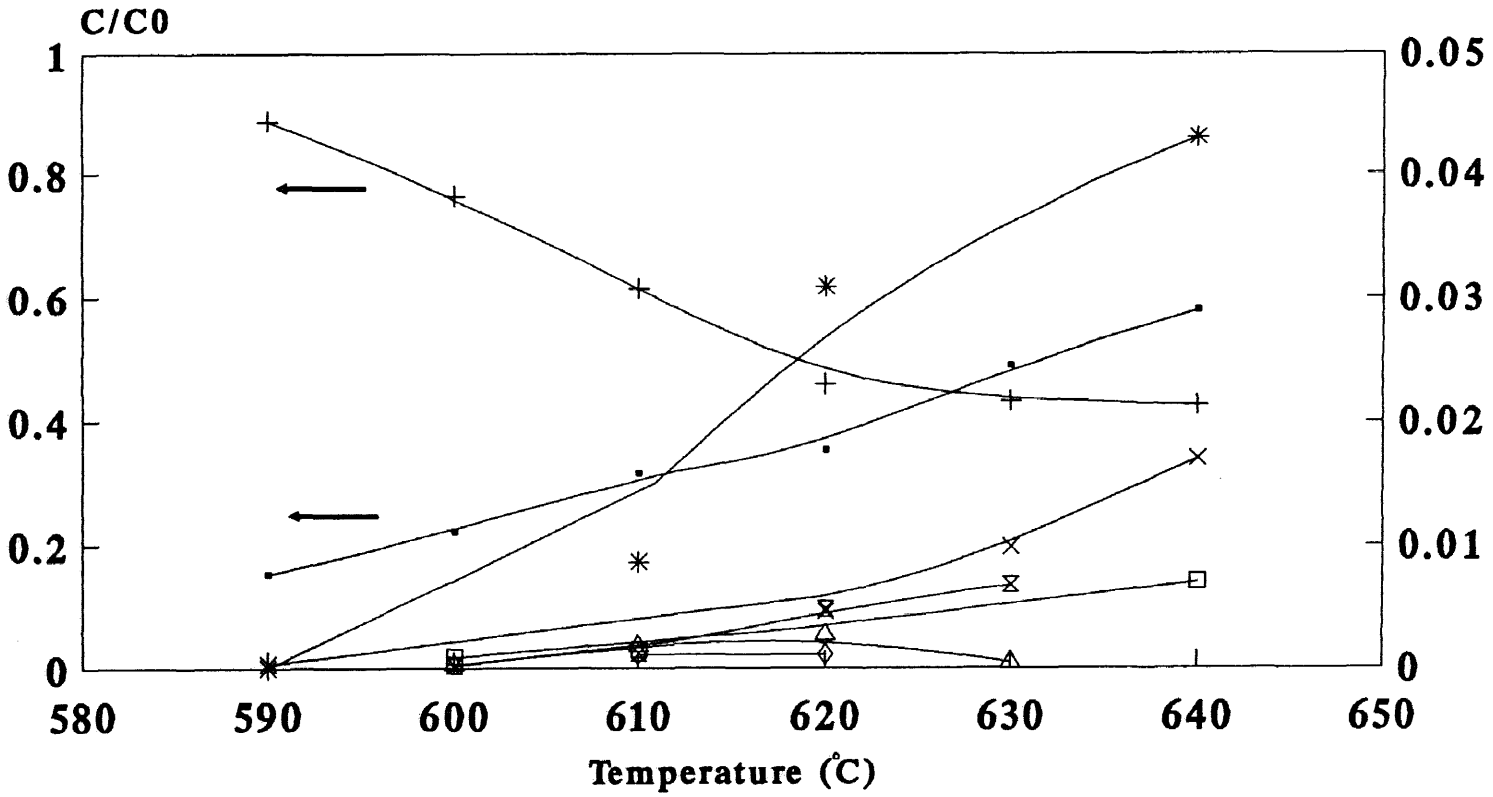

Figure 5.2.4 Product Distribution, O2/H2 = 4%, RT = 0.5sec

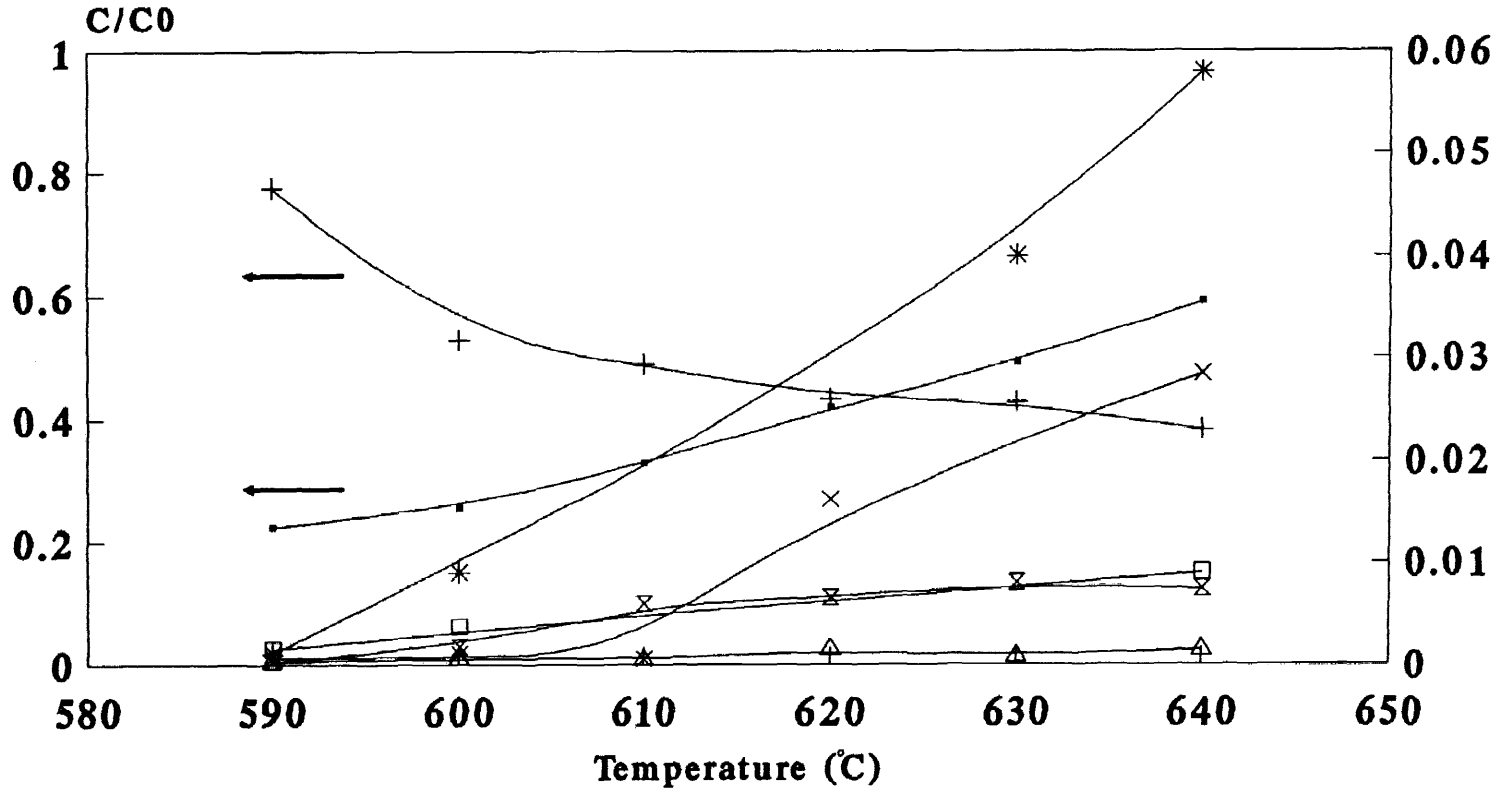

Figure 5.2.5 Product Distribution, O2/H2 = 5%, RT = 0.5sec

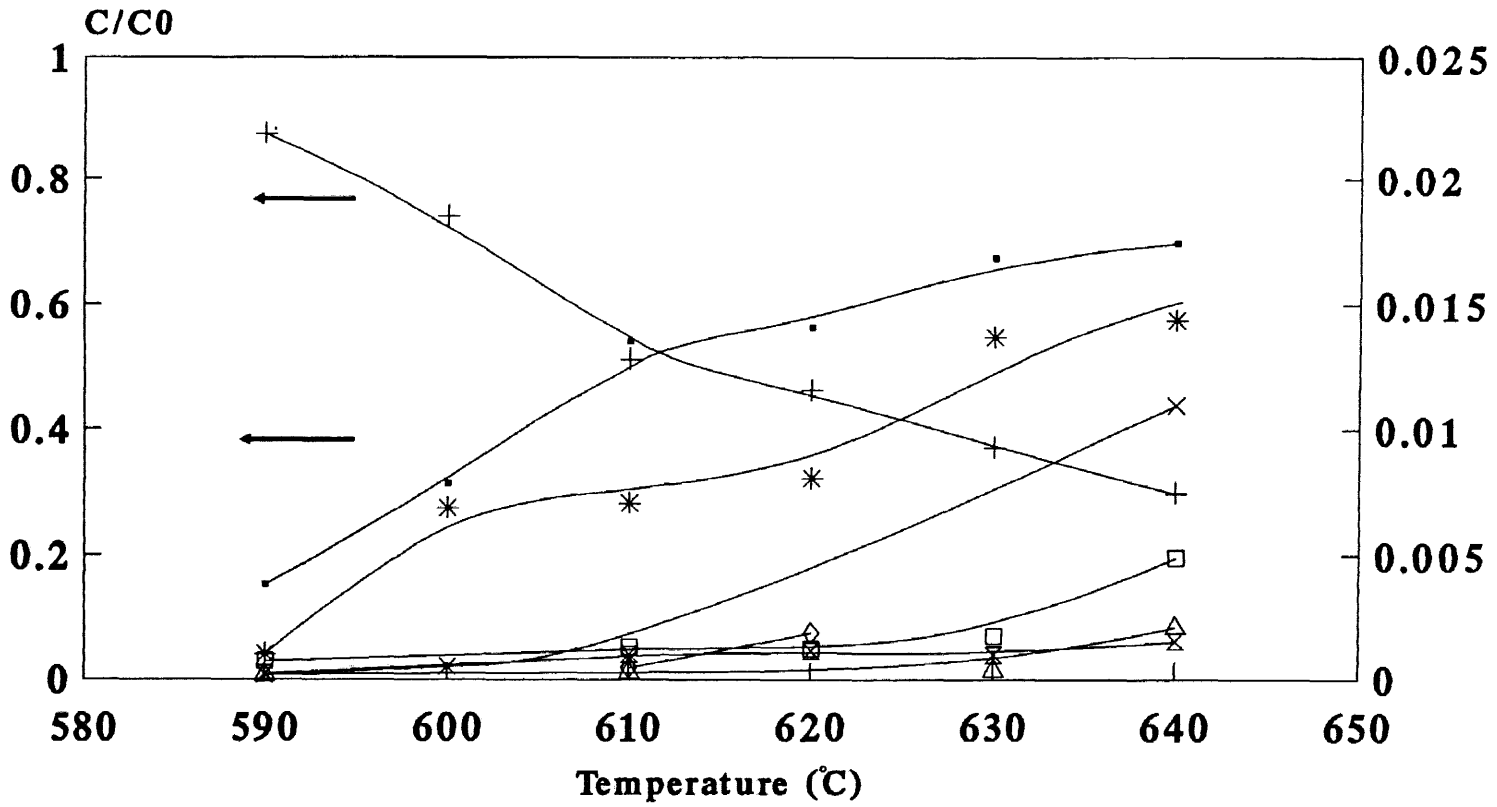

Figure 5.2.6 Product Distribution, O2/H2 = 1%, RT = 1.0sec

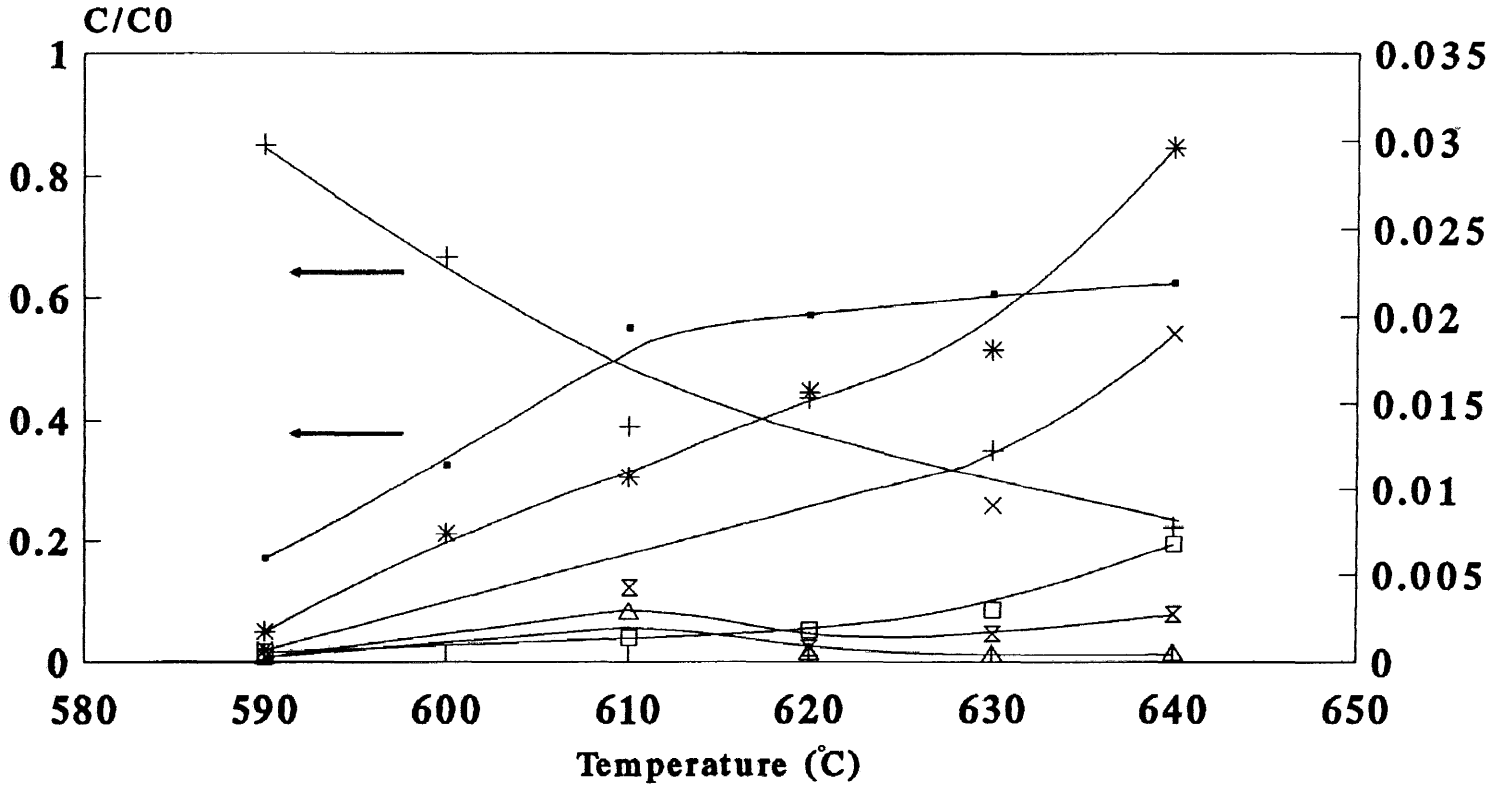

Figure 5.2.7 Product Distribution, O2/H2 = 2%, RT = 1.0 sec

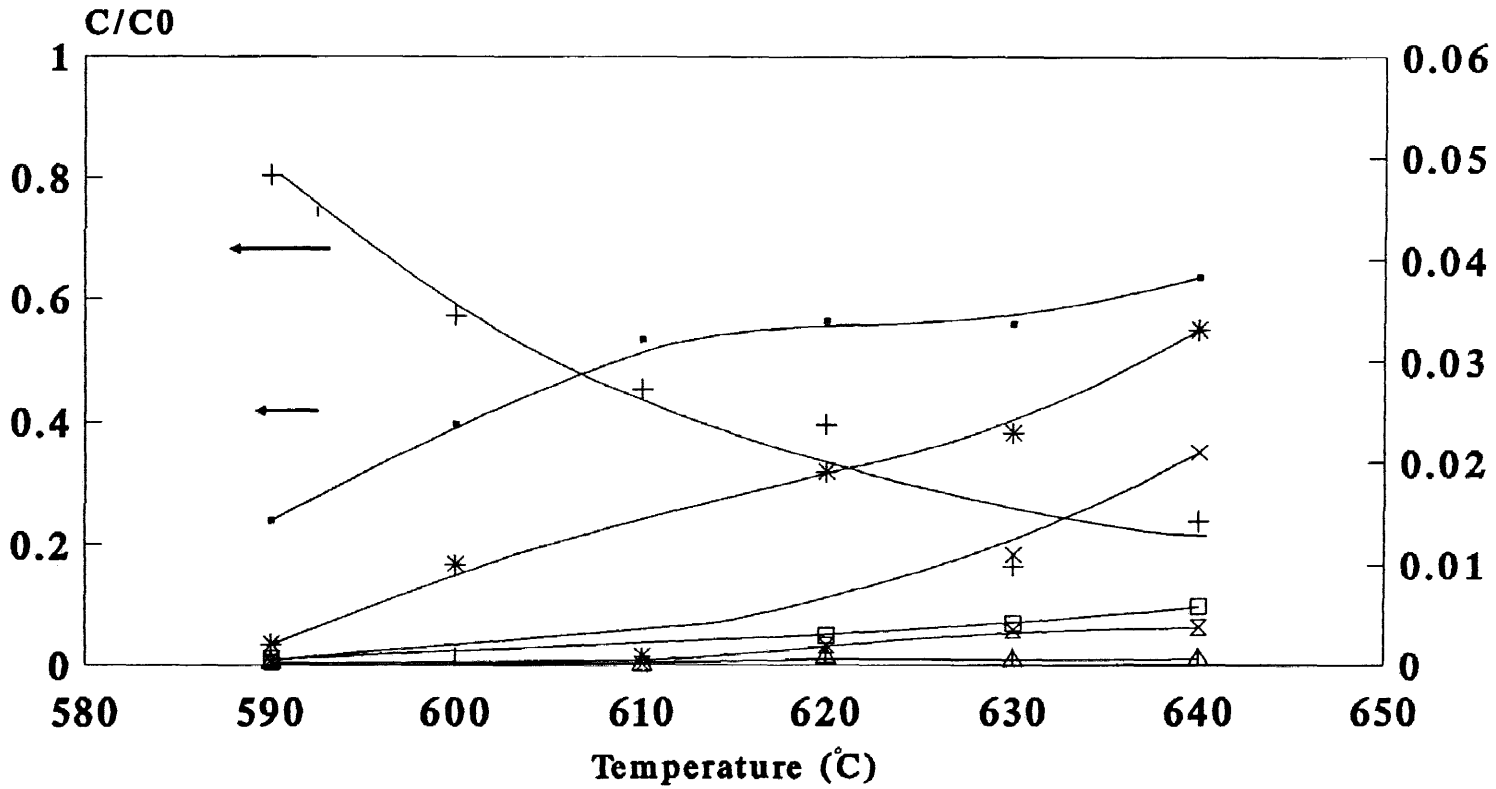

Figure 5.2.8 Product Distribution, O2/H2 = 3%, RT = 1.0sec

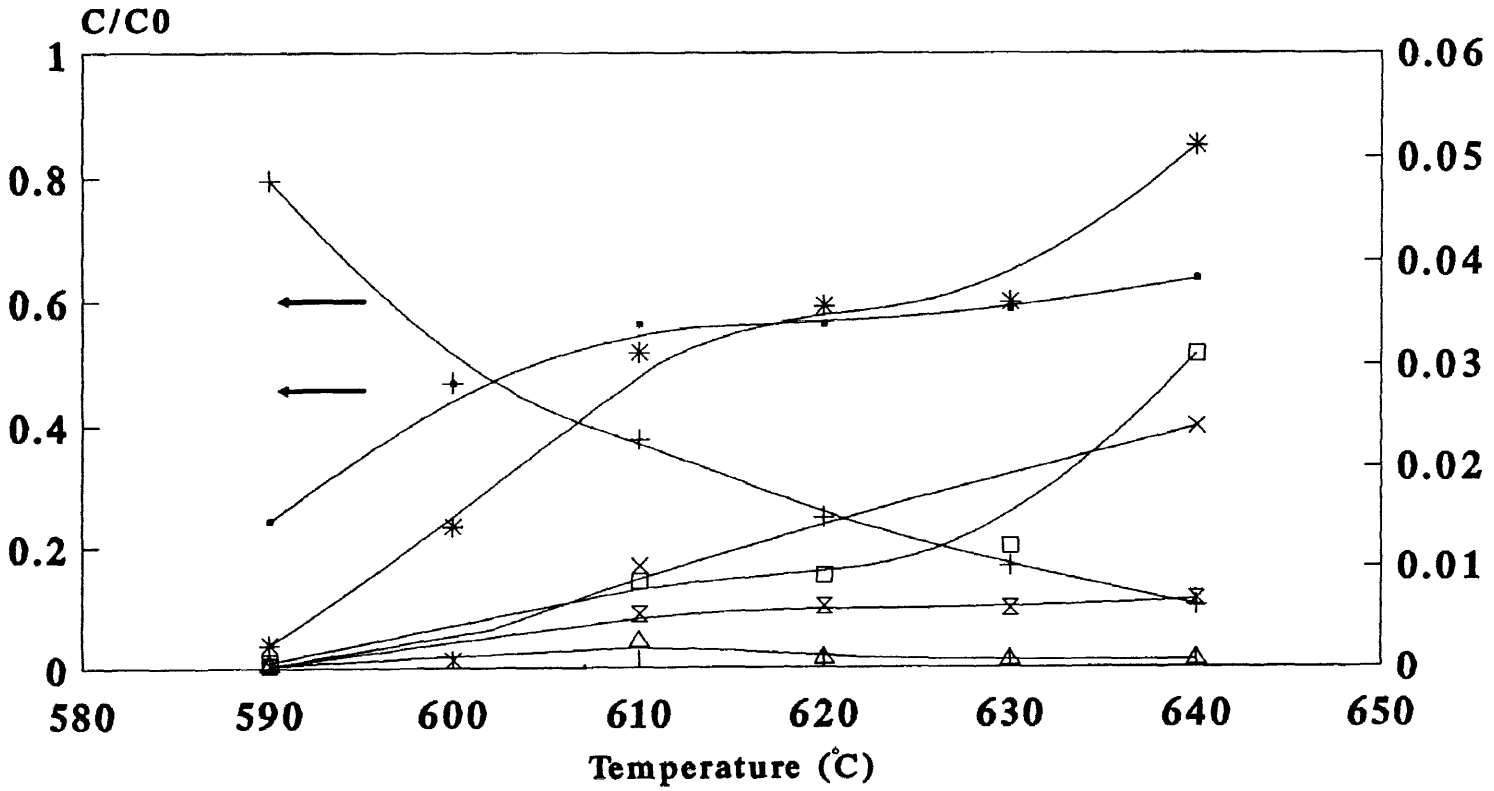

Figure 5.2.9 Product Distribution, O2/H2 = 4%, RT = 1.0sec

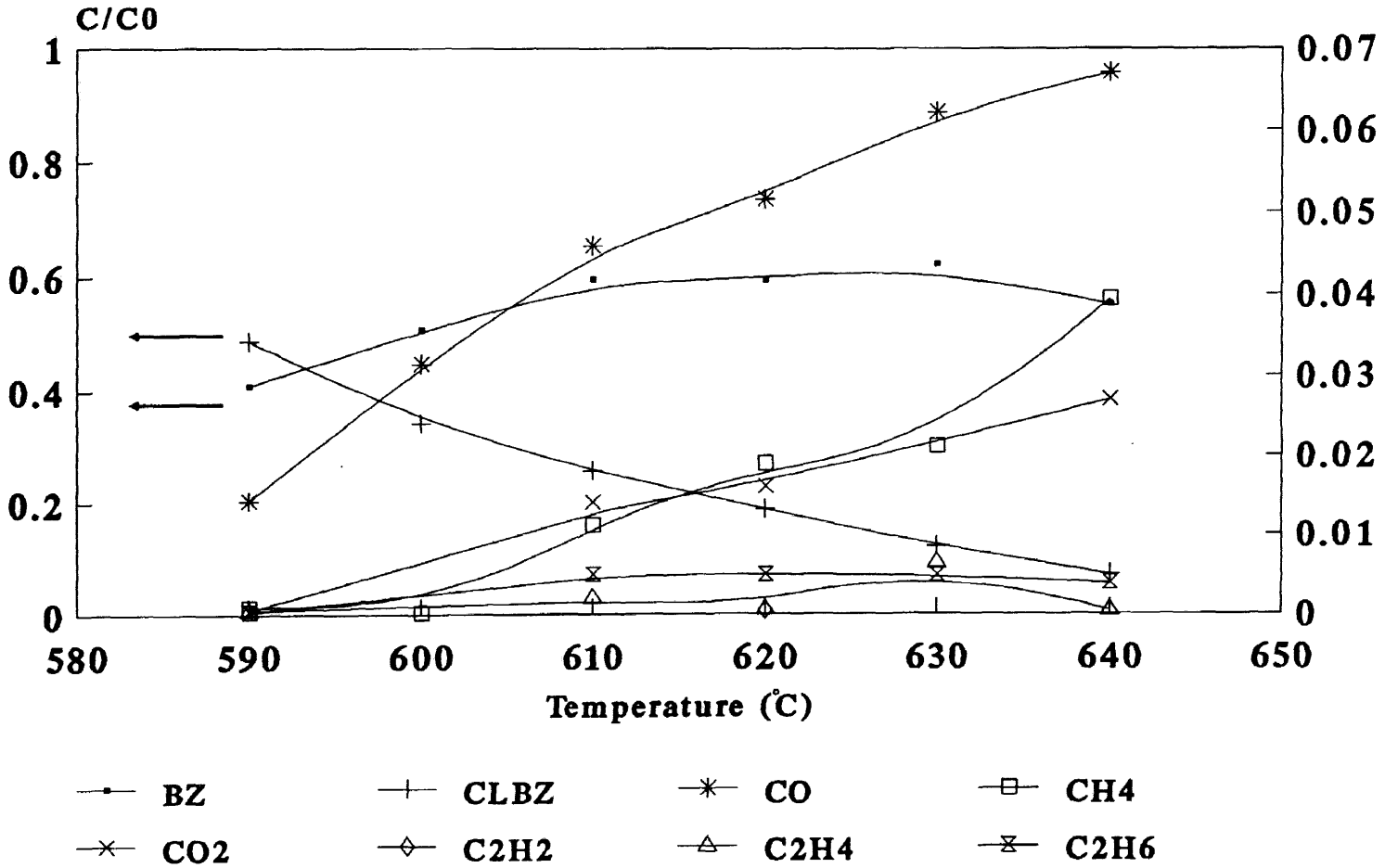

Figure 5.2.10 Product Distribution, O2/H2 = 5%, RT = 1.0sec

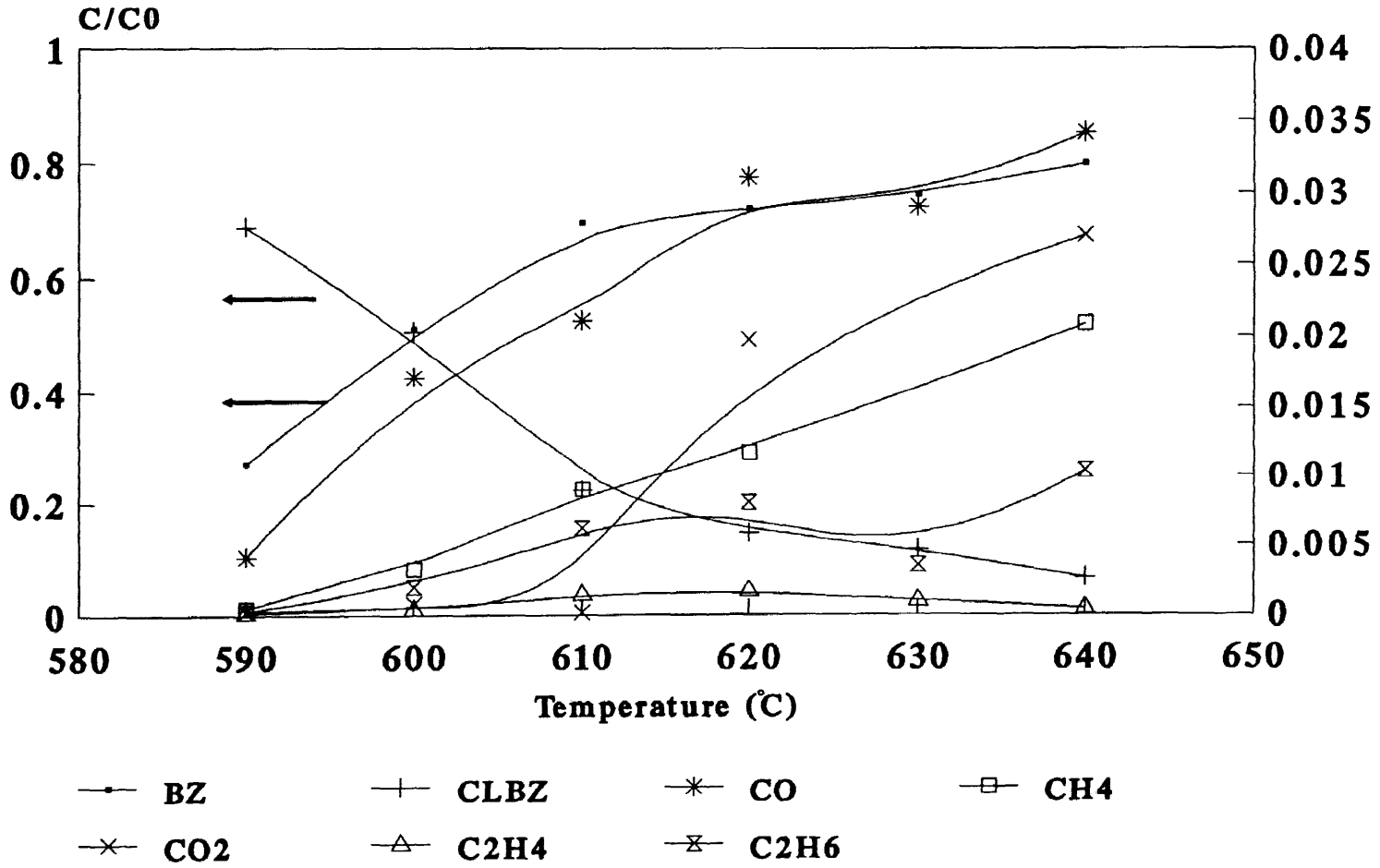

Figure 5.2.11 Product Distribution, O2/H2 = 1%, RT = 2.0sec

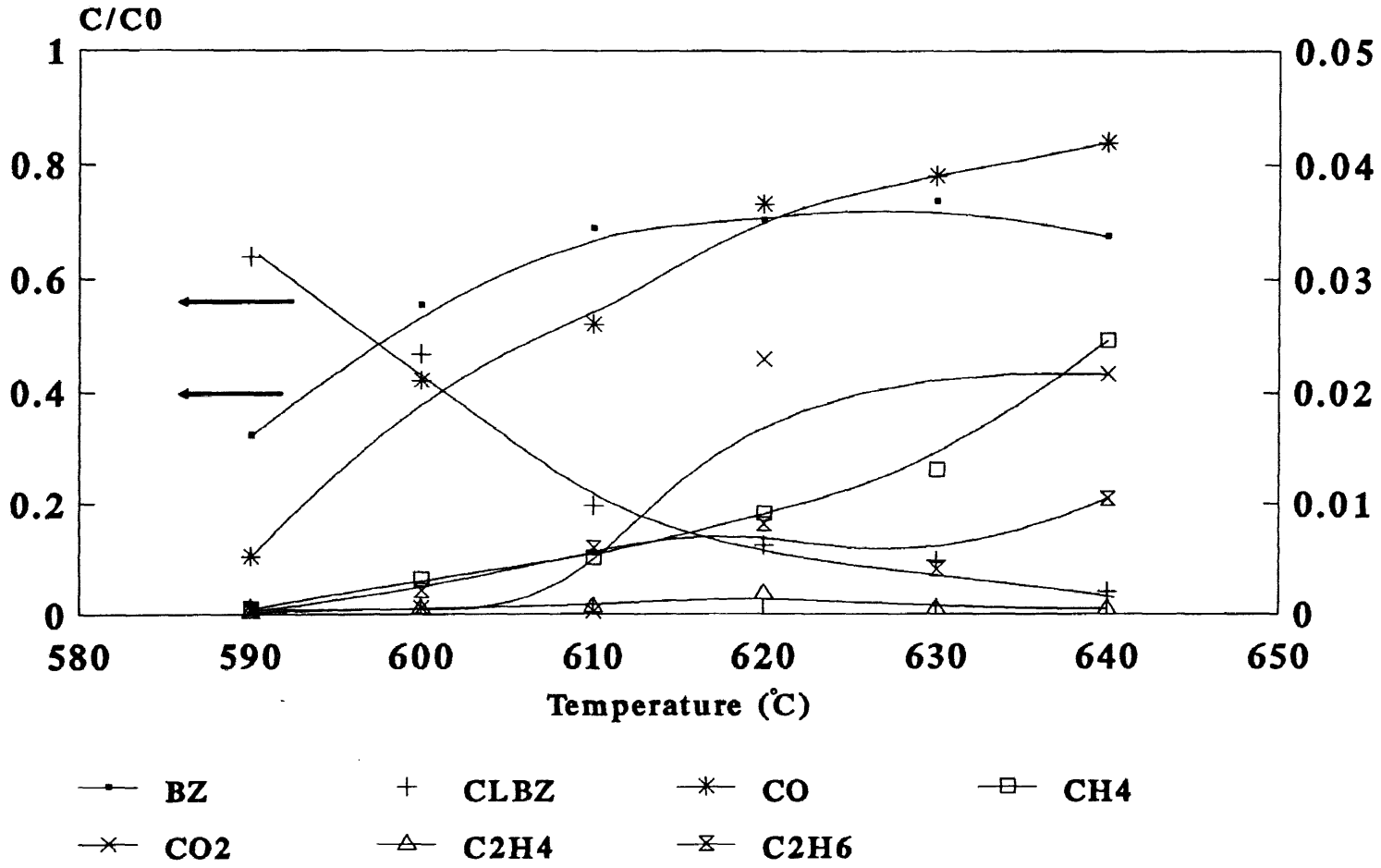

Figure 5.2.12 Product Distribution, O2/H2 = 2%, RT = 2.0sec

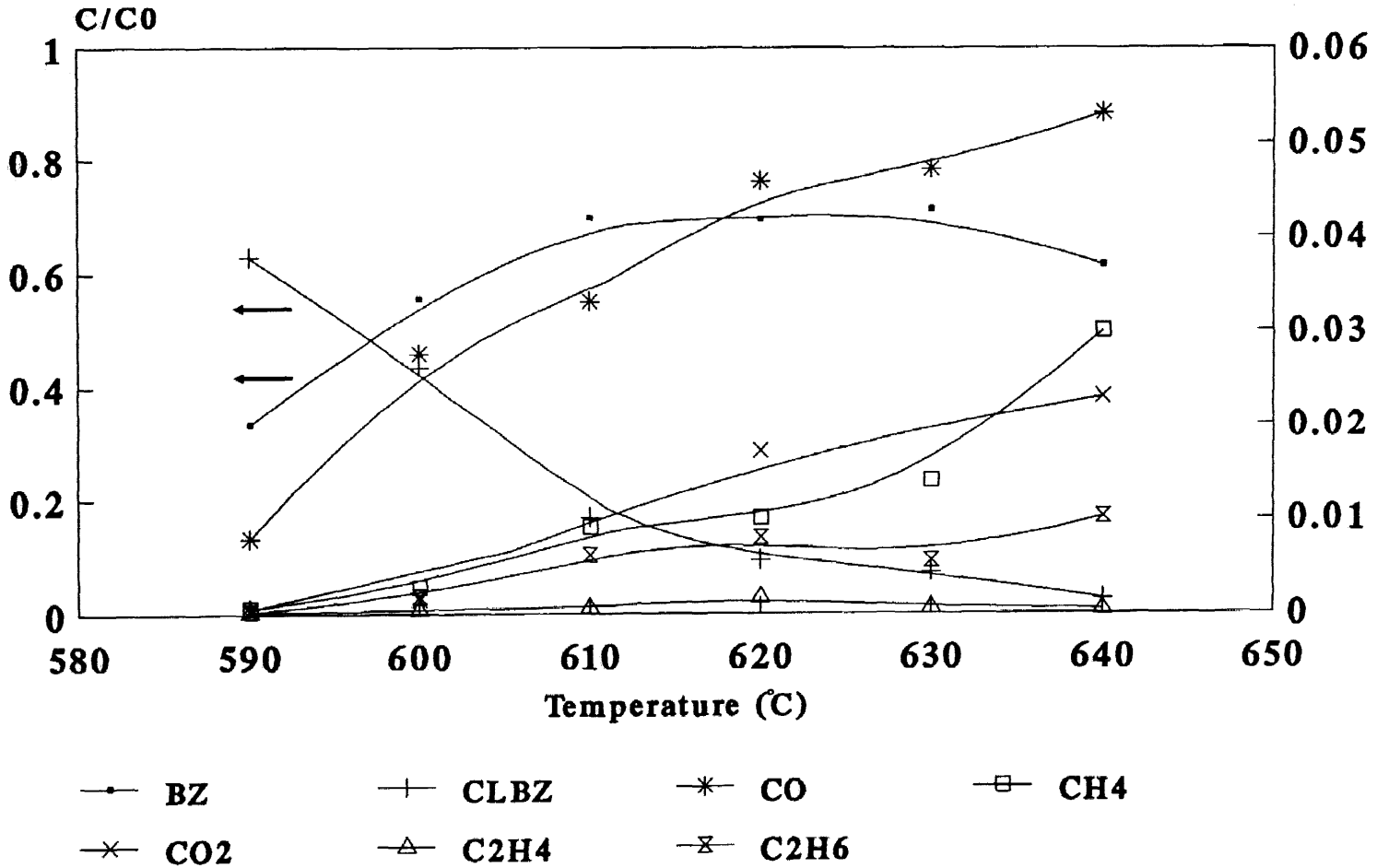

Figure 5.2.13 Product Distribution, O2/H2 = 3%, RT = 2.0sec

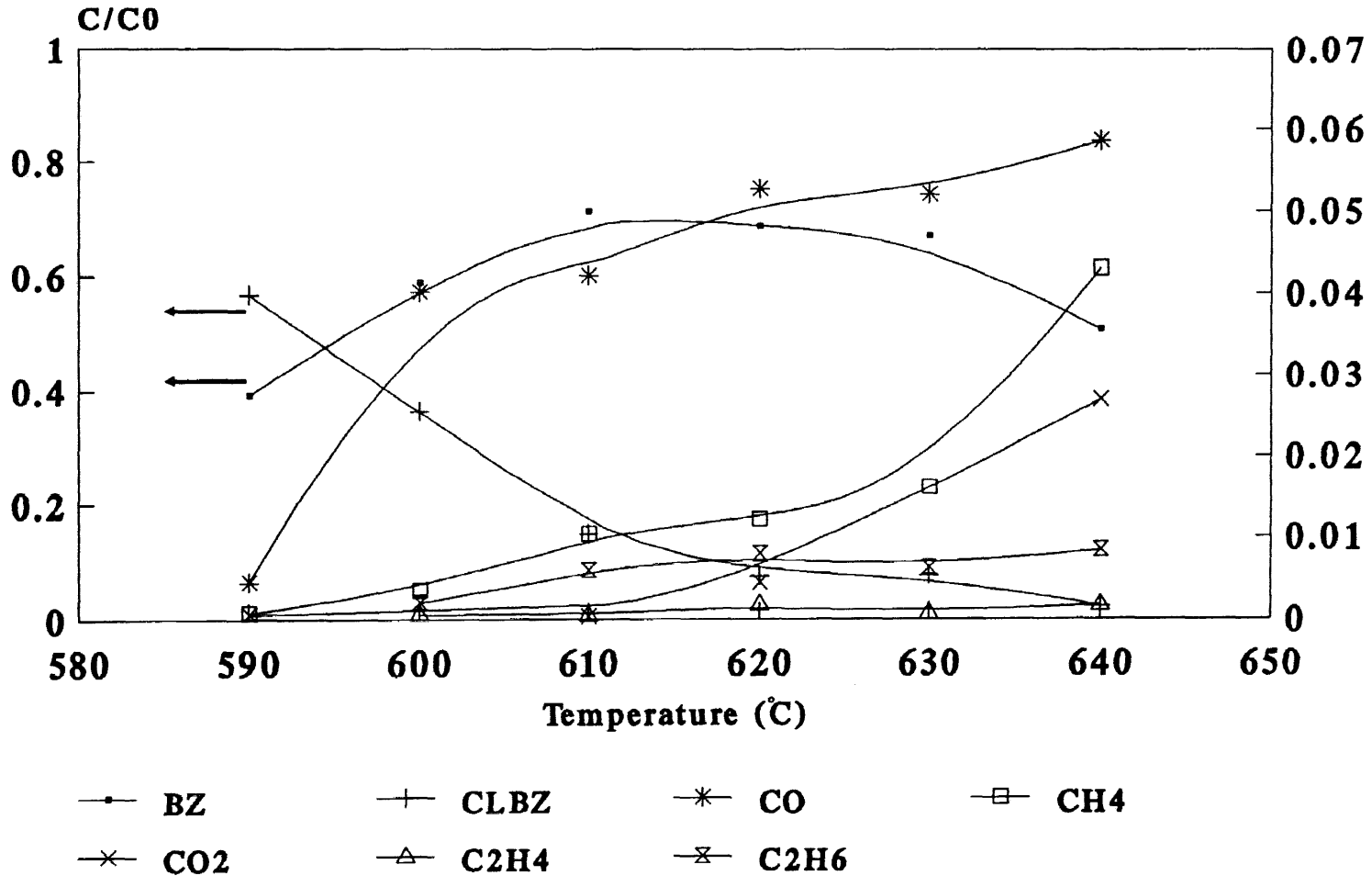

Figure 5.2.14 Product Distribution, O2/H2 = 4%, RT = 2.0sec

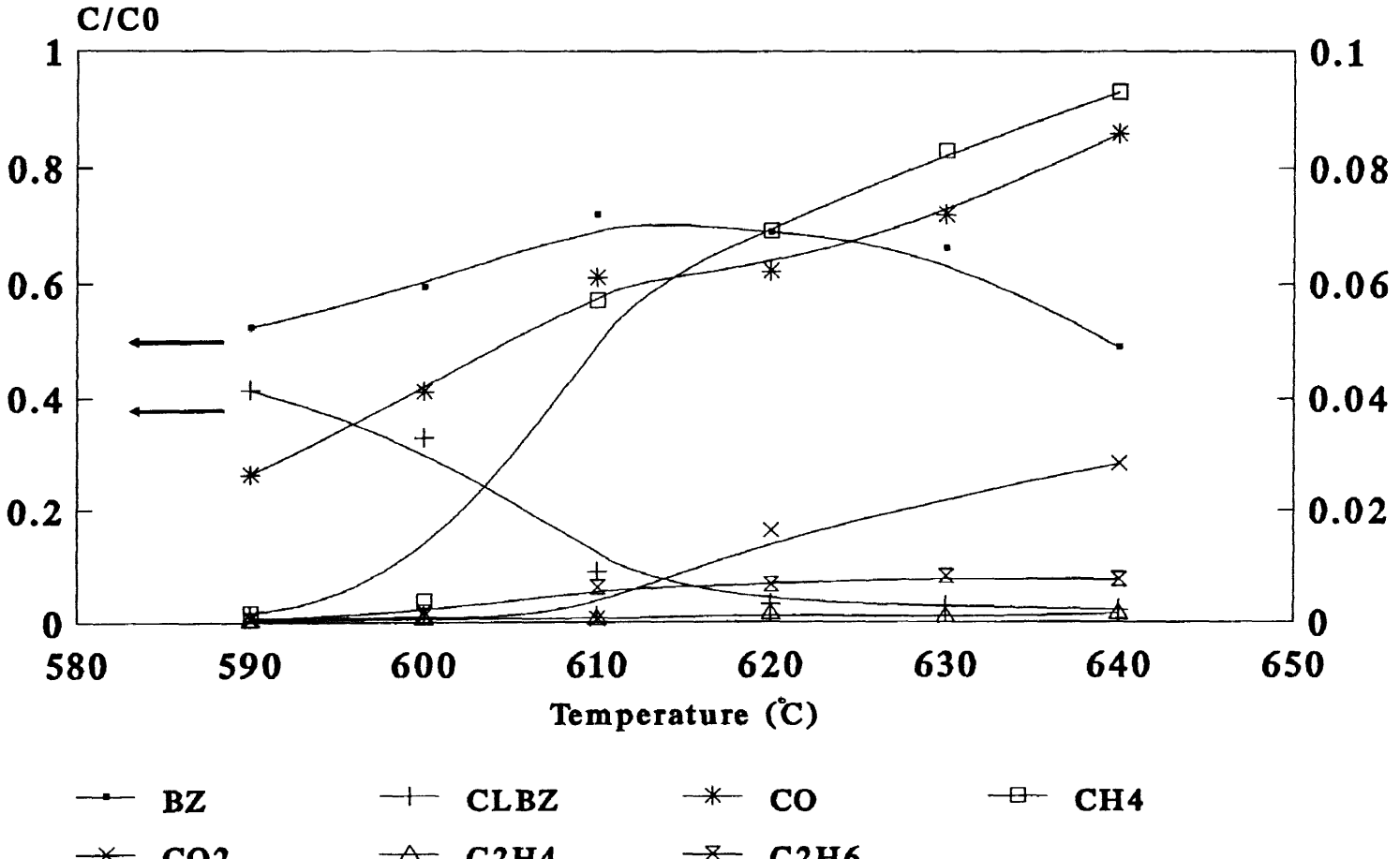

Figure 5.2.15 Product Distribution, O2/H2 = 5%, RT = 2.0sec

Table 5.2.1 Material Balance for 100 moles Carbon

in O_2/H_2 = 1%, Residence Time = 1.0 sec

	Reaction Temperature(°C)					
SPECIES	590	600	610	620	630	640
C6H6	15.25	31.45	53.89	56.23	67.37	69.75
C7H8	0.13	0.28	-	-	-	-
C6H5Cl	87.48	74.04	51.28	46.38	37.24	29.98
CO	0.10	0.69	0.71	0.81	1.37	1.44
CH4	0.07	-	0.13	0.12	0.17	0.49
CO2	0.02	0.05	0.08	-	-	0.11
C2H2	-	-	0.05	0.19	-	-
C2H4	0.02	-	0.03	-	0.04	0.21
C2H6	0.02	-	0.46	0.11	0.10	0.15
TOTAL	103.09	106.51	107.02	103.84	106.29	102.13

Table 5.2.2 Material Balance for 100 moles Carbon in O_2/H_2 = 2%, Residence Time = 1.0 sec

	Reaction Temperature(°C)					
species	590	600	610	620	630	640
C6H6	16.98	32.44	55.14	57.00	60.59	62.62
C7H8	0.09	0.09	-	-	-	-
C6H5Cl	85.08	66.71	43.66	38.80	34.09	22.27
CO	0.17	0.74	1.07	1.56	1.80	2.96
CH4	0.06	-	0.13	0.18	0.29	0.68
CO2	0.06	-	2.01	-	-	2.40
C2H2	-	-	-	-	-	-
C2H4	0.02	-	0.28	0.05	0.03	0.04
C2H6	0.02	-	0.42	0.08	0.16	0.27
TOTAL	102.48	99.98	102.71	97.67	96.96	91.24

Table 5.2.3 Material Balance for 100 moles Carbon

in O_2/H_2 = 3%, Residence Time = 1.0 sec

	Reaction Temperature(^oC)					
species	590	600	610	620	630	640
C6H6	23.76	39.55	53.23	56.24	55.84	63.73
C7H8	0.11	0.13	-	-	-	-
C6H5Cl	80.44	57.27	45.34	39.58	16.44	23.72
CO	0.22	0.98	-	1.92	2.30	3.25
CH4	0.06	-	-	0.28	0.40	0.57
CO2	0.03	-	0.08	-	-	2.21
C2H2	-	-	-	-	-	-
C2H4	0.03	-	-	0.07	0.04	0.05
C2H6	0.02	-	-	0.19	0.34	0.37
TOTAL	104.63	97.88	98.65	98.02	75.36	93.90

Table 5.2.4 Material Balance for 100 moles Carbon in O_2/H_2 = 4%, Residence Time = 1.0 sec

	Reaction Temperature(^oC)					
species	590	600	610	620	630	640
C6H6	24.21	46.85	56.31	56.40	58.76	63.86
C7H8	0.14	0.20	-	-	-	-
C6H5Cl	79.65	46.98	37.60	24.81	16.74	10.23
CO	0.22	1.40	3.11	3.55	3.60	5.11
CH4	0.06	-	0.85	0.91	0.97	1.13
CO2	0.11	-	0.02	0.07	2.40	2.76
C2H2	-	-	-	-	-	-
C2H4	0.02	-	0.26	0.09	0.07	0.07
C2H6	0.02	-	0.52	0.60	0.58	0.67
TOTAL	104.43	95.43	98.67	86.42	83.12	83.83

Table 5.2.5 Material Balance for 100 moles Carbon in O_2/H_2 = 5%, Residence Time = 1.0 sec

	Reaction Temperature(^oC)					
species	590	600	610	620	630	640
C6H6	41.06	50.79	59.55	59.35	62.09	55.29
C7H8	0.19	0.36	-	-	-	-
C6H5Cl	48.94	34.33	25.23	18.82	12.14	7.18
CO	1.43	3.14	4.57	5.15	6.17	6.68
CH4	0.09	0.02	1.11	1.89	2.31	3.94
CO2	0.04	-	0.14	1.16	-	2.76
C2H2	-	-	-	0.05	-	-
C2H4	0.04	-	0.20	0.06	0.64	0.05
C2H6	0.03	-	0.72	0.75	0.49	0.38
TOTAL	91.82	88.64	91.52	87.23	83.84	76.28

5.3 Previous Studies on Chlorobenzene

Several researchers have reported on the pyrolysis of chlorobenzene in different types of reactors, but for the most part, they investigated reaction temperature ranges which are above 900°C (1173K) and did not significantly involve O_2 reactions. Kern[40] et al studied pyrolysis of chlorobenzene in Ne bath gas in a shock tube reactor over the temperature range 1307 - 1727°C and total pressures of 0.3 - 0.5 atm. Time-of-flight mass spectrometry was used for product profiles. The major products they found are acetylene, HCl, and diacetylene. Minor products are C_6H_2, benzene, and C_8H_2. The only radical they detected is phenyl. The products of chlorobenzene reaction were described by Ritter[8], but he did not measure C_1 to C_2 products from pyrolysis of chlorobenzene in excess hydrogen. Zhu[17] however did quantitatively examine formation of light hydrocarbons from $C_6H_5Cl + H_2$ reaction. His study related to initial C_6H_5Cl concentration showed a few percent of CH_4, and C_2H_6. In our study, the major product from oxidation of chlorobenzene was benzene.

Reaction initiation is the bimolecular reaction of $O_2 + H_2$ ---> $HO_2 + H$. The activation energy for dissociation of chlorobenzene is 97 kcal/mole at these temperatures, but Ea for this $O_2 + H_2$ chain branching reaction is only 55.5 kcal/mole. The reaction with both oxygen and hydrogen present should show faster chlorobenzene decomposition rates than the pyrolysis of chlorobenzene in excess of H_2

only; where initiation must be unimolecular decomposition of chlorobenzene. This is because the H atom produced rapidly reacts with C_6H_5Cl via a displacement path.[9]

This work shows significant agreement with Yang's[10] work on chlorobenzene decomposition, benzene formation , and soot formation. The propensity of chlorobenzene to form soot was published by Frenklach et. al.[36]. Solid carbon formatiom inside the reactor as observed in our study, amounts to as much as 25% of the chlorobenzene. (see Table 5.2.5).

This work also shows several differences with respect to that of Yang[10]. This may due to the difference between the two experimental systems and conditions. We found 10% of chlorobenzene's carbon as CH_4 instead of 50% as CH_4 reported by Yang[10]. 50% CH_4 formation occurred in the 16 mm reactor of Yang's experiemnts. We also found up to 3% of CO_2 as a reaction product but Yang did not observe CO_2. Cyclopendiene was also found in Yang's study.

5.4 Kinetic Calculations and Modeling

Energized Complex/QRRK theory as presented by Westmoreland and Dean[37,38] is used for modeling of radical addition and combination reactions. This calculation has been modified by Ritter and Bozzelli[39] to use gamma functions. The QRRK computer code was used to determine the temperature and pressure energy dependent rate constants for all channels. The program incorporates QRRK theory

to calculate rate constants as function of temperature and pressure. It is important in determination of the mechanism and choice of the paths (accurate product prediction from the activated complex).

A QRRK analysis of the chemically activated system, using generic estimates or literature values for high pressure rate constants and species thermodynamic properties for the enthalpies of reaction, yields apparent rate constants at varied temperatures and pressures. The input rate parameters used in these calculations and the results from the calculations are summarized in Table 5.4.1A through 5.4.6B, and Figure 5.4.1.1 through 5.4.4.3. The calculations were performed for each of three pressures 76, 760, and 7600 torr (0.1, 1.0, 10 Atm) and over a temperature range of 773 K to 1273 K.

In the following formulas, " * " will be use to represent a double bond between two atoms.

5.4.1 O + C*C*O Reaction

$$O + C{*}C{*}O \underset{-1}{\overset{1}{<\!\!\!-\!\!\!-\!\!\!-\!\!\!-\!\!\!>}} CH2O.C.{*}O \longrightarrow C.{*}OCHO + H$$

$$CH2O.C.{*}O \underset{-4}{\overset{4}{<\!\!\!-\!\!\!-\!\!\!-\!\!\!-\!\!\!>}} C.HO.CHO \xrightarrow{5} HCO + HCO$$

TABLE 5.4.1A CHEMACT Input Parameters for O + C*C*O

k	A	Ea	source
1	6.10E+12	0.56	a
-1	2.36E+13	39.21	b
2	1.50E+13	24.57	c
4	9.81E+12	25.00	d
-4	1.39E+13	17.53	e
5	1.72E14	5.87	f

$\langle v \rangle$ = 1004 cm^{-1} g

Lennard Jones PARAMETERS: h

σ = 4.49A^{o} ϵ/k = 472 cal

a: From O + CH_2CHCH_3 (Cvetanovic, R.J. J.P.C. 1987)

b: From THERM calculations and microscopic reversibility:
LN (A_f / A_r) = del S / R - (del n) * (ekT)
E_f - E_r = del $H_{(rxn)}$ - del n/RT

c: A_2, E_2 calculated from THERM, A_{-2}=9.0E+12, microscopic reversibility. E_{-2}=2.9 Kcal/mol, from H + C=C (Barat and Bozzelli, J.P.C 1992).

d: $A_4=(10^{13.56-4/4.6})*2$, E_4=25 Kcal/mol (Benson, 1990)

e: calculated from THERM, microscopic reversibility

f: calculated from THERM, A_{-5}=5.19E+11, E_{-5}=6.56 Kcal/mol, which are taken from CC. + CO., treat E_a as addition and microscopic reversibility

g: CPFIT program

h: $\epsilon/k = T_c/1.259$, $\sigma = 0.809V_c^{1/3}$ (Dean, A.M., Bozzelli, J.W., and Ritter, E.R. Combustion Science and Technology, 1991, Vol.80.)
Critical properties T_c and V_c estimated from $C_2H_4O_2$ Acetic Acid data using Lydersen's Method (Reid, R.C., Prausnitz, J.M., and Sherwood, T.K., The Properties of Gases and Liquids McGraw-Hill Book Company.

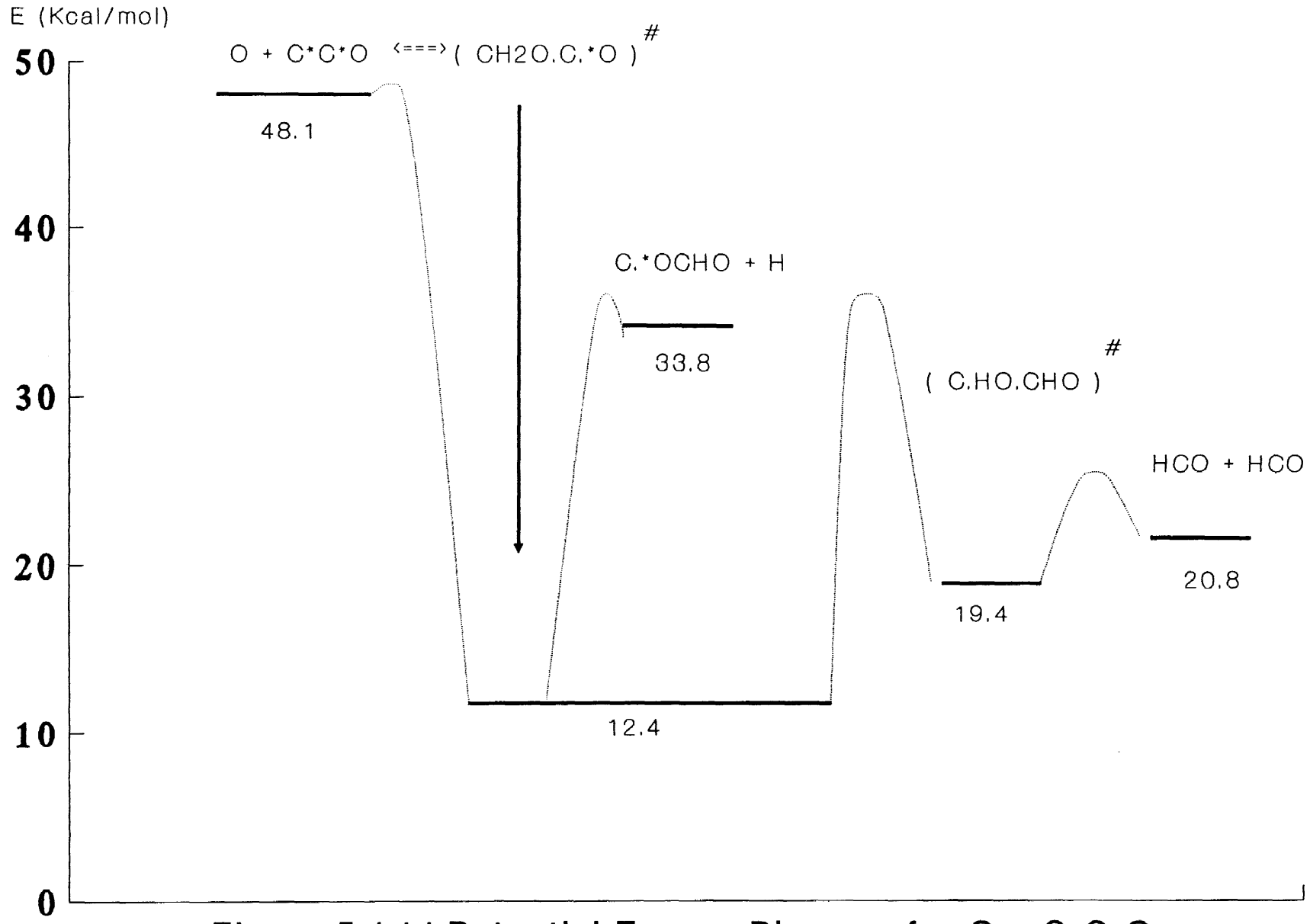

Figure 5.4.1.1 Potential Energy Diagram for O + C*C*O

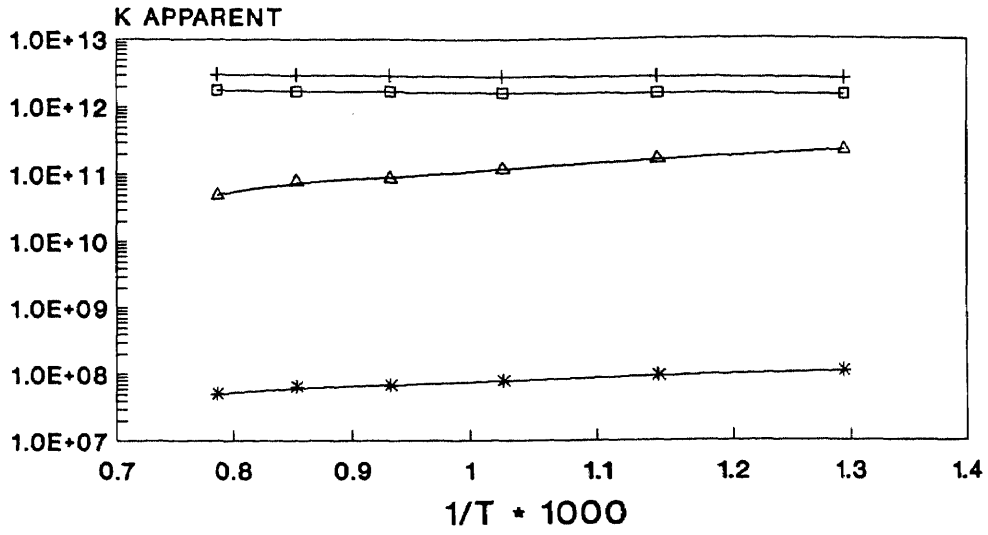

Figure 5.4.1.2 QRRK Analysis: Kapp vs 1/T at 760 Torr

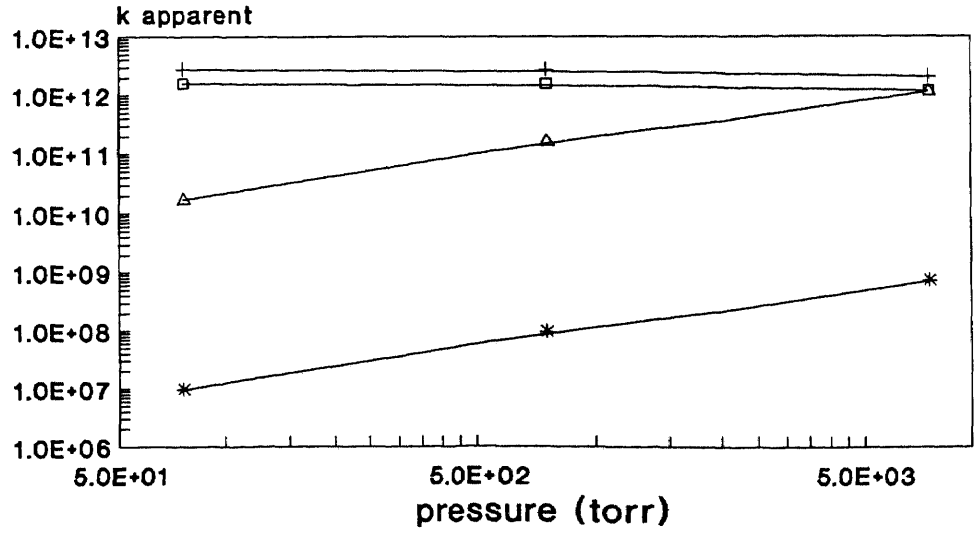

Figure 5.4.1.3 QRRK Analysis: Kapp vs Pressure at 873 K

UNITS: A in cc/mol sec and sec^{-1}, Ea in kcal/mol

TABLE 5.4.1B CHEMACT Results for O + C*C*O

Products	A	n	Ea	Pressure
CH2O.C.*O	2.88E+25	-4.88	3.46	76 Torr
	7.74E+26	-5.00	3.88	760 Torr
	2.13E+29	-5.37	5.84	7600 Torr
C.*OCHO + H	1.13E+13	-0.14	0.76	76 Torr
	3.53E+13	-0.28	1.19	760 Torr
	6.65E+15	-0.90	3.48	7600 Torr
C.HO.CHO	3.14E+14	-2.43	1.47	76 Torr
	9.67E+15	-2.56	1.92	760 Torr
	1.37E+19	-3.14	4.15	7600 Torr
HCO + HCO	4.25E+12	-0.08	0.75	76 Torr
	1.33E+13	-0.22	1.17	760 Torr
	2.60E+15	-0.84	3.47	7600 Torr

Valid from 773 - 1273 K

Best Fit Equation $A*T^n \exp(-Ea/RT)$

UNITS: A in cm^3/mole-sec, Ea in Kcal/mole

The energy diagram of the reaction system is shown in Figure 5.4.1.1,and the calculation results are shown in Figure 5.4.1.2 and Figure 5.4.1.3.

5.4.2 HO2 + HCO Reaction

$$HO2 + HCO \underset{-1}{\overset{1}{<\!\!-\!\!-\!\!-\!\!-\!\!>}} HC(*O)OOH \overset{2}{\longrightarrow} HCO2. + OH$$

$$HC(*O)OOH \overset{3}{\longrightarrow} H2O + CO2$$

TABLE 5.4.2A CHEMACT Input Parameters for HO_2 + HCO

k	A	Ea	source
1	1.00E+13	0.00	a
-1	2.86E+15	81.47	b
2	1.60E+14	37.03	c
3	8.50E+11	33.70	d
<v> = 885.6 cm^{-1}			e
Lennard Jones PARAMETERS:			f
σ = 4.57A^{o}		ϵ/k = 380 cal	

a: From CC. + CC. (Allara and Shaw)

b: From THERM calculations:
LN (A_f / A_r) = del S / R - (del n) * (ekT)
E_f - E_r = del $H_{(rxn)}$ - del n/RT

c: A_2, E_2 calculated from THERM, A_{-2}=2.0E+13, E_{-2}=0 Kcal/mol which were taken from OH + CC. (Tsang, W. and Hampson, R.F. NIST)

d: A_3=($10^{13.56-7.5/4.6}$), HC(*O)OOH loss of two rotors. E_3=33.7 Kcal/mol From literature, C_3COH-->H_2O+C_2C=C C_3CCOH-->H_2O+C_3C=C, E_as = delH + 45. But the above reactions were endothermic. This reaction exothermic by 84 Kcal/mol. If an Evans Polanyi relationship holds then E_3 = 45 - (del H/4) = 24, we elect to take average E_3 = (45 + 24)/2 = 34.5 Kcal/mol.

e: CPFIT program

h: $\epsilon/k = T_c/1.259$, $\sigma = 0.809V_c^{1/3}$ (Dean, A.M., Bozzelli, J.W., and Ritter, E.R. Combustion Science and Technology, 1991, Vol.80.)
Critical properties T_c and V_c estimated by using Lydersen's Method (Reid, R.C., Prausnitz, J.M., and Sher wood, T.K., The Properties of Gases and Liquids McGraw-Hill Book Company.

UNITS: A in cc/mol sec and sec^{-1}, Ea in kcal/mol

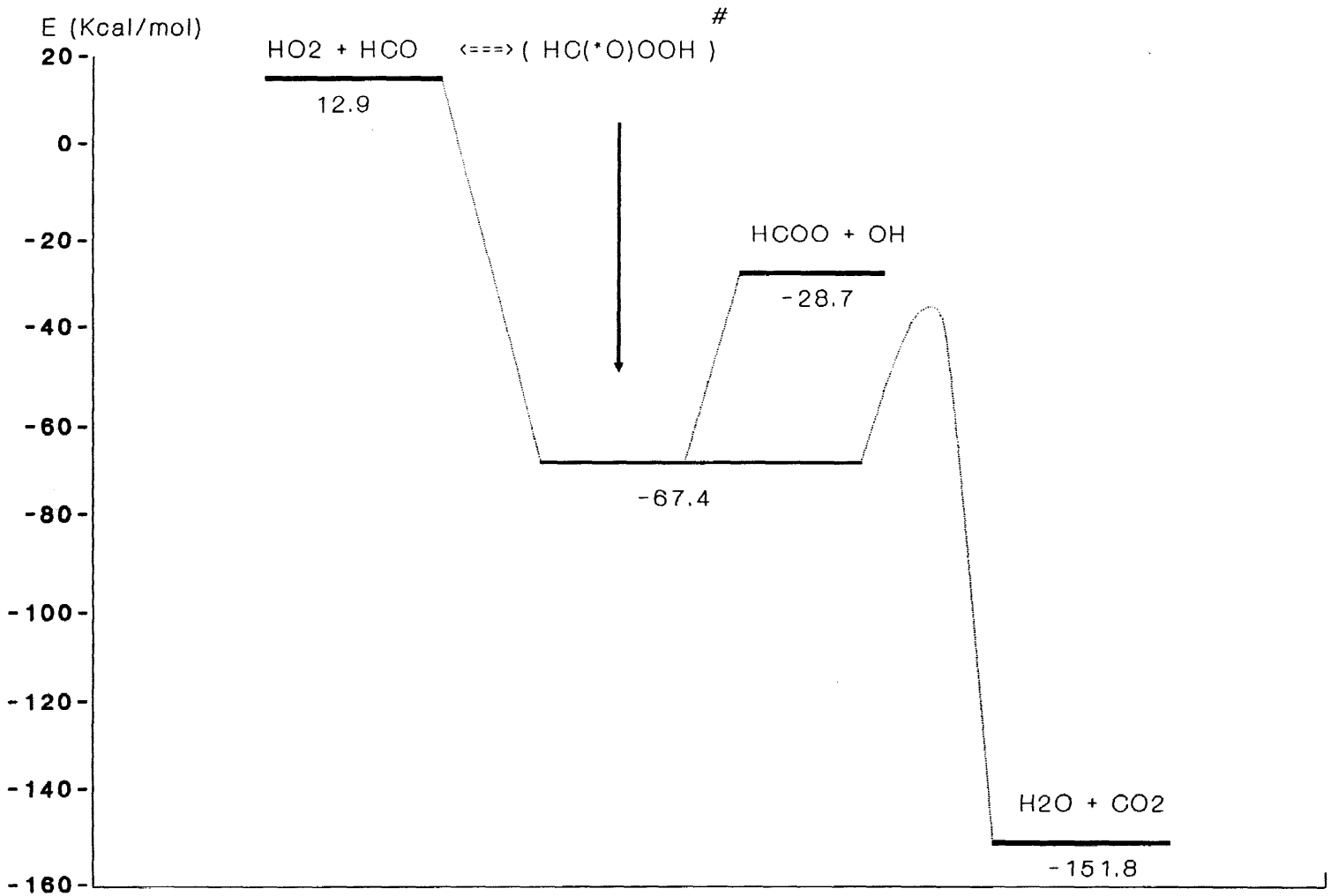

Figure 5.4.2.1 Potential Energy Diagram for HO2 + HCO

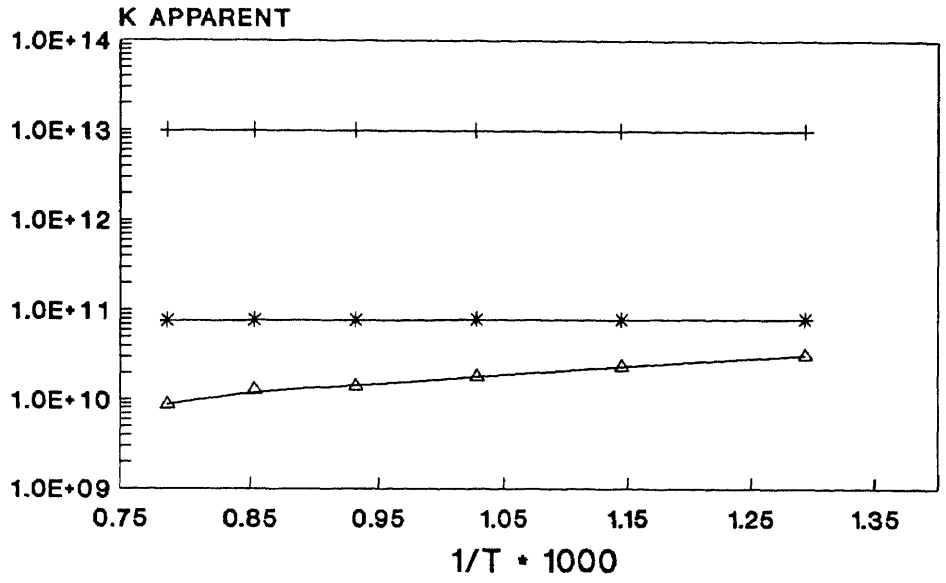

Figure 5.4.2.2 QRRK Analysis: Kapp vs 1/T at 760 Torr

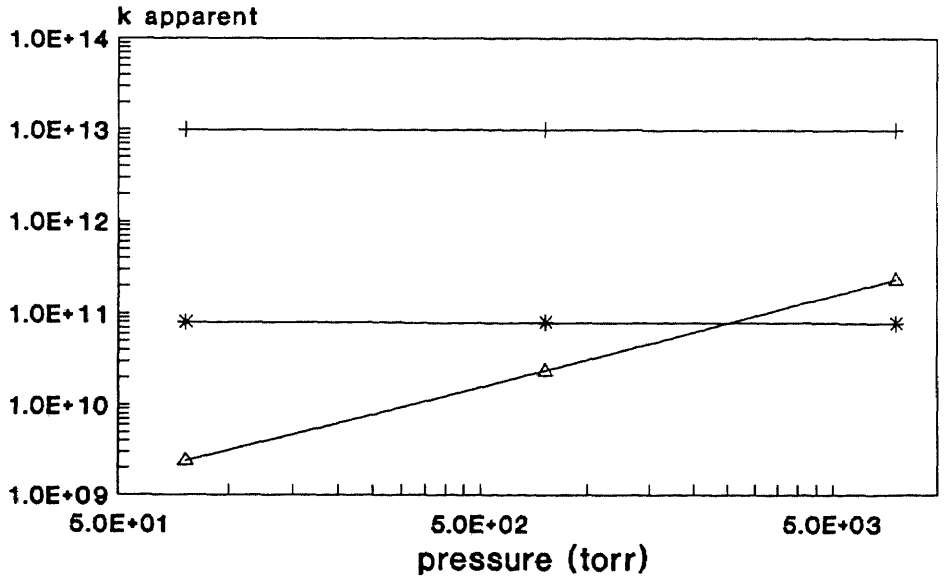

Figure 5.4.2.3 QRRK Analysis: Kapp vs Pressure at 873 K

TABLE 5.4.2B CHEMACT Results for HO_2 + HCO

Products	A	n	Ea	Pressure
HC(*O)OOH	1.64E+20	-3.53	1.84	76 Torr
	1.71E+21	-3.53	1.86	760 Torr
	2.43E+22	-3.57	2.02	7600 Torr
HCO2. + OH	1.24E+13	-0.03	0.05	76Torr
	1.29E+13	-0.03	0.07	760 Torr
	1.89E+13	-0.08	0.23	7600 Torr
H2O + CO2	3.62E+11	-0.21	0.19	76 Torr
	3.77E+11	-0.21	0.21	760 Torr
	5.52E+11	-0.26	0.38	7600 Torr

Valid from 773 - 1273 K

Best Fit Equation $A*T^n \exp(-Ea/RT)$
UNITS: A in cm^3/mole-sec, Ea in Kcal/mole

The energy diagram for the above reaction is illustrated in Figure 5.4.2.1, and the calculation results are shown in Figure 5.4.2.2 and Figure 5.4.2.3.

5.4.3 OH + HCO Reaction

$$OH + HCO \underset{-1}{\overset{1}{<\!\!\!-\!\!\!-\!\!\!-\!\!\!>}} HCO2H \xrightarrow{2} CO + H2O$$

$$HCO2H \xrightarrow{3} HOCO + H$$

TABLE 5.4.3A CHEMACT Input Parameters for HCO + OH

k	A	Ea	source
1	5.00E+13	0.00	a
-1	1.36E+17	109.40	b
2	6.31E+12	49.00	c
3	1.19E+15	94.51	d

<v> =1336.4 cm^{-1} e

Lennard Jones PARAMETERS: f

σ = 4.01A^{o} ϵ/k = 460 cal

a: From HCO + OH = H_2O + CO (OH + CH_3 Washida et al.

b: From THERM calculations:
LN (A_f / A_r) = del S / R - (del n) * (ekT)
E_f - E_r = del $H_{(rxn)}$ - del n/RT

c: A_2 = $10^{12.8}$ (transition state theory),
E_2 = del H + 43 NIST data for C_3COH = H_2O + $C_2C{=}C$

d: A_3 and E_3 calculated using THERM where A_{-3} was taken from H + CC. 2.8E+13 (Tsang, W., 1986) E_{-3} = 0.

e: CPFIT program

f: ϵ/k = $T_c/1.259$, σ = 0.809$V_c^{1/3}$ (Dean, A.M., Bozzelli, J.W., and Ritter, E.R. Combustion Science and Technology, 1991, Vol.80.)
Critical properties T_c and V_c estimated by using Lydersen's Method (Reid, R.C., Prausnitz, J.M., and Sher wood, T.K., The Properties of Gases and Liquids McGraw-Hill Book Company.)

UNITS: A in cc/mol sec and sec^{-1}, Ea in kcal/mol

TABLE 5.4.3B CHEMACT Results for OH + HCO

Products	A	n	Ea	Pressure
HCOOH	4.64E+26	-5.02	4.34	76 Torr
	5.37E+27	-5.03	4.42	760 Torr
	1.41E+29	-5.14	5.03	7600 Torr
H2O + CO	6.15E+22	-2.84	3.67	76Torr
	7.19E+22	-2.86	3.75	760 Torr
	2.07E+23	-2.98	4.38	7600 Torr
HOCO + H	2.54E+16	-1.01	2.33	76 Torr
	3.11E+16	-1.03	2.42	760 Torr
	1.42E+17	-1.21	3.14	7600 Torr

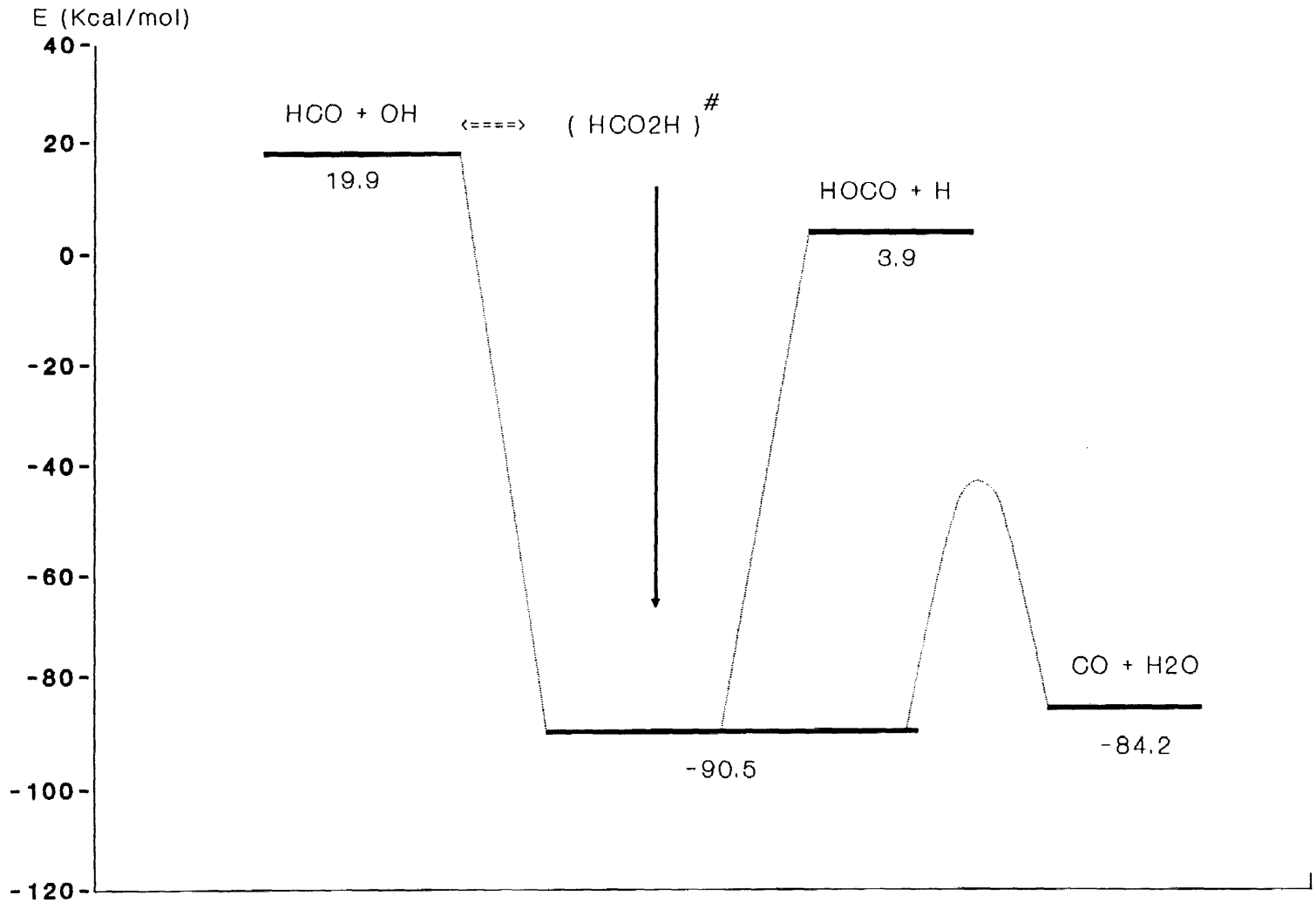

Figure 5.4.3.1 Potential Energy Diagram for HCO + OH

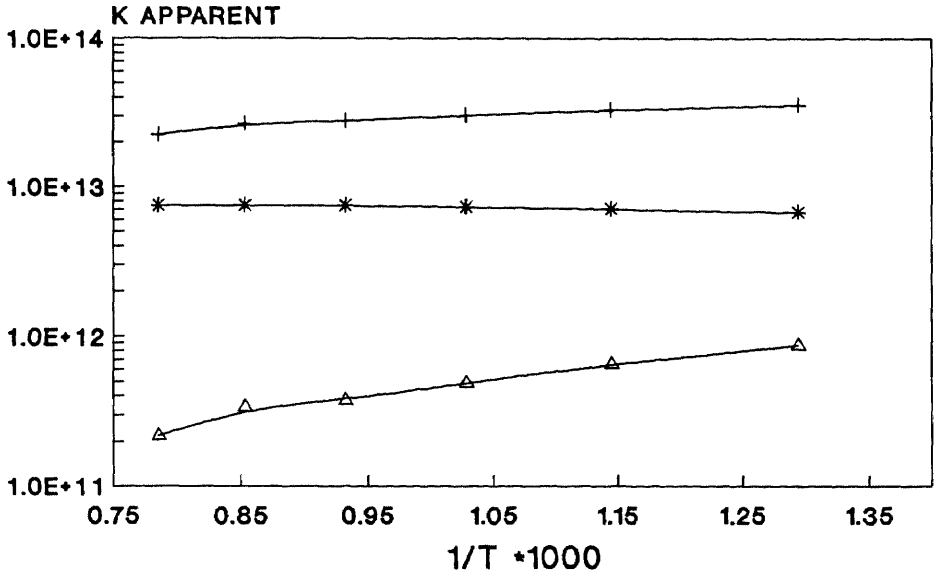

Figure 5.4.3.2 QRRK Analysis: Kapp vs 1/T at 760 Torr

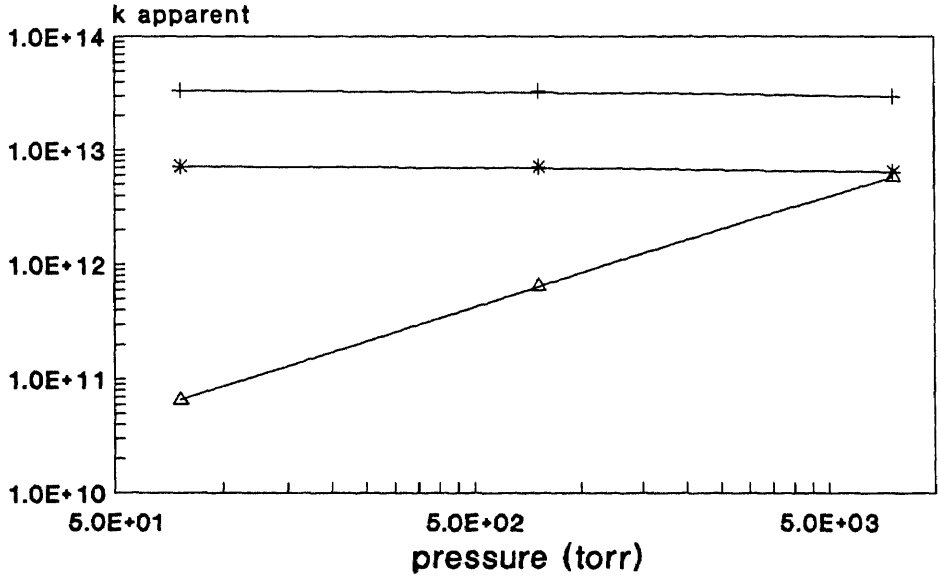

Figure 5.4.3.3 QRRK Analysis: Kapp vs Pressure at 873K

Valid from 773 - 1273 K

Best Fit Equation $A*T^n \exp(-Ea/RT)$

UNITS: A in cm^3/mole-sec, Ea in Kcal/mole

The energy diagram of the reaction system is shown in Figure 5.4.3.1,and the calculation results are shown in Figure 5.4.3.2 and Figure 5.4.3.3.

5.4.4 OH + C*C*O Reaction

$$OH + C*C*O \underset{-1}{\overset{1}{<\!\!\!\!>}} CH2OHC.*O \xrightarrow{2} C.H2OH + CO$$

$$CH2OHC.*O \underset{-4}{\overset{4}{<\!\!\!\!>}} CH2O.CHO \xrightarrow{5} CH2O + HCO$$

TABLE 5.4.4A CHEMACT Input Parameters for OH + C*C*O

k	A	Ea	source
1	7.00E+12	0.45	a
-1	1.05E+14	40.96	b
2	1.44E+11	22.49	c
4	8.50E+12	52.00	d
-4	8.34E+12	35.94	e
5	8.32E14	11.09	f
<v> = 988 cm^{-1}			g
Lennard Jones PARAMETERS:			h
σ = 4.49A^o		ϵ/k = 472 cal	

a: From O + CH_2CHCH_3 (Cvetanovic, R.J. NIST)

b: From THERM calculations: microscopic reversibility
LN (A_f / A_r) = del S / R - (del n) * (ekT)
$E_f - E_r$ = del $H_{(rxn)}$ - del n/RT

c: A_2, E_2 calculated from THERM, CH_3 + CO A_{-2}=5.19E+11, E_{-2}=6.56 Kcal/mol (Anastasic, C. et al. J. Chem. Soc., Faraday Trans. I, 78, 2423, 1982) microscopic reversibility

d: $A_4=(10^{13.56-4/4.6})*2$, E_4=25 Kcal/mol (Benson, 1990)

e: calculated from THERM, microscopic reversibility

f: calculated from THERM, A_{-5}=5.19E+11, E_{-5}=6.56 Kcal/mol, which are taken from CC. + CO., treat E_a as addition, microscopic reversibility.

g: CPFIT program

h: $\epsilon/k = T_c/1.259$, $\sigma = 0.809V_c^{1/3}$ Dean, A.M., Bozzelli, J.W., and Ritter, E.R. Combustion Science and Technology, 1991, Vol.80. Critical properties T_c and V_c estimated from $C_2H_4O_2$ Acetic Acid data using Lydersen's Method

(Reid, R.C., Prausnitz, J.M., and Sherwood, T.K., The Properties of Gases and Liquids McGraw-Hill Book Company.)

UNITS: A in cc/mol sec and sec^{-1}, Ea in kcal/mol

TABLE 5.4.4B CHEMACT Results for OH + C*C*O

Products	A	n	Ea	Pressure
CH2OHC.*O	1.48E+19	-2.91	2.02	76 Torr
	1.81E+20	-2.93	2.13	760 Torr
	4.83E+21	-3.04	2.90	7600 Torr
C.H2OH + CO	5.18E+14	-0.56	1.36	76 Torr
	6.37E+14	-0.58	1.47	760 Torr
	1.77E+15	-0.70	2.24	7600 Torr
CH2O.CHO	7.91E+05	-0.45	13.56	76 Torr
	9.40E+06	-0.47	13.65	760 Torr
	2.77E+08	-0.59	14.34	7600 Torr
CH2O + HCO	7.96E+03	2.06	13.71	76 Torr
	9.58E+03	2.04	13.80	760 Torr
	3.21E+04	1.90	14.51	7600 Torr

Valid from 773 - 1273 K

Best Fit Equation $A*T^n \exp(-Ea/RT)$
UNITS: A in cm^3/mole-sec, Ea in Kcal/mole

The energy diagram for the above reaction is illustrated in Figure 5.4.4.1, and the calculation results are shown in Figure 5.4.4.2 and Figure 5.4.4.3.

5.4.5 C2H4 = C2H3 + H Reaction

$$C2H4 \xrightarrow{1} C2H2 + H2$$

$$\xrightarrow{2} C2H3 + H$$

TABLE 5.4.5A DISSOC Input Parameters for C2H4

k	A	Ea	source
1	3.16E+13	76.00	a
2	2.60E+17	96.56	b
<v> = 1588 cm^{-1}			c
Lennard Jones PARAMETERS:			d
σ = 4.16A^{o}		ϵ/k = 224 cal	

a: H_2 elimination data from C_2H_4 study (Lee, Y.T. ACS Meeting, August 1991, NYC. Also Lee et al, JPC, 1992)

b: From NIST

c: CPFIT program

d: $\epsilon/k = T_c/1.259$, $\sigma = 0.809V_c^{1/3}$ (Dean, A.M., Bozzelli, J.W., and Ritter, E.R. Combustion Science and Technology, 1991, Vol.80.)
Critical properties T_c and V_c estimated using Lydersen's Method, Reid, R.C., Prausnitz, J.M., and Sherwood, T.K., The Properties of Gases and Liquids McGraw-Hill Book Company.

UNITS: A in cc/mol sec and sec^{-1}, Ea in kcal/mol

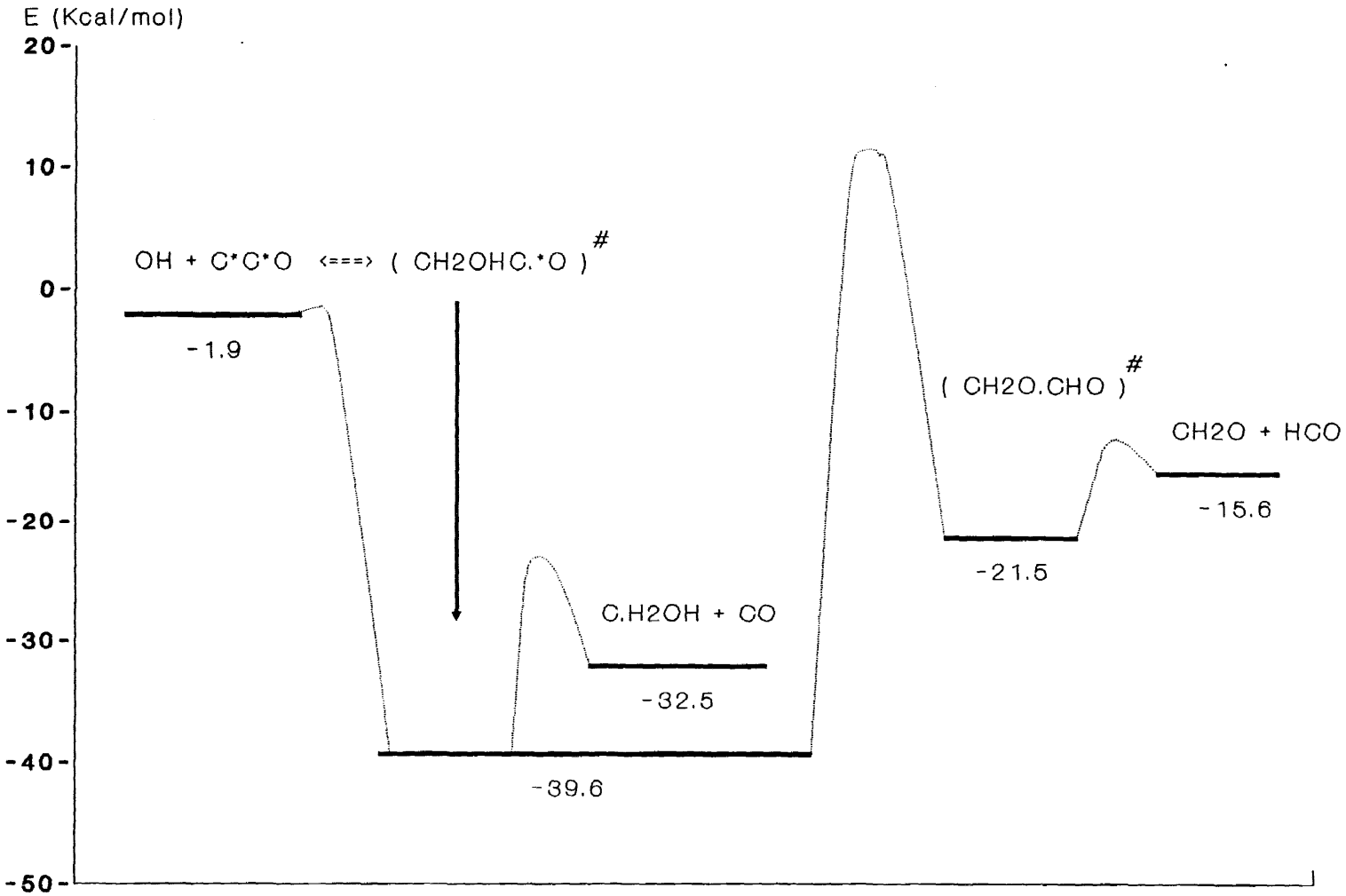

Figure 5.4.4.1 Potential Energy Diagram for OH + C*C*O

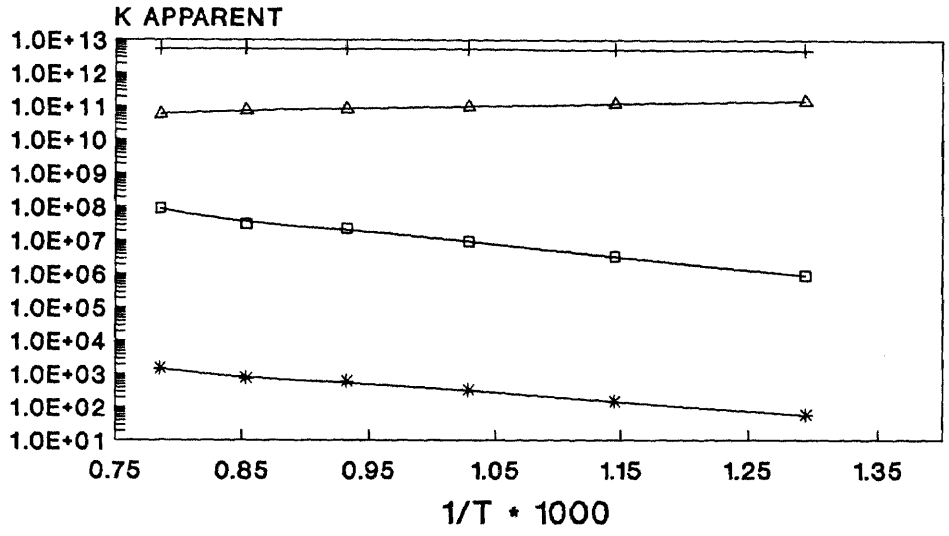

Figure 5.4.4.2 QRRK Analysis: Kapp vs 1/T at 760 Torr

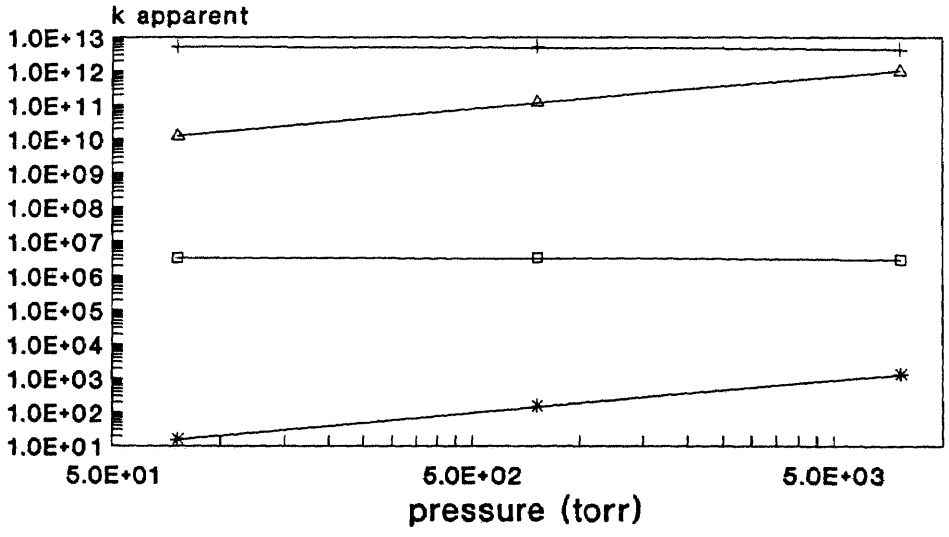

Figure 5.4.4.3 QRRK Analysis: Kapp vs Pressure at 873 K

TABLE 5.4.5B DISSOC Results for C2H4

Products	A	n	Ea	Pressure
C2H2 + H2	6.05E+32	-5.90	88.64	76 Torr
	1.74E+28	-4.49	86.81	760 Torr
	7.36E+26	-4.07	86.21	7600 Torr
C2H3 + H	3.48E+42	-8.49	107.77	76 Torr
	5.01E+43	-8.53	108.05	760 Torr
	9.34E+43	-8.29	108.81	7600 Torr

Valid from 773 - 1023 K

Best Fit Equation $A*T^n \exp(-Ea/RT)$

UNITS: A in cm^3/mole-sec, Ea in Kcal/mole

5.4.6 C2H5 = C2H4 + H Reaction

C2H5 ---> C2H4 + H

TABLE 5.4.6A DISSOC Input Parameters for C2H5

k	A	Ea	source
1	2.00E+13	39.68	a
<v> = 1403 cm^{-1}			b
Lennard Jones PARAMETERS:			c
σ = 4.30A^{o}	ϵ/k = 220 cal		

a: From NIST (Warnatz,J., Rate Coefficients in the C/H/O System, Combustion Chemistry, Spring-Verlag, NY,1984)

b: CPFIT program

c: $\epsilon/k = T_c/1.259$, $\sigma = 0.809V_c^{1/3}$ (Dean, A.M., Bozzelli, J.W., and Ritter, E.R. Combustion Science

and Technology, 1991, Vol.80.)
Critical properties T_c and V_c estimated using Lydersen's Method, Reid, R.C., Prausnitz, J.M., and Sherwood, T.K., The Properties of Gases and Liquids McGraw-Hill Book Company.

UNITS: A in cc/mol sec and sec^{-1}, Ea in kcal/mol

TABLE 5.4.6B DISSOC Results for C2H4

Products	A	n	Ea	Pressure
C2H4 + H	1.55E+33	-6.19	47.82	76 Torr
	6.77E+21	-2.70	43.20	760 Torr
	6.84E+16	-1.18	40.97	7600 Torr

Valid from 773 - 1023 K

Best Fit Equation $A*T^n \exp(-Ea/RT)$
UNITS: A in cm^3/mole-sec, Ea in Kcal/mole

5.5 Kinetic Mechanism

The QRRK calculations were used to estimate apparent rate parameters for addition, recombination, and elementary dissociation reactions. Elementary reaction rate parameters for abstraction reactions are based upon literature comparisons, thermodynamic estimation, and thermochemical methods of Benson<27>.

The reaction mechanism for combustion of chlorobenzene was modified. We started with the mechanism developed by Yang(10) and corrected this. We then added a series of benzene oxidation and pyrolysis reactions. Many the of reactions in the chlorobenzene pyrolysis study by E. Ritter, et al were used as a starting point for the pyrolysis products. The final mechanism composed of 220

elementary reactions, which appears in Appendix B, was found to fit experimental results well in the temperature range from 600 to 630°C.

Experimental data are compared with model predictions in Figure 5.5.1 through Figure 5.5.10 for chlorobenzene decomposition and benzene formation. Figure 5.5.1 through Figure 5.5.5 demonstrate that the experimental data and model prediction are close at 610°C in all residence times and O_2/H_2 ratios. Figure 5.5.6 through Figure 5.5.10 show the experiment and model comparison over the temperature range of this study. The model predictions at 600°C to 630°C are satisfactory. However, at 590°C, the model predicts by 20% less chlorobenzene than is desired (overpredicts decomposition) and overpredicts benzene formation by 20%. The model prediction at 5% O_2/H_2 is much closer to experimental observations, only 5% underprediction occurs for the chlorobenzene level (still overpredicts decomposition). At 640°C reactor temperature and all of the oxygen to hydrogen ratios, the model overpredicts by 15% for chlorobenzene decomposition. The model prediction on benzene formation at this temperature changes from 15% underprediction when the oxygen to hydrogen ratio is one to 15% overprediction when the oxygen to hydrogen ratio is five.

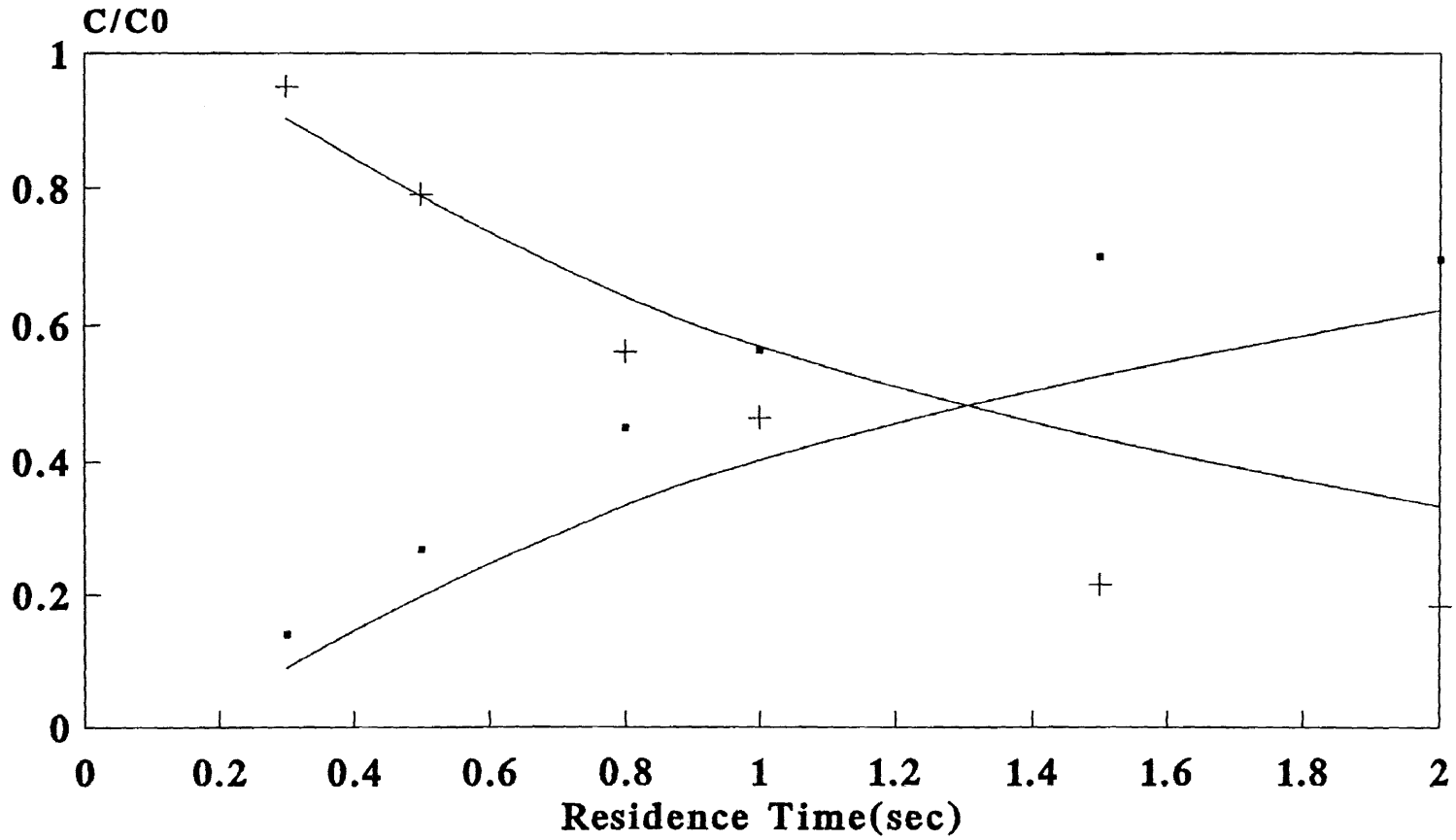

Figure 5.5.1 Model and Experiment Comparison

610 °C, O2/H2=1%

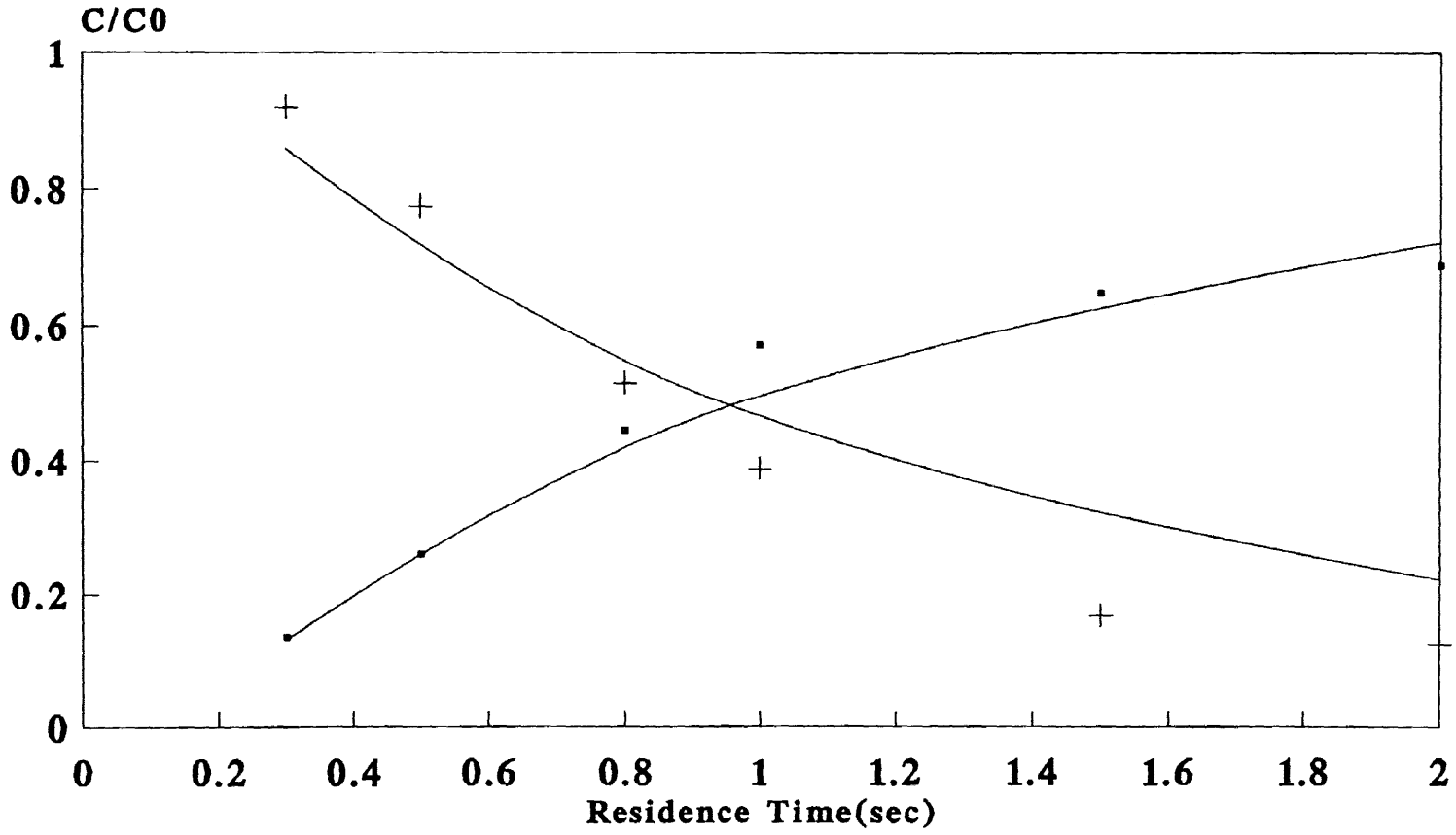

Figure 5.5.2 Model and Experiment Comparison
610 °C, O2/H2=2%

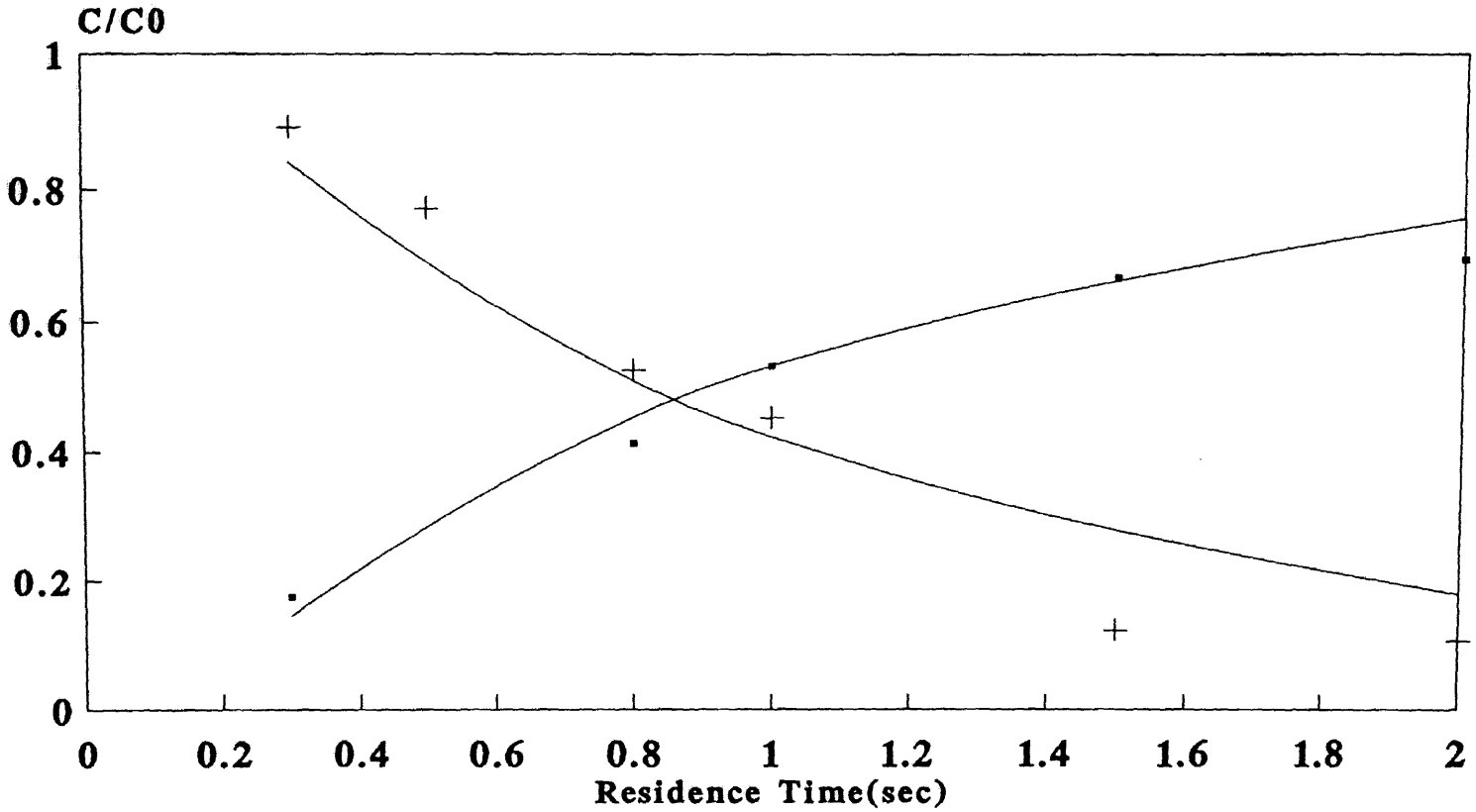

Figure 5.5.3 Model and Experiment Comparison

610 °C, O2/H2=3%

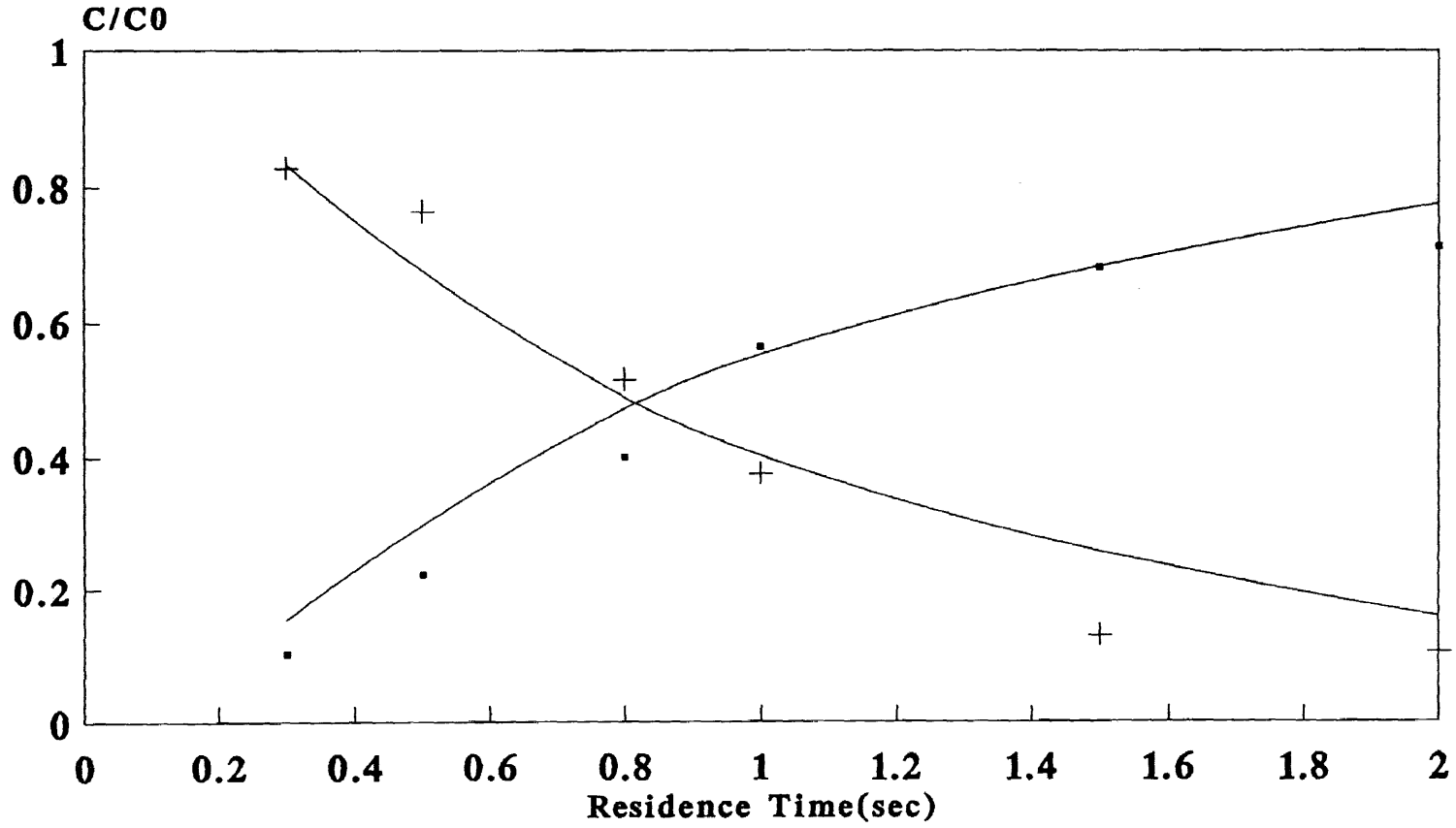

Figure 5.5.4 Model and Experiment Comparison

610 °C, O2/H2=4%

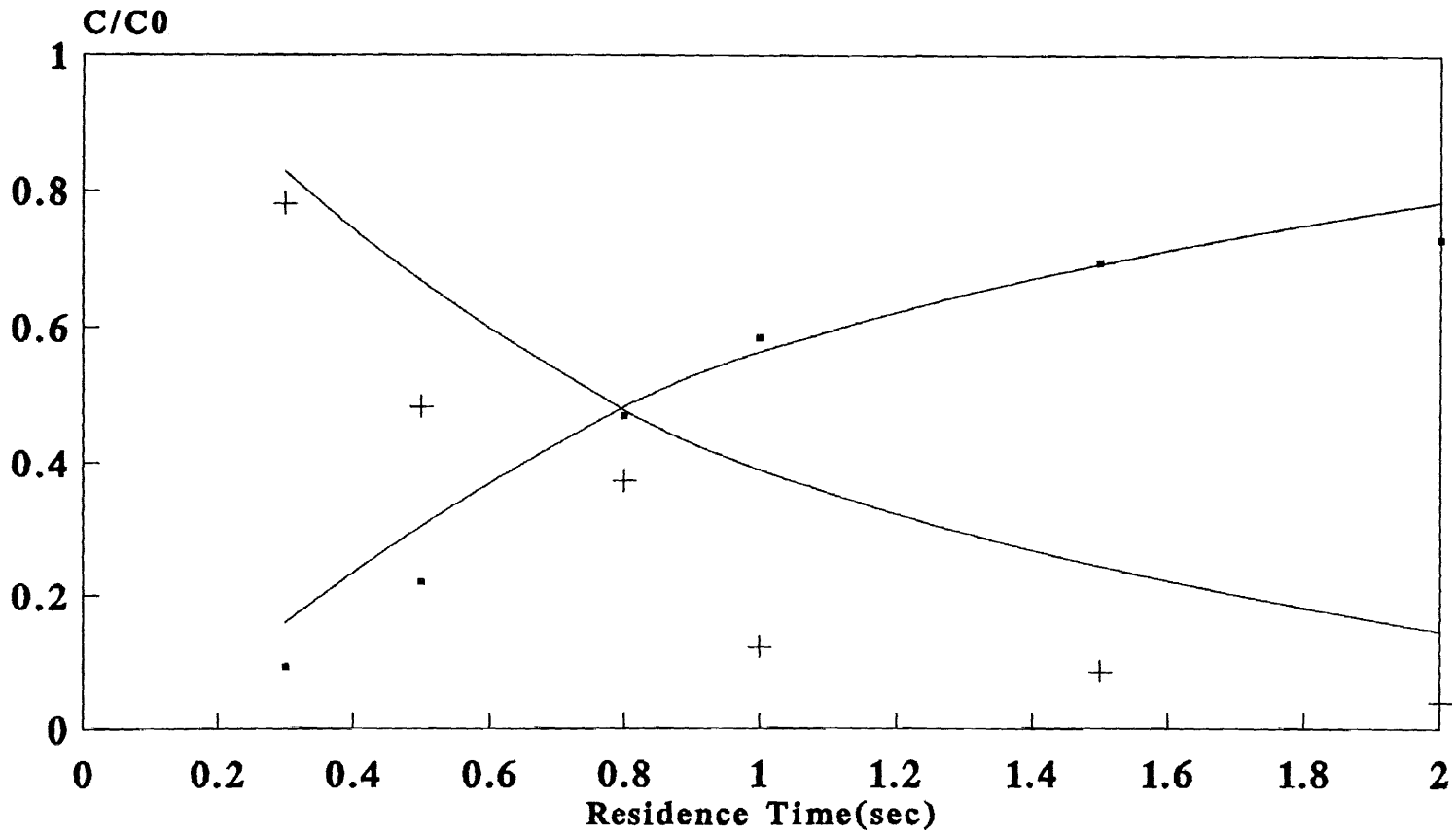

Figure 5.5.5 Model and Experiment Comparison

610 °C, O2/H2=5%

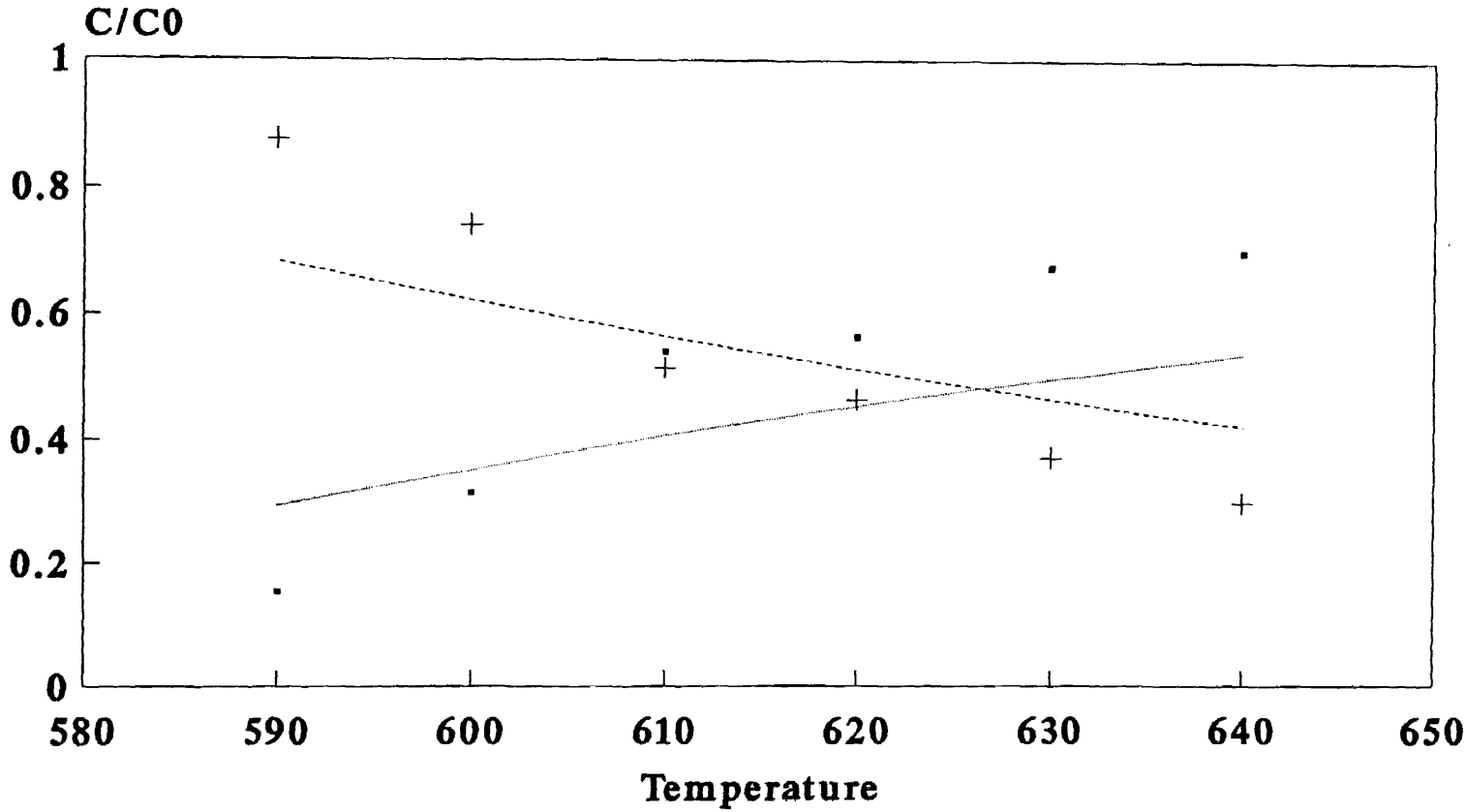

Figure 5.5.6 Model and Experiment Comparison

Residence Time=1.0 sec, O2/H2=1%

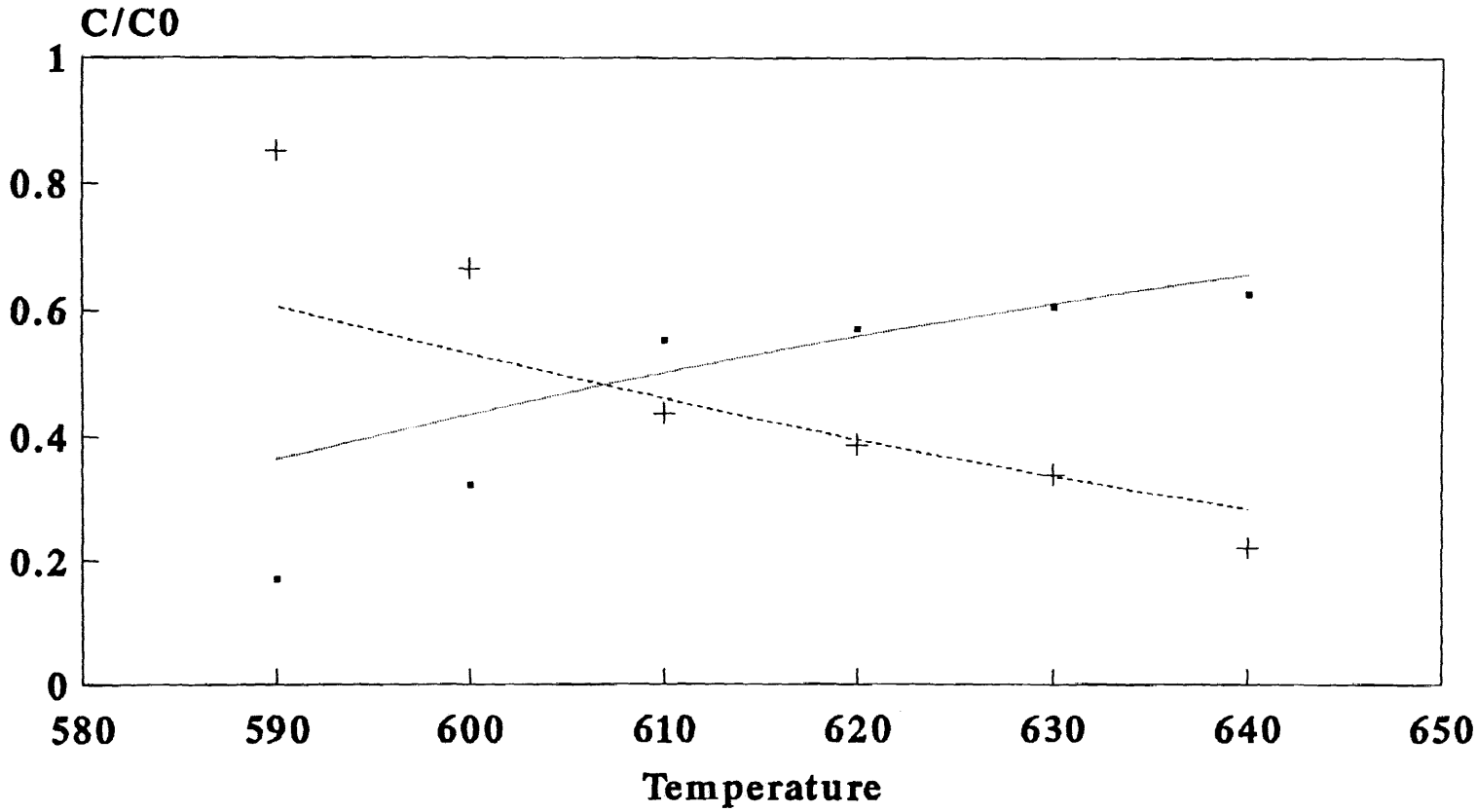

Figure 5.5.7 Model and Experiment Comparison

Residence Time=1.0 sec, O2/H2=2%

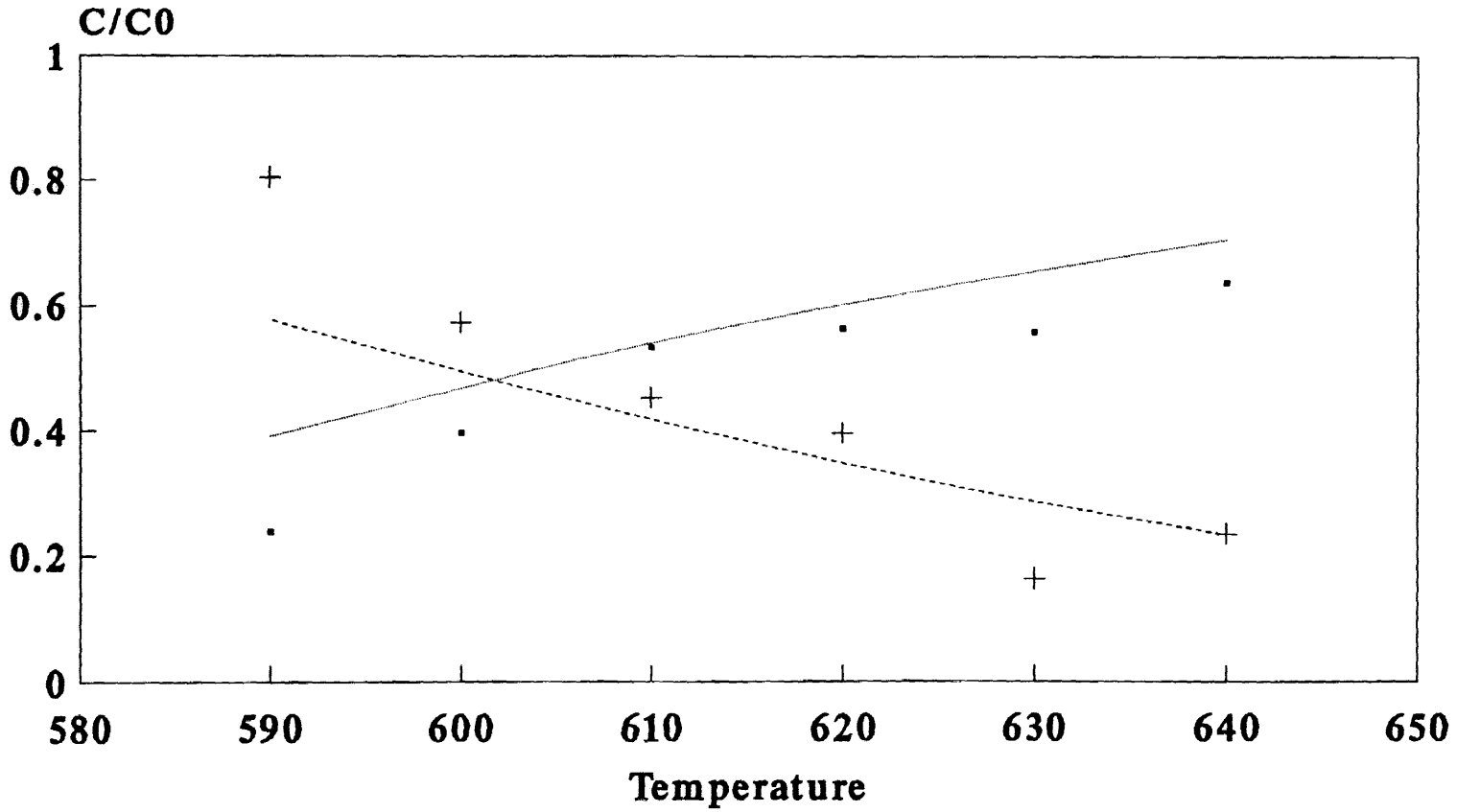

Figure 5.5.8 Model and Experiment Comparison

Residence Time=1.0 sec, O2/H2=3%

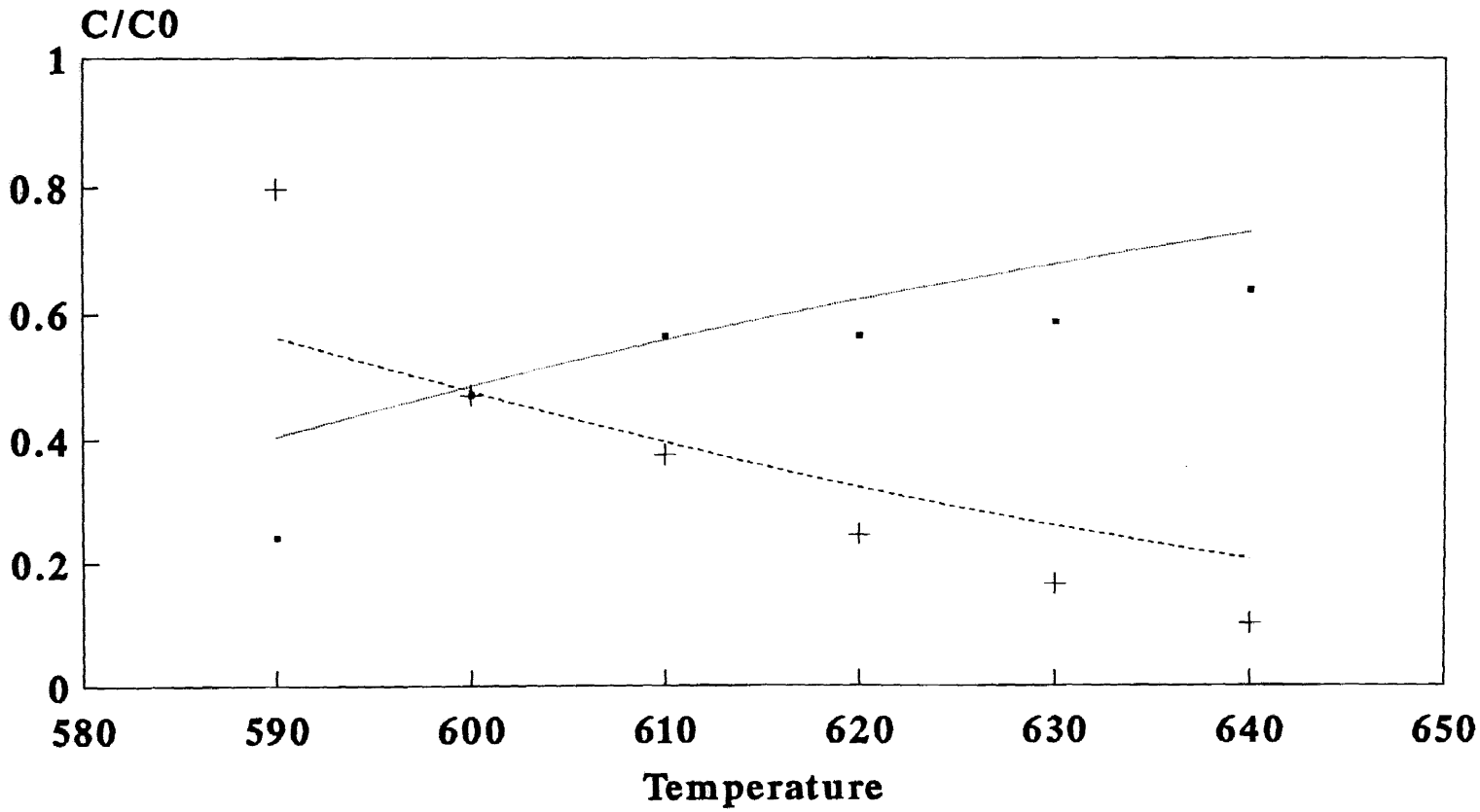

Figure 5.5.9 Model and Experiment Comparison

Residence Time=1.0 sec, O2/H2=4%

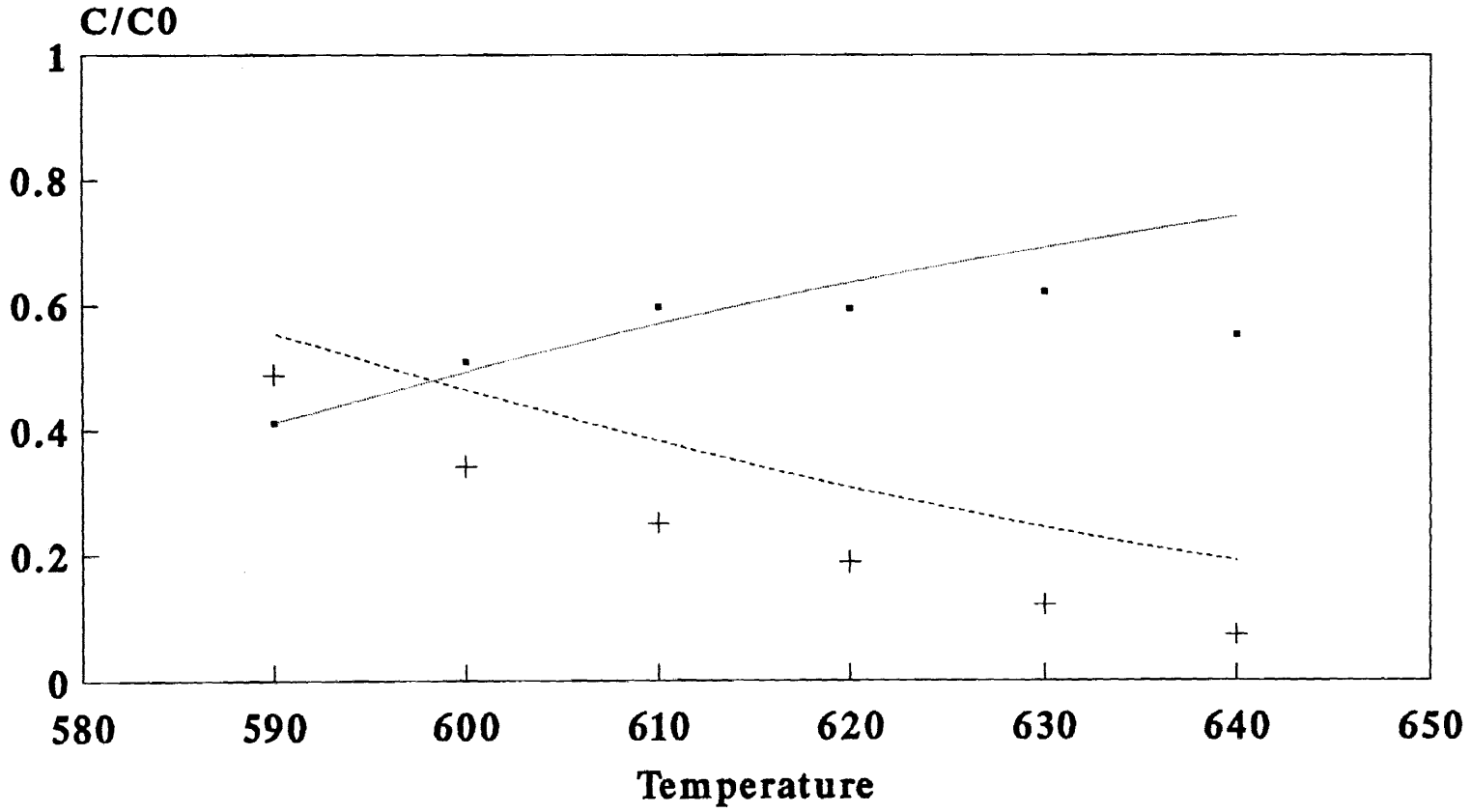

Figure 5.5.10 Model and Experiment Comparison

Residence Time=1.0 sec, O2/H2=5%

CHAPTER 6
CONCLUSION

The study of chlorobenzene decomposition in hydrogen bath gas and low concentrations of oxygen (1% - 5%) was carried out in 10.5 mm tubular flow reactor at 1 atmosphere pressure. Temperature ranged from 590 to 640^{o}C and residence times ranged from 0.3 to 2.0 seconds.

95% decomposition of chlorobenzene occurred at 620^{o}C, O_2/H_2 = 5%, and two seconds residence time. Increases in temperature, oxygen concentration, and residence time accelerated the chlorobenzene decomposition. The major products are benzene and HCl, and the minor products are CH_4, C_2H_4, and C_2H_6. Toluene and C_2H_2 were observed in several experiment conditions.

Oxygen concentration has a very significant effect on the decomposition of chlorobenzene. The reaction of chlorobenzene decomposition occurred faster when more oxygen was added. The higher oxygen concentration, the lower temperature needed for reaction.

The kinetic reaction mechanism which was initially developed by Yang was improved and further modified by adding benzene oxidation and pyrolysis reactions. The experiment data showed that benzene began to be decomposed at 620^{o}C, one second residence time, and 5% product in this study. Over the temperature range of 600^{o}C to 630^{o}C, the model predictions of chlorobenzene

decomposition and benzene formation at one second residence time and 1% to 5% oxygen and hydrogen ratio showed reasonable agreement with experiment results, and model development is on going.

BIBLIOGRAPHY

1 Shaub, W.M. and Tsang W., Environ. Sci. Technol., Vol 7, No. 12, 721 - 730 (1983)

2 Harris, J. C., Anderson, P. C., Goodwin, B. E. and Rechsteiner, C. E., "Dioxin Emission from Combustion Sources: A Review of the Current State of Knowlege", Final Report to ASME, ASME, New York, NY (1980)

3 Graham, J.L., Hall, D.L. and Dellinger, B., Environ. Sci. Tech., 20, 703 (1986)

4 Deichman, W., "Patty's Industrial Hygiene and Toxicology", Vol. II B, 3rd ed., ed. by Clayton,G. and Clayton, F. New York, Willey Interscience, (1981)

5 Rubey, W. A., Dellinger, B., Hall, D. L. and Mazerb, S. L., Chemosphere, 14, 1483 (1985)

6 Gochfeld, M., Gallo, M. and Kahn, P., New Jersey Medicine, Vol 85, 907 (1988)

7 Louw, R., Dijks, J. H. and Mulder, P., J. Chem. and Industry, Oct. 3, 759 (1983)

8 Ritter, E. R., M. Sc. Thesis, NJIT (1986), J. Phys. Chem. accepted July 1989.

9 Ritter, E. R., Bozzelli, J. W., Hazardous Waste and Hazardous Material, 3, 103, (1990)

10 Yang, C.C., M. Sc. Thesis, NJIT (1989)

11 Cullis, C. and Priday, Proc. Roy. Soc. London A, 224, 08 (1954)

12 Cullis, C., Manton, Transcripts of the Faraday Soc., 54, 381 (1958)

13 Louw, R., Dijks, J. H. and Mulder, P., J. of Chemical Soc. Perkin Trans II, 40, 1635 (1973)

14 Manion, J. A., Mulder, P. and Louw, R., Environ. Sci. Technol., Vol. 19, 280 (1985)

15 Yang, Y.D., Ph. D. Thesis, New Jersey Institute of Technology (1986)

16 Hung, M., M. Sc. Thesis, NJIT (1986)

17 Zhu, L. J.,M. Sc. Thesis, NJIT (1988)

18 Cui, J. P., He, Y. Z., and Tsang, W., J. Phys. Chem., Vol 93, pp 724-727 (1989)

19 Madronich, S. and Felder, W., J. Phys. Chem., Vol 89, pp 3556-3561 (1985)

20 Venkat, C., Brezinsky, K., and Glassman, I., Nineteenth Symposium (International) on Combustion/The Combustion Institute, (1982)

21 Bozzelli, J.W., Desai, V., Ritter, E.R., and Dean, A.M., paper accepted

22 Brezinsky, K., Prog. Energy Combust. Sci. 12, 1986,

23 Bittker, D. A., Technical Meeting 1988, Central States Section, The Combustion Institute.

24 Tsang, W., The Eastern Section Meeting of the Combustion Institute, Orlando, FL, Dec.,(1990)

25 Tsang, W., Combustion Sci. and Tech., 74, 99, (1990)

26 Bozzelli, J. W. and Ritter, E. R., Int. J. Chem. Kinet., 1991

27 Benson, S. W., Thermochemical Kinetics, John Wiley and Son, NY, 1976

28 NIST, Chemical Kinetics Database, version 2.0, User's Manual (1990)

29 Kassel, L. S., J. Phys. Chem. 32, 1928, 1065.

30 Dean, A. M., J. Phys. Chem. 89, 1985, 4600.

31 Troe, J., J. Chem. Phys., 66, 1977

32 Dean, A.M., Bozzelli, J.W., and Ritter, E.R., Combust. Sci. and Tech., Vol. 80, 1991

33 Robison, P.J. and Holbrook, K.A., Unimolecular Reactions, John-Wiley, NY (1972)

34 Ritter, E.R., Ph.D Thesis, NJIT, (1988)

35 Chang, S.H. and Bozzelli, J.W., AIChE J., 33, (1987)

36 Frenklach, M., Ramachandra, M., Matula, A.,Symposium (Int.) on Combustion, 20, 871 (1984)

37 Dean, A. M., J. Phys. Chem., 89, 4600 (1985)

38 Westmoreland, P.R. and Dean, A.M., AIChE J., 32, 171 (1986)

39 Ritter, E, and Bozzelli, J.W. and Dean, A.M.'s paper Accepted in J. Phys. Chem. (1989)

40 Kern, R.D., Xie, K., and Chen, H., "A Shock Tube Study of Chlorobenzene Pyrolysis"

APPENDIX A
List of Thermo Data

UNITS:KCAL

thermo data for chlorobenzene decomposition

SPECIES	HF(298)	S(298)	CP300	CP400	CP500	CP600	CP800	CP1000	CP1500	DATE	REF		ELEMENTS				
CO	-26.40	47.20	6.67	6.85	7.02	7.18	7.47	7.72	8.20		121286	C	1 O	1	0	0 G 0	
CO2	-94.01	51.00	8.91	9.80	10.55	11.17	12.13	12.80	13.73		121286	C	1 O	2	0	0 G 0	
HCO	10.40	53.60	8.37	8.85	9.32	9.78	10.65	11.42	12.80		121286	H	1 C	1 O	1	0 G 0	
HO2	3.50	54.70	8.28	8.78	9.26	9.71	10.50	11.16	12.24		20387	H	1 O	2	0	0 G 0	
O	59.51	38.40	5.00	5.00	5.00	5.00	5.00	5.00	5.00		120186	O	1	0	0	0 G 0	
H	52.10	27.30	4.90	4.90	4.90	4.90	4.90	4.90	4.90			H	1	0	0	0 G 0	
H2	0.00	31.20	6.79	6.90	7.00	7.09	7.25	7.37	7.60			H	2	0	0	0 G 0	
CH3	34.80	46.30	9.12	9.91	10.68	11.41	12.75	13.90	16.00		J 6/69	C	1 H	3	0	0 G 0	
CH4	-17.90	44.40	9.07	10.14	11.25	12.37	14.54	16.50	20.02		J 3/61	C	1 H	4	0	0 G 0	
O2	0.00	49.00	6.86	7.10	7.33	7.54	7.89	8.18	8.70			O	2	0	0	0 G 0	
OH	9.50	43.80	6.73	6.81	6.88	6.96	7.10	7.23	7.50			O	1 H	1	0	0 G 0	
BICYC6H5O	42.30	73.81	23.45	29.97	35.36	39.82	46.53	51.18	58.08	3/15/90	THERM	C	6 H	5 O	1	0 G 0	
CH2CO	-14.60	57.81	12.88	15.14	16.88	18.22	20.15	21.54	23.69		12/83	C	2 H	2 O	1	0 G 0	
C*C*O	-14.60	57.81	12.88	15.14	16.88	18.22	20.15	21.54	23.69		12/83	C	2 H	2 O	1	0 G 0	
C*C*C	45.90	58.31	14.29	16.95	19.57	21.97	25.65	27.68	32.00		AP153	C	3 H	4	0	0 G 0	
CYC5H5CHO	3.87	80.45	25.01	32.49	38.71	43.82	51.42	56.45	63.11	5/ 2/91	THERM	C	6 H	6 O	1	0 G 1	
CYC5H5CO	37.77	81.51	24.84	31.83	37.50	42.06	48.61	52.78	58.36	5/ 2/91	THERM	C	6 H	5 O	1	0 G 1	
C6H5OH	-22.30	75.18	24.45	32.02	38.21	43.25	50.65	55.60	62.73	5/ 2/91	THERM	C	6 H	6 O	1	0 G 1	
CYC6H5O	12.10	72.58	23.14	30.07	35.74	40.37	47.19	51.77	58.38	5/ 2/91	THERM	C	6 H	5 O	1	0 G 0	
C6H5O.	12.10	72.58	23.14	30.07	35.74	40.37	47.19	51.77	58.38	5/ 2/91	THERM	C	6 H	5 O	1	0 G 0	
CY13PD	31.26	65.50	18.23	24.76	30.15	34.59	41.25	45.81	52.50	5/ 2/91	THERM	C	5 H	6	0	0 G 0	
CY13PD5.	57.17	63.58	17.86	24.30	29.47	33.58	39.46	43.26	48.68	5/ 2/91	THERM	C	5 H	5	0	0 G 0	
CYC5H5OH	-9.02	75.33	22.08	29.03	34.72	39.34	46.15	50.72	57.40	5/ 2/91	THERM	C	5 H	6 O	1	0 G 1	
CYC5H5O.	42.94	72.73	20.60	27.20	32.60	36.99	43.44	47.73	53.79	5/ 2/91		C	5 H	5 O	1	0 G 0	
CPDOOH	6.38	84.88	26.88	34.57	40.75	45.69	52.76	57.34	63.76	5/ 2/91	THERM	C	5 H	6 O	2	0 G 2	

CYC5H4OH	16.88	75.23	21.69	28.61	34.08	38.38	44.34	48.04	53.24	5/ 2/91		C	5	H	5	O	1	0 G 1
CYPDONE	8.41	71.08	16.56	22.03	26.86	31.07	37.79	42.52	48.45	5/ 2/91	THERM	C	5	H	4	O	1	0 G 0
C*CC*CCO	-2.49	80.16	25.33	31.48	36.53	40.67	46.85	51.12	57.47	5/ 2/91	THERM	C	5	H	6	O	1	0 G 2
C.OC*CC*C	31.41	81.22	25.17	30.79	35.34	38.99	44.30	47.84	53.03	5/ 7/91		C	5	H	5	O	1	0 G 2
C*CC*C	26.08	66.61	19.23	24.25	28.39	31.81	37.00	40.69	46.53	5/ 6/91	THERM	C	4	H	6		0	0 G 1
C*CC*C.	83.99	69.05	19.06	23.57	27.22	30.15	34.45	37.38	42.05	5/ 6/91	THERM	C	4	H	5		0	0 G 1
COC*CCO	-44.62	78.19	22.50	27.30	31.34	34.70	39.82	43.33	48.10	5/ 6/91	THERM	C	4	H	4	O	2	0 G 2
CC*CCO	-22.12	77.49	21.12	25.76	29.90	33.59	39.67	44.25	50.89	5/ 6/91	THERM	C	4	H	6	O	1	0 G 2
CC*CC.O	7.78	78.55	20.99	25.11	28.74	31.91	37.07	40.88	46.35	5/ 6/91	THERM	C	4	H	5	O	1	0 G 2
C*CC#C	68.18	66.78	17.46	21.43	24.69	27.37	31.33	34.01	37.85	5/ 6/91	THERM	C	4	H	4		0	0 G 1
C*CCO	-16.05	67.40	16.35	20.04	23.18	25.84	29.99	32.95	37.22	5/ 6/91	THERM	C	3	H	4	O	1	0 G 1
C*CC.O	13.85	68.46	16.19	19.38	22.02	24.20	27.46	29.66	32.75	5/ 6/91	THERM	C	3	H	3	O	1	0 G 1
C.*CCO	41.85	68.46	16.19	19.38	22.02	24.20	27.46	29.66	32.75	5/ 6/91	THERM	C	3	H	3	O	1	0 G 1
C*CC	4.65	63.82	15.45	19.32	22.74	25.75	30.72	34.51	40.34	5/ 6/91	THERM	C	3	H	6		0	0 G 1
C*CC.	40.75	63.02	14.96	18.61	21.75	24.43	28.67	31.74	36.33	5/ 6/91	THERM	C	3	H	5		0	0 G 1
CC#C	44.28	59.29	13.98	16.64	19.07	21.28	25.00	27.86	31.94	5/ 7/91		C	3	H	4		0	0 G 1
C#CC.	82.39	58.49	14.14	16.52	18.58	20.37	23.20	25.22	27.87	5/ 6/91	THERM	C	3	H	3		0	0 G 1
C2H4	12.52	52.47	10.27	12.79	15.01	16.95	20.13	22.55	26.34	5/ 6/91	THERM	C	2	H	4		0	0 G 0
C2H3	70.43	56.29	10.08	12.12	13.85	15.31	17.60	19.26	21.86	5/ 6/91	THERM	C	2	H	3		0	0 G 0
C2H2	53.86	48.02	10.53	11.86	12.92	13.76	15.00	15.92	17.71	5/ 6/91	THERM	C	2	H	2		0	0 G 0
C2H6	-20.40	55.09	12.41	15.79	18.82	21.53	26.07	29.59	35.08	5/ 6/91	THERM	C	2	H	6		0	0 G 1
C2H5	28.14	59.00	11.64	14.57	17.14	19.38	23.05	25.86	30.34	5/ 6/91	THERM	C	2	H	5		0	0 G 1
CC*C.	62.56	64.88	15.29	18.64	21.56	24.10	28.18	31.22	35.87	5/ 6/91		C	3	H	5		0	0 G 1
CH3OH	-48.00	57.31	10.42	12.38	14.23	15.97	19.00	21.42	25.12	5/ 7/91	THERM	C	1	H	4	O	1	0 G 1
CH3O.	3.96	54.70	8.98	10.57	12.14	13.64	16.33	18.48	21.60	5/ 7/91	THERM	C	1	H	3	O	1	0 G 0
CH2O	-26.00	50.92	8.48	9.49	10.51	11.51	13.33	14.82	16.98	5/ 7/91	THERM	C	1	H	2	O	1	0 G 0
H2O2	-32.60	55.70	10.53	11.76	12.74	13.50	14.58	15.29	16.50	5/ 7/91	THERM	H	2	O	2		0	0 G 1
H2O	-57.80	43.72	8.17	8.88	9.56	10.20	11.30	12.10	12.98	5/ 7/91	THERM	H	2	O	1		0	0 G 0
CYC6H7	49.93	73.40	20.89	28.63	35.11	40.51	48.73	54.44	62.62	5/ 7/91	THERM	C	6	H	7		0	0 G 0
MECY24PD	23.04	73.60	23.54	31.73	38.51	44.11	52.55	58.39	66.99	5/ 7/91	THERM	C	6	H	8		0	0 G 1
MECY24PD1	48.94	73.50	23.13	31.25	37.82	43.11	50.78	55.85	63.16	5/ 7/91	THERM	C	6	H	7		0	0 G 1
ME.CY24PD	71.59	76.13	22.73	30.51	36.84	41.99	49.56	54.67	62.25	5/ 7/91	THERM	C	6	H	7		0	0 G 1

LINC6H8	39.64	79.37	28.21	35.71	41.77	46.67	53.86	58.83	66.71	5/ 7/91	THERM	C	6	H	8		0	0	G 2
LINC6H7	97.55	81.81	28.03	35.03	40.60	45.01	51.31	55.52	62.23	5/ 7/91	THERM	C	6	H	7		0	0	G 2
C6H5CH3	11.81	76.82	25.16	33.34	40.34	46.31	55.67	62.37	72.04	5/ 7/91	THERM	C	7	H	8		0	0	G 1
CH3CHO	-39.18	63.14	13.17	15.83	18.26	20.47	24.19	27.06	31.22	5/ 8/91	THERM	C	2	H	4	O	1	0	G 1
CH2CHO	5.12	63.72	13.62	15.86	17.78	19.42	22.00	23.89	26.79	5/ 8/91	THERM	C	2	H	3	O	1	0	G 1
C.*C*O	42.58	60.63	11.81	13.35	14.61	15.63	17.13	18.10	19.38	5/ /90		C	2	H	1	O	1	0	G 0
HOOCHO	-67.41	72.53	16.11	18.11	19.89	21.44	23.91	25.64	27.67	5/ 9/91	THERM	C	1	H	2	O	3	0	G 2
O.OCHO	-31.30	68.51	14.15	15.36	16.60	17.83	20.08	21.89	24.09	5/ 9/91	THERM	C	1	H	1	O	3	0	G 1
HOOC.O	-33.50	73.59	16.27	17.89	19.16	20.15	21.49	22.25	23.07	5/ 9/91	THERM	C	1	H	1	O	3	0	G 2
CHOCOOH	-112.71	72.52	17.39	20.52	23.10	25.21	28.32	30.36	32.97	5/ 9/91	THERM	C	2	H	2	O	3	0	G 2
O.COCHO	-60.75	69.92	15.29	18.29	20.74	22.72	25.54	27.25	29.05	5/ 9/91	THERM	C	2	H	1	O	3	0	G 1
COC*COH	-51.61	76.89	19.68	23.22	26.35	29.09	33.54	36.78	41.35	5/ 9/91	THERM	C	3	H	4	O	2	0	G 2
COC*CO.	0.35	74.29	18.19	21.41	24.25	26.74	30.79	33.77	37.88	5/ 9/91	THERM	C	3	H	3	O	2	0	G 0
CH	142.00	43.72	6.97	6.98	7.03	7.13	7.41	7.77	8.74		J12/67	C	1	H	1		0	0	G 0
CH+	388.80	31.79	6.97	6.97	7.02	7.11	7.36	7.65	8.24		J12/71	C	1	H	1	E	-1	0	G 0
CH2	92.35	46.33	8.28	8.62	8.99	9.37	10.15	10.88	12.22		J12/72	C	1	H	2		0	0	G 0
CYC6H10	-1.28	74.27	25.24	34.77	42.74	49.37	59.51	66.64	77.28			C	6	H	10		0	0	G 0
BICYC6H8	39.54	69.19	18.61	27.92	35.67	42.07	51.65	58.08	67.70			C	6	H	8		0	0	G 0
C2	200.24	47.64	10.30	9.44	8.91	8.62	8.50	8.62	8.93			C	2		0		0	0	G 0
CYC6H5	81.37	69.20	18.79	25.18	30.52	34.96	41.70	46.36	53.18			C	6	H	5		0	0	G 0
CYC6H6	19.82	64.34	19.55	26.64	33.07	38.79	48.14	54.77	62.26			C	6	H	6		0	0	G 0
CYC6H7	49.86	72.01	20.79	28.58	35.11	40.53	48.74	54.33	62.33			C	6	H	7		0	0	G 0
CY13PD5	54.30	62.40	17.24	24.03	29.40	33.61	39.46	43.13	49.10			C	5	H	5		0	0	G 0
MECY24PD3	81.76	75.80	22.91	29.99	36.09	41.31	49.58	55.57	64.43			C	6	H	7		0	0	G 0
MECY14PD4	79.66	75.40	22.95	30.01	36.09	41.31	49.57	55.57	64.43			C	6	H	7		0	0	G 0
MECY14PD3	48.06	75.36	23.11	30.25	36.37	41.59	49.85	55.83	64.69			C	6	H	7		0	0	G 0
C*CC*CC*C	39.60	80.70	28.09	35.78	41.91	46.76	53.70	58.32	66.32			C	6	H	8		0	0	G 0
C#CC.*C	115.57	68.20	17.50	20.52	22.98	24.97	27.91	29.93	33.27			C	4	H	3		0	0	G 0
C#CC*C.	126.27	69.60	17.50	20.52	22.98	24.97	27.91	29.93	33.27			C	4	H	3		0	0	G 0
C#CC#C	112.30	59.86	17.19	19.77	21.77	23.29	25.32	26.55	28.72			C	4	H	2		0	0	G 0
C#CC#C.	192.20	62.72	14.98	17.00	18.59	19.82	21.50	22.53	24.21			C	4	H	1		0	0	G 0
C#CC#CC#C	170.66	73.74	20.65	24.21	27.51	30.49	35.35	38.60	40.79			C	6	H	2		0	0	G 0

CYC6H4	112.52	68.88	16.38	22.95	28.22	32.42	38.45	42.42	48.70			C	6	H	4		0	0 G 0
CL	28.90	39.47	5.20	5.34	5.40	5.41	5.35	5.30	5.20				0		0	CL	1	0 G 0
CL2	-0.01	53.29	8.10	8.38	8.59	8.74	8.91	8.99	9.10				0		0	CL	2	0 G 0
CLO	24.20	54.10	7.50	7.91	8.21	8.43	8.69	8.81	9.00				0	O	1	CL	1	0 G 0
C6H5CL	12.35	74.79	23.27	30.58	36.47	41.18	47.96	52.41	59.16			C	6	H	5	CL	1	0 G 0
C6H5C6H5	43.50	93.85	35.74	48.74	59.43	68.18	81.19	90.04	103.36			C	12	H	10		0	0 G 0
HCL	-22.06	44.64	6.96	6.95	6.99	7.07	7.29	7.56	8.10				0	H	1	CL	1	0 G 0
C6H4CL	74.34	77.78	22.92	29.16	34.33	38.61	45.16	49.86	57.75			C	6	H	4	CL	1	0 G 0
LINC6H6	82.73	77.88	26.31	32.66	37.79	41.91	47.86	51.75	57.76			C	6	H	6		0	0 G 0
LINC6H5	136.55	80.70	25.50	31.62	36.41	40.12	45.21	48.39	53.56			C	6	H	5		0	0 G 0
BICYC10H9	115.33	82.47	41.50	53.02	62.43	70.06	81.10	88.14	97.06			C	10	H	9		0	0 G 0
C6H3CL2	66.01	82.84	26.90	34.24	38.95	42.01	46.21	51.45	76.83			C	6	H	3	CL	2	0 G 0
CYC6H5CL2	28.16	76.24	28.70	35.98	41.70	46.22	52.97	58.28	71.59			C	6	H	5	CL	2	0 G 0
BICYC6H8	36.88	71.46	21.42	29.39	36.10	41.73	50.51	56.94	67.51			C	6	H	8		0	0 G 0
BICYC6H7.	68.95	76.97	21.04	29.02	35.51	40.78	48.62	54.13	63.66			C	6	H	7		0	0 G 0
CYC5H4CHO	39.18	80.01	23.56	29.56	36.75	42.75	48.25	52.67	57.91			C	6	H	5	O	1	0 G 0
CYPENE4.	54.33	62.51	17.24	23.31	29.39	34.29	39.19	43.00	49.11			C	5	H	7		0	0 G 0
C*CCC*C.	71.41	83.11	21.72	26.83	31.94	37.46	42.99	47.59	54.82			C	5	H	7		0	0 G 0
CH2OHCHO	-73.50	73.57	17.53	20.07	22.34	24.41	28.32	31.01	.00	3/ 5/92	THERM	C	2	H	4	O	2	0 G 2
CH2O.CHO	-21.54	70.97	16.06	18.25	20.22	22.05	25.60	28.04	.00	3/ 5/92	THERM	C	2	H	3	O	2	0 G 1
CH2O.C.O	12.36	72.03	15.90	17.58	19.05	20.40	23.05	24.73	.00	3/ 5/92	THERM	C	2	H	2	O	2	0 G 1
C.HO.CHO	19.36	70.75	16.58	18.27	19.82	21.01	23.20	24.94	.00	3/ 5/92	THERM	C	2	H	2	O	2	0 G 1
CH2OHC.*O	-39.60	74.63	17.37	19.40	21.17	22.76	25.77	27.70	.00	3/ 5/92	THERM	C	2	H	3	O	2	0 G 2

APPENDIX B
Kinetic Mechanism

ELEMENTS

C H O CL

REACTIONS	A	n	Ea
1. C6H5CL=CYC6H5+CL (RITTER)	3.0E+15	0.0	95500.
2. CYC6H6=CYC6H5+H (RITTER)	1.67E+16	0.0	111500.
3. CYC6H7=MECY24PD1 (RITTER)	5.0E+12	0.0	38100.
4. MECY24PD=CY13PD5+CH3 (RITTER)	1.0E+16	0.0	67500.
5. CY13PD=CY13PD5+H (RITTER)	6.0E+14	0.0	75100.
6. CYC6H5=LINC6H5 (RITTER)	3.16E+13	0.0	55200.
7. LINC6H5=C#CC*C.+C2H2 (RITTER)	6.09E+14	0.0	47600.
8. C#CC*C. = C2H + C2H2 (YANG)	3.16E14	0.0	57200.
9. H+CL+M = HCL + M (PRINCETON)	7.20E+21	0.0	0.
10. CL+CL+M = CL2 + M (DUSTIN)	2.34E+14	0.0	-1800.
11. H2 + M = H +H +M (DUSTIN)	4.57E+19	-1.40	104390.
12. C6H5CL=C6H4CL+H (RITTER)	1.3E+16	0.0	110500.
13. CYC6H6+H=MECY24PD1 (RITTER)	2.39E+27	-3.92	29200.
14. C6H5CL+H=CYC6H6+CL (RITTER)	1.50E+13	0.0	7500.
15. CYC6H6+H=CYC6H7 (RITTER)	4.87E+57	-12.73	26800.
16. CYC6H6+H=LINC6H7 (RITTER)	1.22E+22	-1.87	31200.
17. LINC6H7=C*CC*C. + C2H2 (RITTER)	5.50E+14	0.0	41000.
18. CH3+C6H5CL=C6H5CH3+CL (RITTER)	1.96E+14	-0.65	12000.
19. CH3+CYC6H6=C6H5CH3+H (RITTER)	3.4E+26	-4.15	26400.
20. CH3 + H = CH4 (RITTER)	8.09E+36	-7.19	9200.
21. CYC6H6+H=CYC6H5+H2 (RITTER)	2.0E+13	0.0	18600.
22. CH3+H2= CH4 + H (RITTER)	5.00E+12	0.0	11000.
23. C6H5CL+H=CYC6H5+HCL (RITTER)	1.0E+13	0.0	11300.
24. H+C6H5CL=H2+C6H4CL (RITTER)	2.0E+13	0.0	18600.
25. CL+H2=HCL+H (RITTER)	4.8E+13	0.0	5000.
26. CL+C6H5CL=HCL+C6H4CL (RITTER)	1.00E+13	0.0	12500.
27. CL+CYC6H6=HCL+CYC6H5 (RITTER)	1.1E+13	0.0	12500.
28. H + CL2 = CL + HCL (RITTER)	7.94E13	0.0	1200.

29.	MECY24PD1+H=CY13PD5+CH3 (RITTER)	8.0E+13	0.0	0.
30.	CYC6H7=ME.CY24PD (RITTER)	5.5E+10	0.0	23000.
31.	ME.CY24PD+H2=MECY24PD+H (RITTER)	3.98E+12	0.0	14000.
32.	H+CYC6H7=C2H2+C*CC*C (BOZZELLI ESTIMATE)	1.8E+28	-3.4	27900.
33.	C*CC*C= C2H3 + C2H3 (DESAI)	3.98E19	-1.0	98150.
34.	H+CY13PD=CY13PD5+H2 (DESAI)	4.4E+06	2.54	0.
35.	C2H6 = CH3 + CH3 (DUSTIN)	5.34E54	-11.12	112210.
36.	C2H6 + H = C2H5 + H2 (YANG)	5.40E02	3.5	5200.
37.	C2H6 + CH3 = C2H5 + CH4	3.16E11	0.00	10800.
38.	C2H6 + CL = C2H5 + HCL	4.64E13	0.00	179.
39.	C2H6 + O = C2H5 + OH	2.51E13	0.00	6400.
40.	C2H6 + OH = C2H5 + H2O	6.76E13	0.00	3600.
41.	C2H5 = C2H4 + H (DISSOC)	5.65E32	-6.16	50660.
42.	CH3 + CH3 = C2H5 + H (WARNATZ)	8.00E14	0.00	26529.
43.	C2H5 + O = CH2O + CH3 (NIST)	1.61E13	0.00	0.
44.	C2H5 + O2 = C2H4 + HO2 (BOZZELLI)	2.70E10	-5.61	10920.
45.	C2H5 + C2H5 = C2H4 + C2H6 (TSANG)	1.39E12	0.00	0.
46.	C2H4 = C2H3 + H (DISSOC)	5.6E43	-8.54	108080.
47.	C2H4 + O = CH3 + HCO (TSANG)	1.32E08	1.55	427.
48.	C2H4 + OH= CH3 + CH2O (QING-RUI)	1.53E16	-1.46	12170.
49.	C2H4 + OH = C2H3 + H2O (QING-RUI)	9.41E13	0.03	8330.
50.	C2H4 + H = C2H3 + H2 (QING-RUI)	1.31E5	3.10	11400.
51.	C2H3 = C2H2 + H (QING-RUI)	2.00E13	0.00	10000.
52.	C2H3 + O2 = C2H2 + HO2 (BOZZELLI)	1.15E17	-1.71	3290.
53.	C2H3 + O = CH2CO + H (QING-RUI)	9.64E13	0.00	0.
54.	C2H3 + O2 = CH2O + HCO (BOZZELLI)	5.68E26	-4.49	6390.
55.	C2H2 + O = CH2 + CO (QING-RUI)	7.11E14	-0.66	1800.
56.	C2H2 + OH = CH2CO+H (QING-RUI)	2.23E12	0.00	1990.
57.	C2H2 + H = C2H + H2 (QING-RUI)	5.51E13	0.00	22900.
58.	C2H2 + O2 = HCO + HCO (GREG)	1.20E11	0.00	44500.
59.	CH4 + O2 = CH3 + HO2	7.94E13	0.00	55900.
60.	CH4 + O = CH3 + OH	1.20E07	2.1	7620.
61.	CH4 + OH = CH3 + H2O	1.60E06	2.1	2460.
62.	CH4 + CL = CH3 + HCL	5.14E13	0.00	3850.
63.	CH3 + H2O2 = CH4 + HO2 (NIST)	1.21E10	0.00	-596.

64.	CH3 + C2H5 = CH4 + C2H4 (TSANG)	1.95E13	-0.5	0.
65.	CH3 + O2 = CH3O. + O (BOZZELLI)	2.88E15	-1.15	30850.
66.	CH3 + O = CH2O + H (NIST)	8.94E13	-0.03	36.
67.	CH3 + OH = CH2O + H2 (BOZZELLI)	1.60E12	-0.45	10449.
68.	CH3 + OH = CH3O. + H (BOZZELLI)	3.87E12	-0.19	13741.
69.	CH3 + HO2= CH3O. + OH (DUSTIN)	2.00E13	0.0	0.
70.	CH3O. + O2 = CH2O + HO2 (DUSTIN)	6.62E10	0.00	2600.
71.	CH2O + CH3 = CH4 + HCO	1.00E10	0.50	6000.
72.	CH2O+ H = HCO + H2	2.50E13	0.00	3990.
73.	CH2O + O = HCO + OH	3.50E13	0.00	3510.
74.	CH2O + OH= HCO + H2O	3.00E13	0.00	1190.
75.	CH2O + HO2= HCO+ H2O2	1.00E12	0.00	8000.
76.	CH2O + CL = HCO + HCL	5.00E13	0.00	500.
77.	HCO + OH = CO + H2O (CHEMACT)	7.19E22	-2.86	3750.
78.	HCO + M = H + CO + M (NIST)	5.11E21	-2.14	20424.
79.	HCO + H = CO + H2 (NIST)	2.00E14	0.00	0.
80.	HCO + O = CO + OH (NIST)	3.00E13	0.00	0.
81.	HCO + O2 = CO + HO2 (BOZZELLI)	3.04E20	-2.66	2383.
82.	HCO + O2 = CO2 + OH (BOZZELLI)	8.65E18	-2.46	2247.
83.	HCO + HO2=CH2O +O2 (BOZZELLI)	8.00E11	0.00	2000.
84.	HCO + HO2= H2O + CO2 (CHEMACT)	6.31E11	-0.27	250
85.	CH2 + H = CH + H2	4.00E13	0.00	0.
86.	CH2 + O = CO + H +H	5.00E13	0.00	0.
87.	CH2 + O2= CO2 + H +H	1.30E13	0.00	1500.
88.	CH2 + O2= CH2O + O	1.00E14	0.00	3700.
89.	CH2 + CH3= C2H4 + H	4.00E13	0.00	0.
90.	CH + O = CO + H	4.0E13	0.00	0.
91.	CH + O2= CO + OH	2.00E13	0.00	0.
92.	CO + O + M = CO2 + M (NIST)	6.17E14	0.0	3000.
93.	CO + OH = CO2 + H (DESAI)	4.4E+07	1.5	-717.
94.	CO + HO2=CO2+OH	1.51E14	0.00	23600.
95.	CO + O2 = CO2 +O	2.50E12	0.00	48000.
96.	CH2CO + H=CH3 + CO	7.00E12	0.00	3010.
97.	CH2CO + O= HCO + HCO (CHEMACT)	7.30E12	-0.27	1800.
98.	CH2CO + OH = CH2O + HCO (CHEMACT)	2.61E06	1.32	13850.

99. CH2CO + M= CH2 + CO + M	3.00E14	0.00	70930.
100. H + O2 = O + OH (PRINCETON)	1.92E14	0.00	16440.
101. O + H2 = H + OH	1.8E10	1.0	8900.
102. OH + OH = O + H2O	1.51E09	1.14	0.
103. H2 + OH = H + H2O	1.10E09	1.3	3646.
104. H + OH + M = H2O + M	2.2E22	-2.0	0.
105. O2 + M = O + O + M	5.12E15	0.0	11500.
106. H + O + M = OH + M	6.20E16	-0.6	0.
107. H + HO2=OH + OH	1.5E14	0.00	1000.
108. H + HO2 = H2 + O2	2.5E13	0.00	0.
109. O + HO2 = OH + O2	2.00E13	0.00	0.
110. OH + HO2=H2O + O2	2.00E13	0.00	0.
111. H2O2 + OH = H2O + HO2	1.00E13	0.0	1800.
112. H2O2 + H = HO2 + H2 (PRINCETON)	4.82E13	0.0	7948.
113. H2O2 + M = OH + OH + M	1.20E17	0.0	45500.
114. H + O2 + M = HO2 + M (PRINCETON)	6.70E19	-1.42	0.
115. H2 + O2 = OH + OH	1.70E13	0.0	47780.
116. O + HCL = OH + CL	5.24E12	0.00	6400.
117. OH + HCL = CL + H2O	2.45E12	0.00	1100.
118. CL + HO2= HCL + O2	1.30E13	0.00	200.
119. CL + HO2 = CLO + OH (DUSTIN)	2.47E13	0.00	894.
120. CLO + CO = CL + CO2	2.70E11	0.00	4500.
121. CH3 + CLO = CH3O. + CL	9.00E12	0.00	1000.
122. C6H5CL + O = C6H4CL + OH (YANG)	1.80E13	0.0	10000.
123. C6H5CL +OH = C6H4CL +H2O (YANG)	1.44E13	0.0	4490.
124. C6H5CL + HO2 = C6H4CL +H2O2 (BOZZELLI ESTIMATE)	5.00E11	0.0	27500.
125. C6H5CL +O2 =C6H4CL +HO2 (BOZZELLI)	3.00E13	0.0	65370.
126. CYC6H6 + O =CYC6H5 + OH (BOZZELLI)	3.60E13	0.0	15500.
127. CYC6H6 +OH =CYC6H5 +H2O (YANG)	1.40E13	0.0	4490.
128. CYC6H6 +HO2=CYC6H5 + H2O2 (BOZZELLI)	1.00E11	0.0	29040.
129. CYC6H6 +O2 =CYC6H5 +HO2 (BOZZELLI)	6.31E13	0.0	66832.
130. CYC6H6 + O =C6H5OH (DESAI)	3.91E+04	1.59	17190.
131. CYC6H6 + O = C6H5O. + H (DESAI)	6.32E14	-0.4	5640.
132. MECY24PD1+H2=MECY24PD+H (BOZZELLI)	2.00E13	0.0	34500.
133. C6H5OH = C6H5O. + H (YANG)	9.68E14	0.0	83130.

134.	CYC6H6 + OH = C6H5OH + H (YANG)	4.17E12	0.0	13400.
135.	C6H5OH + H = C6H5O. + H2 (DESAI)	1.15E14	0.0	12390.
136.	C6H5OH + OH = C6H5O. + H2O (DESAI)	6.00E12	0.0	0.
137.	C6H5OH + O2 = C6H5O. + HO2 (DESAI)	1.00E13	0.0	32949.
138.	C6H5OH + C*CC*C. = C6H5O. + C*CC*C (DESAI)	1.00E13	0.0	2000.
139.	C6H5OH + CH3 = C6H5O. + CH4 (DESAI)	2.88E11	0.0	5500.
140.	C6H5OH + CY13PD5 = C6H5O. + CY13PD (DESAI)	1.00E13	0.0	25240.
141.	C6H5OH + C*CC. = C6H5O. + C*CC (DESAI)	1.00E13	0.0	2000.
142.	CYC6H5 + C6H5OH = CYC6H6 + C6H5O. (BZ891)	1.00E13	0.0	6064.
143.	C6H5OH + C#CC. = C6H5O. + CC#C (BZ891)	1.00E13	0.0	2000.
144.	CYC6H5 + O2 = C6H5O. + O (BOZZELLI)	6.60E13	0.0	3460.
145.	CYC6H5 + O = CY13PD5 + CO (DESAI)	5.25E14	-0.2	710.
146.	CYC6H5 + OH = C6H5OH (DESAI)	1.59E13	0.0	0.
147.	CYC6H5 + HO2 = C6H5O. + OH (DESAI)	8.00E11	0.0	0.
148.	C6H5CL + O = C6H5O. + CL (YANG)	1.39E13	0.0	4900.
149.	C6H5CL + OH = C6H5OH + CL (YANG)	7.83E12	0.0	4800.
150.	C6H5O. = BICYC6H5O (YANG)	1.31E+22	-2.48	42100.
151.	BICYC6H5O = CYC5H4CHO (YANG)	1.25E16	-2.35	2020.
152.	CYC5H4CHO = CY13PD5 + CO (DESAI)	4.43E14	-1.79	510.
153.	CY13PD + CH3 = CH4 + CY13PD5 (YANG)	3.11E11	0.0	5500.
154.	CY13PD5 + O = CYPDONE + H (DESAI)	2.80E13	-0.02	40.
155.	CY13PD5 + O = C*CC*C. + CO (BZ891)	1.05E14	-0.19	280.
156.	CY13PD5 + HO2 = CYC5H5O. + OH (BZ891)	2.08E20	-1.43	13680.
157.	CYC5H5O. = C*CC*C. + CO (BZ891)	4.53E36	-7.88	31170.
158.	CY13PD5 + OH = CYC5H5OH (BZ891)	2.8E16	-0.8	790.
159.	CYC5H5OH + OH = CYC5H5O. + H2O (DESAI)	1.00E13	0.0	1697.
160.	CYPDONE + H = CO + C*CC*C. (BZ891)	3.61E14	0.26	13550.
161.	C*CC*C. = C2H3 + C2H2 (DESAI)	1.00E14	0.0	43900.
162.	C*CC*C. + O2 = C*CCO +HCO (DESAI)	6.38E12	0.0	0.
163.	C*CC*C + OH = C*CC. + CH2O (DESAI)	1.00E12	0.0	0.
164.	C*CC. = C*C*C + H (DESAI)	2.63E13	0.0	59785.
165.	C*CC. + H = C2H3 + CH3 (DESAI)	4.91E36	-6.0	33070.
166.	C*C*C + O = CO + C2H4 (DESAI)	7.80E12	0.0	1602.
167.	CYPENE4. = CY13PD + H (YANG)	3.88E13	0.0	36171.
168.	CYPENE4. = C*CCC*C. (YANG)	8.72E13	0.0	37379.

169.	C*CC. + C2H2 = C*CCC*C. (YANG)	8.38E30	-6.24	12824.
170.	C*CC. +C2H2 = CYPENE4. (YANG)	1.82E11	0.0	6372.
171.	C*CC + CH3 = C*CC. + CH4 (YANG)	3.80E11	0.0	9000.
172.	C*CC. + C2H2 = CY13PD + H (YANG)	2.95E32	-5.82	25733.
173.	CY13PD5 + HO2 = CPDOOH (BZ891)	5.73E29	-5.14	4800.
174.	CPDOOH = CYC5H5O. + OH (BZ891)	3.07E18	-1.12	44330.
175.	CY13PD + O = C*CC*CCO (BZ891)	5.68E12	0.0	0.
176.	CY13PD + OH = C2H3 + C*CCO (BZ891)	8.02E33	-5.73	25120.
177.	CY13PD + OH = CY13PD5 + H2O (BZ891)	1.00E13	0.0	0.
178.	CY13PD + O2 = CY13PD5 + HO2 (BZ891)	6.00E13	0.0	17349.
179.	CY13PD + C2H3 = CY13PD5 + C2H4 (BZ891)	1.20E-01	4.0	0.
180.	CYC5H4OH = CYPDONE + H (BZ891)	1.00E13	0.0	29830.
181.	CYC5H5OH + H = CYC5H4OH + H2 (BZ891)	3.15E12	0.0	0.
182.	CYC5H5OH + H = CYC5H5O. + H2 (BZ891)	4.00E13	0.0	6094.
183.	CYC5H5OH + O = CYC5H4OH + OH (BZ891)	4.17E11	0.0	0.
184.	CYC5H5OH + O = CYC5H5O. + OH (BZ891)	1.00E13	0.0	4683.
185.	CYC5H5OH + OH = CYC5H4OH + H2O (BZ891)	3.98E12	0.0	0.
186.	CYC5H5OH + HO2 = CYC5H4OH + H2O2 (BZ891)	1.00E11	0.0	0.
187.	CYC5H5OH + HO2 = CYC5H5O. + H2O2 (BZ891)	1.00E13	0.0	15800.
188.	C*CC*CCO + H = C.OC*CC*C + H2 (BZ891)	1.00E13	0.0	0.
189.	C.OC*CC*C = C*CC*C. +CO (BZ891)	1.00E14	0.0	21000.
190.	C*CC#C + H = C*CC*C. (BZ891)	5.50E12	0.0	2400.
191.	C*CC*C. + O2 = CH2O + C.*CCO (BZ891)	7.89E17	-2.05	300.
192.	C.*CCO = HCO + C2H2 (BZ891)	3.16E13	0.0	4000.
193.	C*CC*C. + O2 = H + COC*CCO (BZ891)	6.57E20	-3.03	1160.
194.	C*CC*C. + C2H4 = C*CC*C + C2H3 (BZ891)	6.31E11	0.0	7800.
195.	C*CC*C + H = C*CC*C. + H2 (BZ891)	1.00E13	0.0	4700.
196.	C2H3 + C2H4 = C*CC*C + H (BZ891)	5.00E11	0.0	7304.
197.	CC*CCO + H = CC*CC.O + H2 (BZ891)	1.00E13	0.0	0.
198.	CC*C. + CO = CC*CC.O (BZ891)	6.98E11	0.0	5000.
199.	C*CCO + H = C*CC.O + H2 (BZ891)	8.09E11	0.0	0.
200.	C*CCO + O = C*CC.O + OH (BZ891)	4.70E12	0.0	1999.
201.	C*CCO + OH = C*CC.O + H2O (BZ891)	1.60E13	0.0	0.
202.	C*CCO + HO2 = C*CC.O + H2O2 (BZ891)	1.98E12	0.0	9800.
203.	CO + C2H3 = C*CC.O (BZ891)	1.51E11	0.0	4809.

204.	C*CC. + H = C*CC (BZ891)	3.33E15	-0.55	1800.
205.	C*CC = CC*C. + H (BZ891)	7.59E14	0.0	101271.
206.	C*C*C = CC#C (BZ891)	1.48E13	0.0	60395.
207.	C*C*C + H = C#CC. +H2 (BZ891)	3.30E05	2.54	3000.
208.	C*C*C + O = C#CC. + OH (BZ891)	1.00E13	0.0	3000.
209.	CC#C + O = C#CC. + OH (BZ891)	1.00E13	0.0	3000.
210.	C2H3 + O2 = CH2CHO + O (BZ891)	2.03E13	-0.09	4210.
211.	CH2O + C2H3 = HCO + C2H4 (BZ891)	1.20E-01	4.0	3600.
212.	C2H2 + HO2 = C*C*O + OH (BZ891)	6.03E09	0.0	7948.
213.	C*C*O + OH = HCO + CH2O (BZ891)	2.80E13	0.0	0.
214.	CH2O = CO + H2 (BZ891)	4.52E15	0.0	35295.
215.	CH2O + C2H5 = HCO + C2H6 (BZ891)	6.00E-02	4.0	4600.
216.	CH3 + O2 = CH2O + OH (BZ891)	1.13E12	-0.17	15560.
217.	HCO = CO + H (BZ891)	2.50E14	0.0	16800.
218.	C*CC#C + O = C.*C*O + C2H3 (BZ891)	5.00E13	0.0	0.
219.	C.*C*O + O2 = CO2 + HCO (BZ891)	4.00E12	0.0	0.
220.	C*C*O + OH = H2O + C.*C*O (BZ891)	7.24E12	0.0	1400.